Estudi de la biodisponibilitat del *trans*-resveratrol i el seu efecte quimiopreventiu del càncer de còlon induït per 1,2-dimetilhidrazina en rata

Irene Alfaras Cardenal

III. RESULTATS

L'apartat de Resultats d'aquest treball es troba subdividit en cinc capítols, cadascun dels quals es correspon a un dels objectius plantejats. La introducció, el material i mètodes, els resultats, la discussió i les conclusions que pertanyen a cada capítol es troben recollits en articles publicats, exceptuant el cas del primer apartat del segon capítol, del tercer capítol i del segon apartat del quart capítol, que es troben redactats en català, però en format article.

Resultats ~ Capítol 1

CAPÍTOL 1. POSTA A PUNT D'UN MÈTODE PER A LA DETERMINACIÓ DEL DIHIDRORESVERATROL EN PLASMA DE RATA

Els resultats presentats en el capítol es troben recollits a l'article 1:

Determination of dihydroresveratrol in rat plasma by HPLC.
Juan, M.E., Alfaras, I., Planas, J.M.
J. Agric. Food Chem. 2010, 58, 7472-7475

Els resultats obtinguts han donat lloc a la següent comunicació a congrés:

- *Determination of dihydroresveratrol in rat plasma by HPLC*
  Alfaras I, Prados A, Planas JM, Juan ME.

  Presentada com a pòster en el congrés:

  4th International Conference on Polyphenols and Health (ICPH2009)
  Harrogate, Anglaterra, 7 - 11 de desembre de 2009

Determination of dihydroresveratrol in rat plasma by HPLC

J. Agric. Food Chem. 2010, 58, 7472-7475

1.1. Resum de l'article 1

Objectius: El dihidroresveratrol és un metabòlit del *trans*-resveratrol que es forma mitjançant la hidrogenació del doble enllaç per acció de la microbiota intestinal. Per tant, es va posar a punt un mètode per a la determinació del dihidroresveratrol a plasma de rata i quantificar la seva concentració plasmàtica després de l'administració de 60 mg/kg a rates Sprague-Dawley.

Material i mètodes: El dihidroresveratrol va ser extret del plasma acidificat amb àcid acètic per extracció en fase sòlida emprant un cartutx C18. L'elució del compost retingut al cartutx es va fer amb metanol 100% (v/v) i es va evaporar a 45ºC fins a un volum final d'uns 400 µL abans del seu anàlisi per cromatografia líquida d'alta resolució (HPLC). La fase mòbil utilitzada a l'HPLC estava constituïda per un solvent A, àcid acètic al 3%, i un solvent B que consistia en el 20% de solvent A i un 80% d'acetonitril. Els cromatogrames es van obtenir a 276 nm, màxim d'absorbància del dihidroresveratrol. El mètode es va validar afegint concentracions creixents d'estàndard de dihidroresveratrol a plasma blanc de rata. Es va determinar la linealitat, la precisió, la recuperació, l'exactitud, la sensibilitat i la selectivitat. Posteriorment, es va administrar oralment 60 mg/kg de dihidroresveratrol a rates Sprague-Dawley per avaluar la validesa del mètode i es va extraure sang als 10 i 30 minuts després de l'administració.

Resultats: La validació del mètode va donar una correlació linear en un rang de 5 a 100 µM i una bona precisió inter- i intra-dia (<7%). La recuperació mitjana va ser de 96,7% i l'exactitud va ser de 93,0 i 98,9% a les concentracions de 10 i 50 µM. El mètode va ser selectiu per al dihidroresveratrol, evitant la interferència amb altres pics. El límits de detecció i quantificació van ser de 275 nM i 578 nM, respectivament. Després de l'administració a rates, es confirmà per HPLC-MS el pic del dihidroresveratrol (*m/z* 229) i s'identificaren dos pics més corresponents als seus conjugats glucurònid (*m/z* 405) i sulfat (*m/z* 309). El dihidroresveratrol es va trobar a plasma en concentracions de 1,06 ± 0,20 i 0,88 ± 0,22 µM als 10 i 30 minuts, respectivament. El glucurònid va ser el compost més abundant a plasma amb concentracions de 12,6 ± 1,1 i 33,5 ± 0,9 µM als 10 i 30 minuts, respectivament. Les concentracions de sulfat als 10 i 30 minuts foren de 4,41 ± 1,30 i 6,40 ± 1,26 µM.

Conclusió: El mètode per HPLC de determinació del dihidroresveratrol a plasma de rata és sensible, exacte i reproduïble. A més, aquest mètode permet la separació i

quantificació dels metabòlits del dihidroresveratrol, glucurònid i sulfat, quan aquest és administrat per via oral a rates.

DOI:10.1021/jf100836j

JOURNAL OF AGRICULTURAL AND FOOD CHEMISTRY
ARTICLE

Determination of Dihydroresveratrol in Rat Plasma by HPLC

M. Emília Juan,*,† Irene Alfaras,† and Joana M. Planas†

†Departament de Fisiologia (Farmàcia) and Institut de Recerca en Nutrició i Seguretat Alimentària (INSA-UB), Universitat de Barcelona, Spain

Dihydroresveratrol is a metabolite of *trans*-resveratrol formed in the intestine by the hydrogenation of the double bond by microflora. The aim of the present study was to validate a method to measure dihydroresveratrol in rat plasma and then to quantify its plasmatic concentration after the oral administration of 60 mg/kg to Sprague−Dawley rats. Dihydroresveratrol was extracted from acidified plasma with a C18 cartridge, eluted with methanol, and concentrated prior to HPLC analysis with diode-array detection (HPLC-DAD) at 276 nm. The method was validated by spiking blank plasma samples with pure dihydroresveratrol, obtaining a linear correlation and good interday and intraday precisions, expressed as coefficient of variation (<7%). The average recovery was 96.7% and the limit of detection was 275 nM. The oral administration of dihydroresveratrol to rats and its subsequent detection, along with dihydroresveratrol glucuronide and sulfate, provides evidence of its absorption and metabolism.

KEYWORDS: Dihydroresveratrol; HPLC-DAD; method validation; rat plasma; resveratrol

INTRODUCTION

Dihydroresveratrol (*trans*-3,5,4′-trihydroxybibenzyl) (**Figure 1**) belongs to the family of stilbenoids, which are a class of plant secondary metabolites produced in a number of unrelated species. Dihydroresveratrol has been identified as a phytoalexin in *Orchidaceae* (*1*), in *Cannabis sativa* L. (*2*), and in the tuber of *Dioscorea dumetorum*, where its production seems to be elicited by fungal infection (*3*). In addition, this phytochemical has been found in *Maackia amurensis*, a major component of the Russian hepatoprotective preparation Maksar (*4*). The functions of stilbenoids in plants include constitutive and inducible defense mechanisms, plant growth inhibitors, and dormancy factors (*5*).

Dihydroresveratrol was also detected in humans as a metabolite of *trans*-resveratrol (*6*), a natural antioxidant with beneficial effects on health (*7*). After the oral administration of 25 mg of ^{14}C-resveratrol, Walle et al. (2004) identified in urine two resveratrol monoglucuronides, two monosulfates, and interestingly, dihydroresveratrol glucuronide and sulfate (*6*). The latter may have been produced by the intestinal microflora, since it involved the hydrogenation of the aliphatic double bond of *trans*-resveratrol. Later, dihydroresveratrol and its sulfate conjugate were detected in rats (*8*). Recently, a study that evaluated the interactions of this polyphenol with animal-associated bacteria identified dihydroresveratrol as a metabolite produced by *Eggerthella lenta* and *Bacteroides uniformis*. Both of these microorganisms have been isolated from human fecal samples, thus supporting the involvement of intestinal flora in the synthesis of this metabolite (*9*). The information regarding the human health protecting properties of dihydroresveratrol is limited. This compound has been reported to have antiproliferative effects in human prostate cancer cells (*10*, *11*). Moreover, dihydroresveratrol is a potassium channel modulator (*12*), an antioxidant, and it inhibits DNA synthesis (*13*).

Because the reduction of the stilbenic double bond of *trans*-resveratrol appears to be produced by the intestinal microflora, dihydroresveratrol might be absorbed through the colonic epithelium to reach blood and finally be excreted in urine. The presence of dihydroresveratrol in plasma has yet to be reported, which could be attributed not only to the lack of accurate methods but also to the absence of a commercially available pure standard. Here we present a simple, accurate, and sensitive method for identifying and quantifying dihydroresveratrol in rat plasma by means of solid-phase extraction, followed by HPLC analysis with photodiode array detection. The performance of the method was assessed by oral administration of dihydroresveratrol to Sprague−Dawley rats and its measurement in plasma.

MATERIALS AND METHODS

Chemicals and Reagents. Dihydroresveratrol was provided by Biopharmalab SL (Alicante, Spain). Stock solutions of 1 mM dihydroresveratrol in ethanol 20% (v/v) were prepared weekly and stored at room temperature. Acetonitrile and methanol were purchased from J. T. Baker (Deventer, Netherlands) and acetic acid was provided by Scharlau Chemie SA (Barcelona, Spain). All solvents were HPLC grade. Ascorbic acid (ref A5960) was purchased from Sigma-Aldrich (St. Louis, MO). Other chemicals used were analytical grade and obtained from Sigma-Aldrich. Reversed-phase C_{18} Sep-Pak classic cartridge for manual operation (ref WAT051910) were purchased from Waters (Milford, MA). Water used in all experiments was passed through a Milli-Q water purification system (18 MΩ) (Millipore, Milan, Italy).

Instrumentation. A Concentrator 5301 (Eppendorf Iberica SL, San Sebastian de los Reyes, Spain) was used to evaporate methanol from samples. The determination of dihydroresveratrol and its metabolites was carried out using a gradient liquid chromatograph Agilent model 1100

*To whom correspondence should be addressed. Phone: +34 93 4024505. Fax: +34 93 4035901. E-mail: mejuan@ub.edu.

 Published on Web 05/28/2010

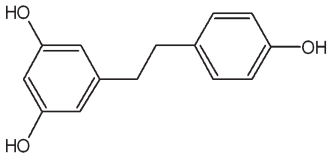

Figure 1. Chemical structure of dihydroresveratrol.

(Agilent Technologies, Palo Alto, CA) equipped with an automatic injector, a Synergi Fusion-RP 80A column (250 mm × 4.6 mm; 4 μm; Phenomenex, Torrance, CA) with a C18 guard column cartridge and a diode array UV−visible detector. Agilent Chemstation software controlled all the equipment and performed the data processing. An Applied Biosystems API 3000 triple quadrupole mass spectrometer (Applied Biosystems, PE Sciex, Concord, Ontario, Canada), equipped with a Turbo IonSpray source in the negative ion mode, was used to obtain the mass spectrometry.

Solid-Phase Extraction of Dihydroresveratrol from Plasma Samples. Blood was collected from Sprague−Dawley rats by cardiac puncture and was placed in tubes containing EDTA-K_3 as anticoagulant. Samples were centrifuged at 1500*g* for 15 min at 4 °C, and the plasma was immediately separated from cells. Plasma (200 μL) was acidified with 6 μL of acetic acid and stirred in a vortex for 2 min. Prior to use, the Sep-Pack cartridge used for the extraction was conditioned with 4 mL of methanol followed by equilibration with 10 mL of water. Then plasma was slowly loaded into the cartridge, followed by 5 mL of water. The dihydroresveratrol contained in the cartridge was eluted with 4 mL of methanol. Ascorbic acid (10 μL) at 15% were added to the eluate as an antioxidant, which was then evaporated at 45 °C to a final volume of 400 μL. Finally, it was placed in a sealed amber vial for HPLC analysis.

HPLC and HPLC-MS Analyses. The temperature of the column oven was set at 40 °C, and the injection volume was 100 μL. The mobile phase included solvent A consisting of an acetic acid solution (3%, v/v) and solvent B, which was a mixture of phase A:acetonitrile (20:80, v/v). The flow rate was 1.5 mL/min. The gradient elution was: min 0 with 22% solvent B to min 2; 2−6 min, linear gradient from 22 to 30% B; 6−14 min, linear from 30 to 50% B; 14−18 min, increasing to 60% B; 18−25 min, linear from 60 to 100% B; followed by washing and reconditioning the column.

The chromatograms were obtained at 276 nm at which the absorbance of dihydroresveratrol presents a maximum (**Figure 2**). The compound was identified using comparative retention times of pure standard and photodiode array spectra (from 200 to 400 nm). Quantification of dihydroresveratrol was performed using standard curves constructed after spiking relevant concentrations of this compound in blank plasma. As dihydroresveratrol metabolites were not available, their quantities were calculated based on the assumption that recovery characteristics and relationship between peak area ratios and concentrations were the same as those for dihydroresveratrol.

Dihydroresveratrol and its conjugates were identified by mass spectrometry. The ion spray voltage was 3500 V, with nitrogen as the nebulizer gas, 10 (arbitrary units), and curtain gas, 15 (arbitrary units). The detecting conditions were optimized with a standard solution of dihydroresveratrol in the presence of LC mobile phase, as follows: declustering potential, −70 V; focusing potential, −200 V; drying gas (N_2) heated to 400 °C and introduced at a flow rate of 5000 cm^3/min. Mass spectra were acquired in the 100−500 *m*/*z* range.

Method Validation. The solid-phase extraction (SPE) of dihydroresveratrol from rat plasma followed by HPLC analysis was validated according to *The United States Pharmacopoeia* (2008) (*14*). Blank rat plasma was obtained by cardiac puncture from rats that had not received dihydroresveratrol. Aliquots of the pooled plasma were stored at −20 °C until the analyses were performed, then 200 μL of plasma were spiked with known amounts of dihydroresveratrol and subsequently stirred in a vortex for 1 min before being extracted as indicated above.

Linearity. Spiked plasma samples containing increasing concentrations of dihydroresveratrol: 5, 10, 25, 50, 75, and 100 μM were analyzed according to the procedure described above. Integrated peak areas were plotted against analyte concentration, and linear regression was performed by the least-squares method.

Precision. The precision of the analytical method was determined by assaying a sufficient number of plasma samples (n = 4−6) at six different concentrations of dihydroresveratrol ranging from 5 to 100 μM and was expressed as relative standard deviation (RSD). The intraday precision was determined by analyzing the spiked samples prepared within a day, whereas the interday precision assessed spiked samples prepared on three different days. Peak areas were considered for the calculation of the concentration and to establish the precision.

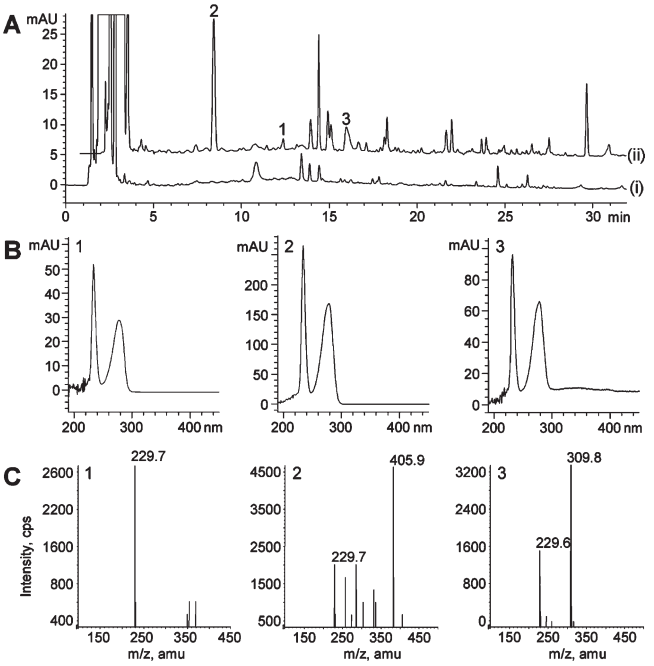

Figure 2. HPLC chromatograms and UV and mass spectra of dihydroresveratrol and its glucuronide and sulfate conjugates. (**A**) HPLC chromatogram at 276 nm of (i) blank plasma and (ii) plasma of rats administered with 60 mg/kg of dihydroresveratrol. Peaks of (1) dihydroresveratrol and its conjugates (2) glucuronide and (3) sulfate are indicated. (**B**) UV spectra obtained by diode-array detection of (1) dihydroresveratrol, (2) glucuronide and (3) sulfate. (**C**) Full-scan product ion mass spectra of (1) dihydroresveratrol, (2) glucuronide, and (3) sulfate.

Recovery. Recoveries of dihydroresveratrol from plasma were measured by spiking 200 μL of blank samples at final concentrations of 5, 10, 25, 50, 75, and 100 μM. Absolute recoveries were calculated by comparing the peak area ratio from spiked samples to those of the corresponding concentrations injected directly into the HPLC system without extraction.

Accuracy. First, 500 μL of plasma and 500 μL of water as control were spiked with dihydroresveratrol at concentrations of 10 and 50 μM. The samples were purified by SPE and analyzed by HPLC as described. Accuracy was calculated by comparing the values for the plasma samples and control: results are expressed as percentages of analyte recovered.

Sensitivity. The limit of detection (LOD) and the limit of quantification (LOQ) were calculated by measuring the analytical background response, running six blanks of plasma using the maximum sensitivity allowed by the system. The signal-to-noise ratio was used to determine the LOD, and it was estimated as the concentration of dihydroresveratrol in plasma samples that generated a peak with an area at least 3 times higher than the baseline noise. LOQ was considered to be 10 times the standard deviation of the six blank samples analyzed using the maximum sensitivity allowed by the system. The LOQ was subsequently validated by the analysis of six plasma samples known to be near the LOQ.

Selectivity. The presence of interfering substances in blank plasma at the retention time of dihydroresveratrol as well as its glucuronide and sulfate conjugates was evaluated. The selectivity of the method was determined by comparing the chromatograms of blank plasma with the corresponding spiked plasma samples.

Animal Studies. Male Sprague−Dawley rats (200−250 g) were housed three per cage, in a temperature-controlled room, with a light−dark cycle of 12 h and free access to water and a commercial rat chow. Animal treatment was in full accordance with the European Community

Table 1. Precision, Accuracy, and Recovery of *trans*-Resveratrol in Spiked Rat Plasma Samples

	precision (% RSD)		
dihydroresveratrol (μM)	intraday	interday	recovery (%)
5 (n = 6)	3.05	3.50	96.8 ± 5.9
10 (n = 6)	5.85	5.14	95.2 ± 6.9
25 (n = 6)	1.30	6.62	95.8 ± 2.2
50 (n = 6)	5.16	6.66	97.5 ± 5.6
75 (n = 6)	5.23	5.60	96.5 ± 6.7
100 (n = 6)	1.73	3.34	98.3 ± 2.7

Guidelines for the care and management of laboratory animals. Dihydroresveratrol dissolved in water was administered orally by gavage to overnight-fasted rats at a dose of 60 mg/kg, except for the control group, which was given only water. Rats were fasted overnight and anesthetized by intramuscular injection of 90 mg/kg ketamine (Imalgene 1000, Merial Laboratorios SA, Barcelona, Spain) and 10 mg/kg xylacine (Rompun 2%, Química Farmaceutica Bayer SA, Barcelona, Spain). Blood was withdrawn by cardiac puncture and transferred to a tube containing EDTA-K3 as anticoagulant, at 10 and 30 min after the administration. Immediately after obtaining the plasma by centrifugation at 1500*g* for 15 min at 4 °C, the analyte was purified using the SPE procedure described above.

Statistical Analysis. Data are reported as the mean ± SEM. A commercially available package (Prism version 4.02; GraphPad Software Inc., San Diego, CA) was used for all statistical tests. Data were evaluated by one-way ANOVA and post hoc Bonferroni's Multiple Comparison tests (Graph Pad Prism). A $p < 0.05$ level was taken as significant.

RESULTS

Method Validation. The analytical performance parameters assessed for the overall assay were linearity, precision, accuracy, sensitivity, and selectivity.

Linearity. The response was linear in the range of concentrations evaluated from 5 to 100 μM, giving an equation of $y = 8.75x - 1.26$ ($n = 31$) and a regression coefficient of 0.998.

Precision. Intraday and interday precision (% RSD) ranged from 1.30% to 6.66% (**Table 1**) and were within the acceptable limits to meet the guidelines for bioanalytical method validation, which is considered to be ≤20% (*15*). The precision data indicate that the analytical method is repeatable.

Recovery. The extraction recoveries of dihydroresveratrol were assayed in plasma samples at six different concentrations (**Table 1**). The mean recovery in plasma was 96.7 ± 5.0%, thus indicating the high extraction efficiency of this procedure.

Accuracy. The accuracy was determined for the overall assay by measuring the percentage of recovery after the addition of known amounts of standard to a control (water) and to a pool of blank plasma, at two different concentrations. The mean recoveries at 10 and 50 μM were 93.0 ± 2.1% and 98.9 ± 3.3%, respectively.

Sensitivity. The LOD was 275 nM on the basis of a signal-to-noise ratio of 3. The LOQ was 578 nM.

Selectivity. Dihydroresveratrol was well resolved and free from interference peaks. This compound was quantified at 276 nm, its maximum absorbance to improve selectivity, and the identity of the chromatographic peak was confirmed not only by its retention time but also by its spectrum (**Figure 2**).

Animal Studies. Dihydroresveratrol was orally administered to rats at a dose of 60 mg/kg, and blood was withdrawn at 5 and 30 min to assess the validity of the method. The representative HPLC profile (**Figure 2A**) was characterized not only by the presence of dihydroresveratrol but also by two more peaks with the same absorbance spectrum, which were identified by means of MS. The peak with retention time of 8.1 min gave a deprotonated molecular ion $[M - H]^-$ at m/z 405 (**Figure 2C**) with a dihydroresveratrol fragment at m/z 229, thus allowing its identification as dihydroresveratrol glucuronide. The second peak (retention time 15.8 min) was identified as the sulfate conjugate because it showed a deprotonated molecular ion $[M - H]^-$ at m/z 309 (**Figure 2C**) and also the dihydroresveratrol fragment at m/z 229.

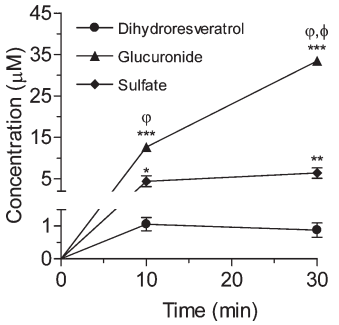

Figure 3. Plasmatic concentrations after the oral administration of 60 mg/kg of dihydroresveratrol. Data are presented as means ± SEM (n = 4), $^*p < 0.05$, $^{**}p < 0.01$, and $^{***}p < 0.001$, conjugates vs dihydroresveratrol. $^{\varphi}p < 0.001$, glucuronide vs sulfate. $^{\Phi}p < 0.001$, 30 min vs 10 min.

Dihydroresveratrol was detected in plasma at 10 and 30 min (**Figure 3**) with concentrations of 1.06 ± 0.20 and 0.88 ± 0.22 μM, respectively. However, its glucuronide conjugate was the most abundant compound in plasma, with concentrations of 12.6 ± 1.1 μM and 33.5 ± 0.9 μM, at 10 and 30 min, respectively. The sulfate conjugate was also present with 4.4 ± 1.3 μM and 6.4 ± 1.3 μM at 10 and 30 min, respectively.

DISCUSSION

The development of a method to measure dihydroresveratrol that provides insight into its plasmatic concentration and metabolism is not trivial. First, because it is a metabolite of *trans*-resveratrol, and although comprehensive data are available on the oral bioavailability of *trans*-resveratrol (*16*−*18*), there are still some unanswered questions in terms of the complete identification and quantification of its metabolites. In addition, given that the in vivo concentrations of individual metabolites are higher than those of the parent compound, *trans*-resveratrol conjugates might act as a pool from which free *trans*-resveratrol could be released in various tissues or be active on themselves in promoting many of the health benefits attributed to *trans*-resveratrol (*19*). The last could be the case of dihydroresveratrol, which is a phytoalexin like *trans*-resveratrol (*1*). Dihydroresveratrol is synthesized by the condensation of one molecule of dihydro-*p*-coumaroyl-CoA and three molecules of malonyl-CoA as an intermediate in the biosynthetic pathway of stilbenoids in plants (*20*). Although the biological properties of dihydroresveratrol have not been completely established, it shows antiproliferative activity in human prostate cancer cells, with an IC_{50} of around 25 μM (*10*, *11*). Moreover, dihydroresveratrol displayed a higher potential as a potassium channel modulator than *trans*-resveratrol in mouse neuroblastoma cells (*12*). This activity has also been reported in other tissues in connection with antitumor (tamoxifen) and cardiac antiarythmic (tedisamil) agents.

Dihydroresveratrol is a scarcely known metabolite of *trans*-resveratrol. This lack of knowledge can be attributed, in part, to the absence of a commercially available pure standard, which hinders the development of sensitive methods for measuring this compound in plasma and body fluids. The present study validates a method that allows the measurement of dihydroresveratrol and its conjugates in rat plasma. The results show that the method is reliable, reproducible, and easy to apply to biological samples. Solid-phase extraction of dihydroresveratrol from plasma with a C18 cartridge was appropriate for its measurement because it avoided analyte losses and provided maximal sensitivity with minimal handling. Solid-phase extractions with different sorbents

were also used when dihydroresveratrol was detected in urine samples (*6*,*8*). However, these authors did not validate the methods, nor did they quantify dihydroresveratrol or its conjugates.

The average extraction recoveries were 96.7% in the six concentrations assayed in plasma. However, the LOD was 275 nM, which could be attributed to the poor UV absorbance of dihydroresveratrol. Indeed, the validation of the instrument for this compound gave an LOD of 50 nM and an LOQ of 170 nM (data not shown). The precision of the method was acceptable, as shown by the intraday and interday coefficients of variation which were below 15%, which is considered acceptable (*15*). Moreover, the HPLC method was reproducible and linear over a wide range of concentrations (5−100 μM). Consequently, the validation of the method showed good reproducibility, accuracy, precision, and recovery in the assays of dihydroresveratrol in rat plasma.

Once the method was validated, it was applied to the detection of dihydroresveratrol and its metabolites in rat plasma after the oral administration of 60 mg/kg. This compound was detected in plasma, along with its glucuronide and sulfate conjugates, which were identified by HPLC-MS. Dihydroresveratrol was extensively metabolized, and 30 min after its oral administration, the concentrations of its glucuronide and sulfate conjugates were 38- and 6-fold higher, respectively, than the parent compound. In a previous study by our group, the chemopreventive activity of *trans*-resveratrol in a rat model of colon cancer induced by 1,2-dimethylhydrazine was assessed. After the oral administration of 60 mg/kg of *trans*-resveratrol for 49 days, dihydroresveratrol was the most abundant compound in colon, followed by *trans*-resveratrol glucuronide and small amounts of *trans*-resveratrol and its sulfate conjugate (*21*). Consequently, dihydroresveratrol formed in the colon could be absorbed, thus reaching blood and urine as indicated previously (*6*, *8*).

Although the different *trans*-resveratrol conjugates have been comprehensively described (*16*), little is known about dihydroresveratrol. The hydrogenation of the aliphatic double bond of *trans*-resveratrol by the intestinal flora rendered a metabolite with different UV absorption properties from the parent compound. The poor sensitivity observed for dihydroresveratrol even when dissolved in water indicates that it might not be detected at low concentrations. In addition, the UV maximum changed from 306 nm for *trans*-resveratrol to 276 nm for dihydroresveratrol. Therefore, when monitoring samples for *trans*-resveratrol, unless the detectors were also set at 276 nm, dihydroresveratrol might have been unnoticed. Boocock et al. (2007) reported their inability to find dihydroresveratrol in their samples since neither their UV-HPLC conditions nor their LC-MS/MS system was optimized for its detection (*22*). Moreover, the different UV spectra obtained by diode-array detection could have constituted an additional drawback to the detection of this metabolite.

In conclusion, the HPLC method described herein possesses appropriate sensitivity, accuracy, and reproducibility for analysis of dihydroresveratrol in preclinical investigations. Furthermore, HPLC analysis enables the separation of dihydroresveratrol metabolites, and when coupled with tandem mass spectrometry, provides a useful tool for metabolism studies.

ABBREVIATIONS USED

LOD, limit of detection; LOQ, limit of quantification; SPE, solid-phase extraction; RSD, relative standard deviation.

LITERATURE CITED

(1) Fritzemeier, K. H.; Kindl, H. 9,10-Dihydrophenanthrenes as Phytoalexins of Orchidaceae. *Eur. J. Biochem.* **1983**, *133*, 545–550.

(2) El-Feraly, F. S. Isolation, characterization, and synthesis of 3,5,4′-trihydrozybibenzyl from *Cannabis sativa*. *J. Nat. Prod.* **1984**, *47*, 89–92.

(3) Adesanya, S. A.; Ogundana, S. K.; Roberts, M. F. Dihydrostilbene phytoalexins from *Dioscorea bulbifer*a and *D. Dumentorum*. *Phytochemistry* **1989**, *28*, 713–174.

(4) Kulesh, N. I.; Vasilevskaya, N. A.; Veselova, M. V.; Denisenko, V. A.; Fedoreev, S. A. Minor polyphenols from *Maackia amurensis* wood. *Chem. Nat. Compd.* **2008**, *44*, 712–714.

(5) Gorham, J.; Tori, M.; Asakawa, Y. The biochemistry of stilbenoids. In *The Biochemistry of Natural Products*; Harborne, J. B., Baxter, H., Eds; Chapman & Hall: London, 1995; Vol. 1, p 262.

(6) Walle, T.; Hsieh, F.; DeLegge, M. H.; Oatis, J. E., Jr; Walle, U. K. High absorption but very low bioavailability of oral resveratrol in humans. *Drug Metab. Dispos.* **2004**, *32*, 1377–1382.

(7) Pervaiz, S.; Holme, A. L. Resveratrol: its biologic targets and functional activity. *Antioxid. Redox Signaling* **2009**, *11*, 2851–2897.

(8) Wang, D.; Hang, T.; Wu, C.; Liu, W. Identification of the major metabolites of resveratrol in rat urine by HPLC-MS/MS. *J. Chromatogr., B: Anal. Technol. Biomed. Life Sci.* **2005**, *829*, 97–106.

(9) Jung, C. M.; Heinze, T. M.; Schnackenberg, L. K.; Mullis, L. B.; Elkins, S. A.; Elkins, C. A.; Steele, R. S.; Sutherland, J. B. Interaction of dietary resveratrol with animal-associated bacteria. *Chem. Biodiversity* **2009**, *6*, 1193–1201.

(10) Cardile, V.; Lombardo, L.; Spatafora, C.; Tringali, C. Chemoenzymatic synthesis and cell-growth inhibition activity of resveratrol analogues. *Bioorg. Chem.* **2005**, *33*, 22–33.

(11) Xie, C. F.; Yuanb, H. Q.; Qua, J. B.; Xinga, J.; Lü, B. B.; Wanga, X. N.; Jia, M.; Lou, H. X. Biocatalytic production of acyclic bis[bibenzyls] from dihydroresveratrol by crude *Momordica charantia* peroxidase. *Chem. Biodiversity* **2009**, *6*, 1193–1201.

(12) Orsini, F.; Verotta, L.; Lecchi, M.; Restano, R.; Curia, G.; Redaelli, E.; Wanke, E. Resveratrol derivatives and their role as potassium channels modulators. *J. Nat. Prod.* **2004**, *67*, 421–426.

(13) Stivala, L. A.; Savio, M.; Carafoli, F.; Perucca, P.; Bianchi, L.; Maga, G.; Forti, L.; Pagnoni, U. M.; Albini, A.; Prosperi, E.; Vannini, V. Specific structural determinants are responsible for the antioxidant activity and the cell cycle effects of resveratrol. *J. Biol. Chem.* **2001**, *276*, 22586–22594.

(14) *The United States Pharmacopoeia*, USP31-NF26, 2008; Vol. *1225*, pp 752−756.

(15) Bansal, S.; DeStefano, A. Key Elements of Bioanalytical Method Validation for Small Molecules. *AAPS J.* **2007**, *9*, 109–114.

(16) Cottart, C. H.; Nivet-Antoine, V.; Laguillier-Morizot, C.; Beaudeux, J. L. Resveratrol bioavailability and toxicity in humans. *Mol. Nutr. Food Res.* **2010**, *54*, 7–16.

(17) Juan, M. E.; González-Pons, E.; Planas, J. M. Multidrug resistance proteins restrain the intestinal absorption of *trans*-resveratrol. *J. Nutr.* **2010**, *140*, 489–495.

(18) Alfaras, I.; Pérez, M.; Juan, M. E.; Merino, G.; Prieto, J. G.; Planas, J. M.; Álvarez, A. I. Involvement of breast cancer resistance protein (BCRP1/ABCG2) on the bioavailability and tissue distribution of *trans*-resveratrol in knockout mice. *J. Agric. Food Chem.* **2010**, *58*, 4523–4528.

(19) Baur, J. A.; Sinclair, D. A. Therapeutic potential of resveratrol: the in vivo evidence. *Nature Rev. Drug Discovery* **2006**, *5*, 493–506.

(20) Flores-Sanchez, I. J.; Verpoorte, R. Secondary metabolism in *Cannabis*. *Phytochem. Rev.* **2008**, *7*, 615–639.

(21) Alfaras, I.; Juan, M. E.; Planas, J. M. *trans*-Resveratrol reduces precancerous colonic lesions in dimethylhydrazine treated rats *J. Agric. Food Chem.* **2010**, *58*, DOI 10.1021/jf100702x.

(22) Boocock, D. J.; Patel, K. R.; Faust, G. E.; Normolle, D. P.; Marczylo, T. H.; Crowell, J. A.; Brenner, D. E.; Booth, T. D.; Gescher, A.; Steward, W. P. Quantitation of *trans*-resveratrol and detection of its metabolites in human plasma and urine by high performance liquid chromatography. *J. Chromatogr., B: Anal. Technol. Biomed. Life Sci.* **2007**, *848*, 182–187.

Received for review March 1, 2010. Revised manuscript received May 13, 2010. Accepted May 23, 2010. Supported by grant AGL2005-05728 from the Ministerio de Ciencia y Tecnología and grant 2009-SGR-471 from the Generalitat de Catalunya, Spain. The group is member of the Network for Cooperative Research on Membrane Transport Proteins (REIT) (grant BFU2007-30688-E/BFI).

Resultats ~ Capítol 2

CAPÍTOL 2. ESTUDI DE L'EFECTE QUIMIOPROTECTOR DEL *trans*-RESVERATROL EN UN MODEL DE LESIONS PRENEOPLÀSTIQUES INDUÏDES PER 1,2-DIMETILHIDRAZINA EN CÒLON EN RATA

Aquest capítol es troba desglossat en dos apartats. El primer, redactat en català sota el format d'article, recull la posta a punt d'un model animal d'inducció de lesions preneoplàstiques per 1,2-dimetilhidrazina en rata. El segon apartat mostra els resultats de l'efecte protector del *trans*-resveratrol recollits en l'article 2.

Article 2:

trans-Resveratrol reduces precancerous colonic lesions in dimethylhydrazine-treated rats.
Alfaras, I., Juan, M.E., Planas, J.M.
J. Agric. Food Chem. 2010, 58, 8104-8110.

Els resultats obtinguts han donat lloc a les següents comunicacions a congressos:

- *Daily oral administration of trans-resveratrol reduces aberrant cript foci in 1,2-dimethylhydrazine treated rats*
  Alfaras, I., Juan, M.E., Planas, J.M.

  Presentada com a pòster en el congrés:

  XXIVth International Conference on Polyphenols
  Salamanaca, 8 – 11 de juliol de 2008

- *Determination of trans-resveratrol and its metabolites in colon content and their effects in a colon cancer model in rat*
  Alfaras, I., Juan, M.E., Lozano, G., Planas, J.M.

  Presentada com a pòster en el congrés:

  5th International Meeting, Advances in Antioxidants (Trace Elements, Vitamins and Polyphenols): Molecular mechanisms, nutritional and Clinical Aspects
  Monastir – Sousse, Tunísia, 11 - 15 d'octubre de 2008

2.1. Posta a punt d'un model de càncer de còlon en rata

2.1.1. Introducció

La carcinogènesi és un procés molt complex de caràcter maligne, en el qual intervenen successos a nivell cel·lular, molecular i morfològic. El procés es pot dividir en tres etapes: iniciació, promoció i progressió. La iniciació es produeix quan les cèl·lules normals s'exposen a agents carcinògens químics, vírics o físics a la natura, que donen com a resultat canvis a nivell genòmic que proporcionen a les cèl·lules capacitats per proliferar. La promoció és l'expansió clonal de les cèl·lules iniciades que normalment ve associada a alteracions morfològiques i fenotípiques. I, finalment, en la progressió intervenen canvis genotípics i fenotípics associats amb malignitat i metàstasi (Sugimura, 1992).

2.1.1.1. Inducció de càncer de còlon en rates

La majoria de carcinomes a còlon es desenvolupen a partir de focus de criptes aberrants (FCA). Ara bé, aquest desenvolupament pot seguir diferents vies donant lloc a tumors esporàdics, poliposi adenomatosa familiar (PAF) i càncer colorectal hereditari no polipós.

Atès que el desenvolupament espontani de càncer de còlon en rates té una freqüència molt baixa (Wells *et al.*, 1938), l'ús de carcinògens és necessari per a la seva inducció. Es creu que els tumors induïts químicament en rosegadors són els millors models que es tenen a l'abast per obtenir resultats traslladables a la clínica. El creixement tumoral en rosegadors comparteix moltes característiques histològiques i genètiques amb el dels humans. Per tant, aquests models reproduïbles permeten estudiar les influències que poden modificar l'inici i desenvolupament del càncer de còlon sota condicions estrictament controlades (Corpet i Pierre, 2005).

2.1.1.2. Dihidroclorur d'1,2-dimetilhidrazina (DMH)

Druckrey *et al.* (1967) van descriure que la DMH tenia la capacitat de produir càncer de còlon a diferents espècies de rosegadors. Aquesta especificitat depèn de la dosi administrada, la via d'administració i el moment d'observació. L'administració intraperitoneal del carcinogen provoca la formació de tumors al còlon, en canvi, l'administració oral o subcutània pot donar també tumors a altres òrgans. Actualment és el carcinogen intestinal més utilitzat, ja que indueix càncer de còlon en més del 80% de les rates administrades.

La DMH té activitat alquilant en l'ADN i també té propietats mutagèniques (Maskens, 1981). La lesió pre-mutagènica O^6-metilguanina, que indueix la transició GT → AT, ha estat detectada a l'ADN de teixits de rates exposades a aquest compost (Herron i Shank, 1982).

Aquesta hidrazina és un procarcinogen que requereix activació metabòlica a dins l'organisme per produir el carcinogen actiu. La DMH és metabolitzada pels hepatòcits però el còlon per si mateix també té la capacitat de metabolitzar aquest carcinogen fins a donar metabòlits també actius amb les mateixes propietats carcinògenes que la DMH (Glauert i Bennink, 1983). Aquests metabòlits actius són l'azoximetà (AOM) i el metilazoximetanol (MAM), aquest últim no és tan organoespecífic a còlon com la DMH o l'AOM (Figura III.1.). Després el MAM donarà un intermediari altament reactiu que es diu ió metildiazoni (MD). Aquest ió es descompondrà en nitrogen molecular i ió carboni, el qual és capaç de metilar l'ADN, l'ARN i les proteïnes.

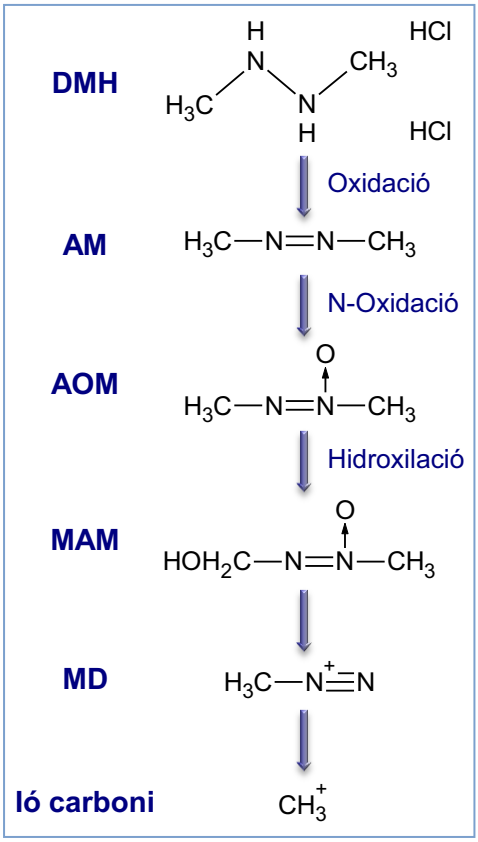

Figura III.1. Metabolisme de la 1,2-dimetilhidrazina (DMH). AM: azometà; AOM: azoximetà; MAM: metazoximetanol; MD: metildiazoni.

Els catabòlits de la DMH s'excreten principalment per pulmó i per via renal, també per via biliar en menys proporció. Els principals metabòlits en aire expirat són CO_2 i azometà (AM), i en orina trobem DMH inalterada, AM, AOM i MAM (Fiala, 1975).

2.1.1.3. Descripció de lesions preneoplàstiques induïdes per DMH

S'ha vist que la mutació del gen que codifica la proteïna APC (acrònim de l'anglès *adenomatous polyposis coli*) és característica de la PAF i també és present en la majoria dels càncers colorectals esporàdics (Kinzler i Vogelstein, 1996). La proteïna APC forma un complex amb l'axina i la quinasa glicogensintasa-3β permetent la fosforilació i posterior degradació d'una altra proteïna, la β-catenina (Xing *et al.*, 2003). Si es dóna la mutació al gen *Apc*, es produeix una acumulació al citosol de β-catenina no fosforilada que viatja al nucli i s'associa amb un factor de transcripció, el *Tcf4*, induint la proliferació cel·lular no controlada.

A les lesions preneoplàstiques induïdes per DMH, freqüentment hi ha mutacions *k-ras*, tal com succeeix en els tumors humans, però en pocs casos hi ha mutació del gen *Apc* i mai hi ha mutació al gen *p53* (Sohn *et al.*, 1999). Ara bé, tot i que el gen *Apc* quasi no es veu afectat, s'ha vist una acumulació de β-catenina al nucli a causa d'una mutació d'un altre

gen, el *Ctnnb1*, que provoca que la β-catenina no es degradi i indueixi una proliferació cel·lular descontrolada, així com succeeix en els tumors humans (Femia *et al.*, 2005).

- Focus de criptes aberrants (FCA)

Els FCA es consideren lesions preneoplàstiques, i consisteixen en el primer canvi morfològic identificable en la formació d'un càncer colorectal (Kinzler i Vogelstein, 1996). La displàsia que exhibeixen alguns FCA és una característica de cèl·lules precanceroses a diversos òrgans, i mostren característiques atípiques tant proliferatives com genotípiques que també es veuen en càncer de còlon. Per tant, els FCA es poden correlacionar amb el risc de patir càncer de còlon així com amb el nombre i la mida dels adenomes en humans.

Els FCA van ser identificats per primer cop en còlon de rosegadors tractats amb carcinogen mitjançant un mètode senzill, l'observació a microscopi de la superfície de la mucosa tenyida amb blau de metilè (Bird, 1987). Els FCA apareixen ràpidament després de l'exposició al carcinogen i es mantenen al còlon temps després. Però la majoria d'aquests FCA romanen a la mucosa durant llargs períodes sense que es produeixi cap canvi morfològic. Són lesions hiperplàstiques que no tenen potencial per tornar-se malignes. Per altre banda, hi ha un petit grup dels FCA denominats per alguns investigadors com a displàsics (Takahashi *et al.*, 2000) que tenen potencial neoplàstic tant en rosegadors com en humans.

L'examen de la superfície de la mucosa permet la quantificació del nombre, la distribució al llarg de l'intestí gros i la determinació de la multiplicitat dels FCA. El número de FCA es considera predictiu en rosegadors i el seu creixement pot ser modificat per moduladors del càncer de còlon (Wargovich *et al.*, 2000).

- Focus amb depleció de mucines (FDM)

Els FDM són FCA que es caracteritzen per l'absència total o gairebé total de producció de mucines. Aquestes lesions es poden visualitzar a la superfície de la mucosa mitjançant la tinció anomenada ferro diamina-blau alcià (HID-AB, acrònim anglès de *high-iron diamine alcian blue*) que permet diferenciar les criptes aberrants que presenten mucina de les que no en secreten o FDM (Caderni *et al.* 2003).

Histològicament, els FDM són lesions més displàstiques que els FCA comuns, els quals no tenen una disminució en la producció de mucines. Consegüentment, el nombre d'FDM és menor al d'FCA en rates exposades a la mateixa dosi de carcinogen (Caderni *et al.* 2003). S'han realitzat diversos estudis d'aquestes lesions i s'ha vist que la proporció d'FDM respecte al número total d'FCA augmenta en presència de promotors de la carcinogènesi del còlon com l'àcid còlic, la vedella i la botifarra de sang (Femia *et al.*,

2004; Pierre *et al.*, 2004) i disminueix amb agents quimiopreventius com el piroxicam o els simbiòtics (Caderni *et al.*, 2003; Femia *et al.*, 2004).

El nombre d'FDM, així com el d'FCA, és dependent de la dosi de DMH administrada a les rates (Femia *et al.*, 2005). Per tant, alguns grups d'investigació han utilitzat no només el recompte d'FCA, sinó també el recompte d'FDM en la mucosa colònica com a un criteri més específic per a l'estudi de predicció de càncer de còlon en rates mitjançant la inducció amb carcinògens.

2.1.2. Material i mètodes

2.1.2.1. Reactius i substàncies utilitzades

La DMH (ref. 40690), la formalina neutra tamponada al 10% (HT501128) i els colorants necessaris per a les tincions es van obtenir de Sigma-Aldrich (St. Louis, EE.UU). L'àcid acètic va ser de Sharlau Chemie S.A. (Barcelona, Espanya). L'hidròxid sòdic és va adquirir a Merck (Darmstadt, Alemanya) i l'àcid etilendiamintetraacètic (EDTA) a Farmitalia Carlo Erba (Milà, Itàlia). L'aigua utilitzada a tots els experiments es va passar a través d'un sistema de purificació Milli-Q (18 mΩ, Millipore, Milà, Itàlia).

2.1.2.2. Animals d'experimentació

Es van utilitzat 16 rates mascle Sprague-Dawley que van estar alimentades amb pinso estàndard de manteniment (2014 Teklad Global 14% Protein Rodent Maintenance Diet, Harlan, Espanya) i aigua *ad libitum*. Els animals es mantingueren en condicions de temperatura (22 ± 3ºC) i humitat (50 ± 10%) controlades i amb cicles de llum-foscor de 12 hores a l'estabulari de la Facultat de Farmàcia de la Universitat de Barcelona.

2.1.2.3. Tractament

La inducció del càncer de còlon es realitzà amb l'administració per via intraperitoneal de DMH a la dosi de 20 mg DMH/kg un cop per setmana. La solució es va preparar immediatament abans de ser administrada a sota la campana de gasos i complertes mesures de seguretat, a partir d'una solució d'EDTA 1 mM a pH 6.5. A les rates control se'ls administrà el mateix nombre d'injeccions que a les tractades amb DMH però es va utilitzar solament la solució d'EDTA, sense el carcinogen. El volum a injectar va ser 1 mL/kg i s'ajusta per cada animal a partir del pes corporal en el moment de l'administració.

Per tal de posar a punt el model animal, s'establiren els següents grups experimentals:

- Control. Els animals reberen per injecció intraperitoneal el solvent. El sacrifici es realitzà a les setmanes 2, 3 i 4 respectivament, a partir de la primera administració (n = 4).

- Grup 1: 2 DMH + 1 set. S'administraren dues dosis de 20 mg/kg de DMH, una per setmana, i una setmana després (la setmana 2) es van sacrificar les rates (n = 4).
- Grup 2: 3 DMH + 1 set. S'administraren tres dosis de 20 mg/kg de DMH, una cada setmana, i s'esperà una setmana (setmana 3) abans del sacrifici (n = 4).
- Grup 3: 3 DMH + 2 set. També s'administraren dosis de 20 mg/kg de DMH setmanals, durant 3 setmanes. Però després van passar dues setmanes sense rebre cap administració abans del sacrifici (n = 4).

Durant tot el procés es va controlar el pes corporal així com el consum d'aigua i pinso. La manipulació dels animals al llarg de tot el tractament, així com el seu sacrifici, es duren a terme segons els procediments autoritzats pel Comitè Ètic d'Experimentació Animal de la Universitat de Barcelona i seguint les recomanacions de la Federation of European Laboratory Animal Science Associations (1995).

2.1.2.4. Obtenció de mostres

Els experiments es van realitzar sempre a primera hora del matí sense sotmetre els animals a dejuni previ. Primer de tot s'anestesiaren les rates amb xilacina (Rompun® Bayer Leverkusen, Alemanya) i ketamina (Imalgene® 500 Rhône Mérieux, Lyon, França), a una dosi de 0,1% i 0,01% volum/pes corporal. Un cop anestesiades, es realitzà una laparotomia i es va extreure el còlon. L'extracció es realitzà des del cec fins al recte. El còlon es va dividir en tres parts d'aproximadament la mateixa longitud, corresponents al segments proximal (més proper al cec), medial (la part central del còlon) i distal (més proper al recte). Les tres parts obtingudes del còlon es netejaren per dintre amb tampó fosfat salí (PBS) amb ajuda d'una xeringa de 10 mL. Seguidament, s'assecaren lleugerament amb paper de filtre i es mesurà el pes humit.

Els segments es col·locaren sobre una placa de poliestirè i se'ls va fer un tall longitudinal seguint el mesenteri per fixar-los oberts. Un cop oberts s'estiraren procurant que l'amplada fos constant al llarg de cada tros d'intestí. De cada segment es mesurà la longitud de l'intestí i l'amplada; a partir d'aquestes dades es va calcular l'àrea de cada segment. Seguidament es subjectaren els extrems del teixit amb agulles 25G a la placa de poliestirè. Les diferents parts del còlon es col·locaren en un recipient rectangular i es va afegir un volum de formalina tamponada suficient com per cobrir completament les mostres. Es tancaren hermèticament i es mantingueren a 4ºC durant un mínim de 24 hores.

2.1.2.5. Recompte de focus de criptes aberrants

La tinció amb blau de metilè al 0,2% s'utilitzà per observar les criptes aberrants. La solució del colorant es va preparar dissolent en calent el blau de metilè en PBS. El còlon es va submergir en un bany de blau de metilè que es filtrà just abans de la seva utilització. Els temps de tinció foren diferents en funció del segment, així doncs el segment proximal es va tenyir durant 8 minuts i el medial i el distal 10 minuts.

Acte seguit, es va preparar la mostra per a l'observació en microscopi òptic. El tros d'intestí tenyit es col·locà amb cura en un portaobjectes, seguidament s'afegiren unes gotes de PBS per a una millor observació i per evitar l'assecament de l'intestí durant el procés. Les mostres s'observaren a 10 augments i en casos concrets a 20 augments per a una millor visió puntual d'alguna cripta aberrant.

El criteri seguit per al recompte va ser aquell descrit per Bird (1987) en el qual es va establir que les criptes aberrants presenten una mida de 2 a 3 vegades superiors a les normals, són més elevades que les criptes normals, presenten una obertura allargada i queden més tenyides amb blau de metilè que les criptes normals. Es va fer el recompte d'FCA així com del nombre de criptes aberrants (CA) present a cada focus.

2.1.2.6. Recompte de focus amb depleció de mucines

Un cop mesurats els FCA, els còlons es van mantenir en formalina tamponada neutra al 10% a 4ºC, fins al seu ús amb la tinció HID-AB que permet la visualització de la producció de mucines, seguint un protocol descrit anteriorment (Caderni *et al.*, 2003).

El teixit a tenyir va passar per diferents solucions realitzant la tinció en dos fases. A la primera fase, el teixit prèviament rentat amb PBS es deixà submergit en la solució ferro diamina entre 18 i 24 hores a temperatura ambient i a les fosques. Per a la preparació d'aquest colorant es va fer primer una solució de clorur de ferro al 60%. Després, per a la solució ferro diamina, es va dissoldre 120 mg de N,N-dimetil-*p*-fenilendiamina i 20 mg de N,N-dimetil-*m*-fenilendiamina en 50 mL d'aigua mQ, i a aquesta solució es va afegir 1,4 mL de la solució de clorur de ferro al 60% prèviament preparada. Tots aquests reactius es protegiren de la llum.

En una segona fase, passades entre 18 i 24 hores, el teixit es rentà un altre cop amb PBS i es va procedir a la tinció amb els colorants blau alcià i vermell neutre. El blau alcià es preparà a l'1% en una solució aquosa d'àcid acètic al 3%. Un cop dissolt, s'ajustà el pH a 2,5 i es va filtrar. Després s'afegiren uns cristalls de timol com a conservant. La solució de vermell neutre es va preparar mitjançant la dissolució d'1 g de vermell neutre i 2 mL d'una solució aquosa d'àcid acètic a l'1% en 1000 mL d'aigua mQ. Un cop dissolt es va filtrar la solució. El teixit rentat es tenyí durant uns 5 minuts aproximadament en la solució de blau

alcià. Després es va rentar amb PBS i es deixà uns 2 minuts més en la solució de vermell neutre. Finalment, es va tornar a rentar amb PBS.

Un cop el còlon va estar tenyit es situà en un portaobjectes, s'afegiren unes gotes de PBS per a millorar l'observació al microscopi i es va fer el recompte dels FDM. La classificació dels FDM es realitza de la mateixa manera que es van classificar els FCA tenyits amb blau de metilè. Aquesta tinció permet veure la producció de sulfomucines i mucines carboxilades ja que queden tenyides de color blau fosc, per tant, aquelles CA que no es van tenyir mitjançant la tinció HID-AB es consideraren CA amb depleció de mucines. L'observació al microscopi es realitzà a 10 augments, podent utilitzar augments superiors en cas de dubte. El criteri seguit per al recompte va ser igual a l'anterior sols que en els FDM hi va haver una depleció o quasi depleció de mucines tenyides.

2.1.2.7. Tractament de les dades

Els resultats s'han expressat com a mitjana ± error estàndard. L'anàlisi estadística es va dur a terme amb el programa GraphPad Prism 3.02. Les diferències entre grups es van avaluar mitjançant el test de la *t* de Student. Els valors de $P < 0,05$ es van considerar com a diferències estadísticament significatives. Les imatges de la superfície de la mucosa es van obtenir amb el programa informàtic de captació d'imatges KAPPA Image Base - Control 2.6 (KAPPA optp-electronics GmbH, Gleichen, Alemanya).

2.1.3. Resultats

2.1.3.1. Evolució del pes corporal

Per tal de comprovar que el tractament amb DMH no afectava a l'evolució del pes corporal de les rates durant l'experiment, es va fer un seguiment periòdic del pes. En la Figura III.2. es pot veure que entre l'evolució del pes corporal de les rates tractades i el de les rates control no hi ha diferències.

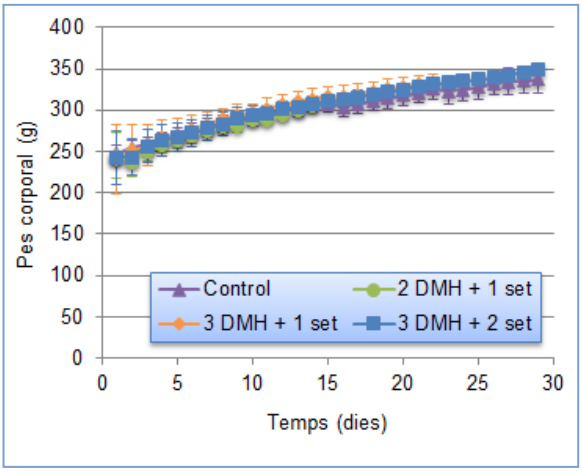

Figura III.2. Evolució del pes corporal. Els resultats s'expressen com a mitjana ± error estàndard. No s'observen diferències estadístiques. DMH: 1,2-dimetilhidrazina.

Les rates del grup 1 han evolucionat de 244 ± 27,2 g fins a 312 ± 3,5 g. L'increment de les rates del grup 2 és de 240 ± 42,5 g fins a 352 ± 5,50 g. El de les del grup 3 és de 243 ± 32,5 fins a 349 ± 2,73 g. L'evolució de les rates control és de 248 ± 9,70 g a l'inici de l'experiment, 309 ± 10,3 g a la segona setmana, 326 ± 12,1 a la tercera setmana i 338 ± 17,2 g a l'últim dia. Aquesta evolució és constant al llarg del temps tal i com

s'observa a la Figura III.2. L'anàlisi estadística mostra que no hi ha diferències significatives entre els grups.

2.1.3.2. Consum de pinso i aigua

També s'ha fet un seguiment periòdic del consum de pinso i d'aigua, per veure si el tractament modifica el consum de les rates tractades amb el carcinogen.

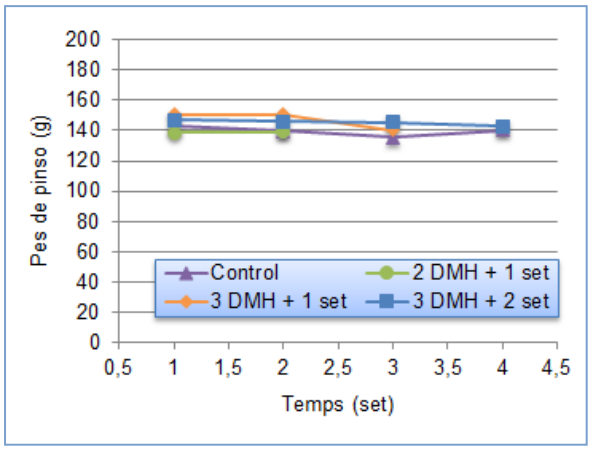

Figura III.3. Consum de pinso setmanal. Els resultats s'expressen com a mitjana ± error estàndard. No s'observen diferències estadístiques. DMH: 1,2-dimetilhidrazina.

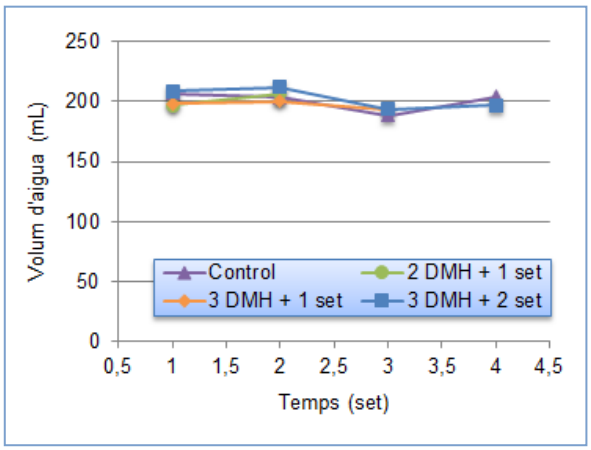

Figura III.4. Consum d'aigua setmanal. Els resultats s'expressen com a mitjana ± error estàndard. No s'observen diferències estadístiques. DMH: 1,2-dimetilhidrazina.

El consum de pinso setmanal es manté constant durant tot l'experiment i tal i com mostra la Figura III.3. El consum mitjà setmanal de pinso de les rates control és de 140 ± 1,46 g. El consum de les rates del grup 1, 2 i 3 és de 139 ± 0,39 g, 147 ± 3,45 g i 145 ± 0,98 g respectivament. Aquests resultats no donen diferències significatives al realitzar l'anàlisi estadística excepte entre els grups 1 i 3 ($P < 0,01$).

El consum setmanal d'aigua es pot veure a la Figura III.4. El consum d'aigua mitjà setmanal del grup control és de 200 ± 4,23 mL. Els dels grups 1, 2, i 3 són de 202 ± 4,99 mL, 197 ± 2,00 mL i 203 ± 4,38 mL, respectivament. No hi ha diferències significatives en el consum d'aigua entre els diferents grups.

2.1.3.3. Dades morfomètriques

Un cop extret el segment del còlon s'ha mesurat el pes humit, la longitud i l'amplada. A partir de la longitud i l'amplada es calcula l'àrea de cada segment i l'àrea total. Tal i com s'observa a la Taula III.1., l'àrea del còlon dels diferents grups no mostren diferències significatives amb la del grup control. Quan l'àrea s'ha normalitzat pel pes tampoc s'han evidenciat diferències entre els diferents grups.

Grup	Segment	Pes humit (g)	Àrea (cm^2)	Àrea / pes còlon (cm^2/g)	Àrea còlon (cm^2)	Àrea / pes còlon (cm^2/g)
Control	Proximal	0,68 ± 0,09	8,11 ± 0,37	13,4 ± 2,03	20,3 ± 2,86	14,2 ± 2,10
	Medial	0,40 ± 0,05	6,25 ± 1,21	15,1 ± 1,42		
	Distal	0,34 ± 0,04	5,91 ± 1,92	16,6 ± 3,89		
Grup 1	Proximal	0,61 ± 0,06	8,90 ± 1,17	14,5 ± 0,816	26,0 ± 1,64	14,1 ± 0,870
	Medial	0,56 ± 0,02	8,44 ± 0,39$^{\theta}$	15,2 ± 0,216		
	Distal	0,44 ± 0,01	8,59 ± 0,61	19,3 ± 1,14		
Grup 2	Proximal	0,60 ± 0,02	9,34 ± 0,73	15,5 ± 0,922	27,8 ± 2,21	16,0 ± 0,594
	Medial	0,54 ± 0,02	7,56 ± 0,78	13,9 ± 0,803		
	Distal	0,58 ± 0,05	10,9 ± 1,12$^{\theta}$	18,6 ± 1,04		
Grup 3	Proximal	0,56 ± 0,05	8,80 ± 0,30	15,6 ± 1,09	25,5 ± 1,56	18,1 ± 1,38
	Medial	0,46 ± 0,03	7,53 ± 0,23$^{\varphi}$	16,6 ± 0,776		
	Distal	0,39 ± 0,02	9,13 ± 1,30$^{\Psi}$	23,2 ± 2,48		

Taula III.1. Mesures morfomètriques dels segments de còlon i àrea total del còlon. Els resultats s'expressen com a mitjana ± error estàndard. $P < 0,05$, $^{\theta}$ *vs.* Control; $^{\varphi}$ *vs.* Grup 1; $^{\Psi}$ *vs.* Grup 2.

2.1.3.4. Recompte de focus de criptes aberrants

El recompte s'ha portat a terme per a cada segment de còlon. Els FCA observats es classifiquen segons el número de CA que els formen: 1, 2, 3, 4, 5, 6 i més de 6 CA. El recompte total d'FCA al còlon s'ha realitzat amb l'objectiu de comprovar la relació directa entre el número de dosis de DMH administrades intraperitonealment a les rates amb l'aparició de les lesions preneoplàstiques. Com es pot veure a la Figura III.5. a més dosis, més número d'FCA són observats. El número total d'FCA del grup 1 és de 59,7 ± 18,7. I el dels grups 2 i 3 és de 227 ± 24,0 i 224 ± 38,3 respectivament. En el grup control no s'han trobat FCA.

Per tal de veure quina part del còlon presenta més FCA, també s'ha tingut en compte el número d'FCA que hi ha a cada segment. S'ha comprovat que l'aparició dels FCA augmenta a mesura que ens apropem més al recte. Per tant, a la part distal del còlon és on trobem més FCA i a la part proximal del còlon gairebé no apareixen CA com mostra la gràfica de la Figura III.6.

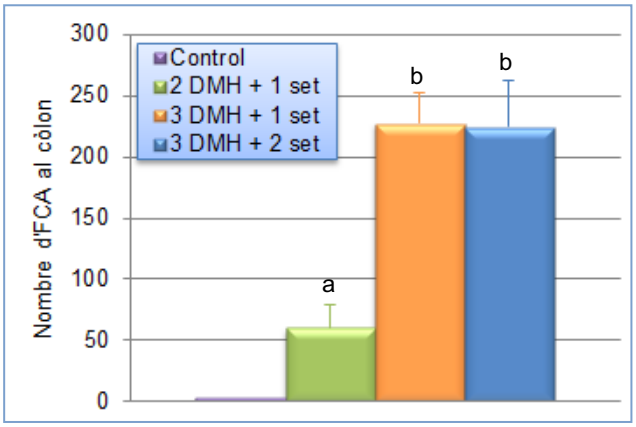

Figura III.5. Recompte total de focus de criptes aberrants (FCA) a còlon sencer. El resultat s'expressa com a mitjana ± error estàndard. Les mitjanes amb lletres distintes presenten diferències estadísticament significatives ($P < 0,05$). DMH: 1,2-dimetilhidrazina.

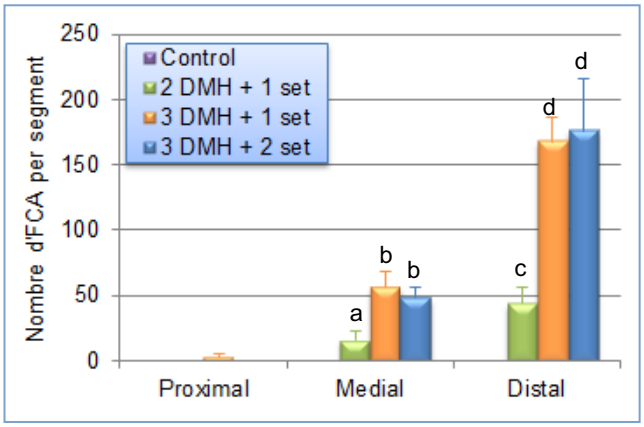

Figura III.6. Recompte de focus de criptes aberrants (FCA) a cada segment de còlon. El resultat s'expressa com a mitjana ± error estàndard. Les mitjanes amb lletres distintes presenten diferències estadísticament significatives entre grups. Diferències entres els segments de cada grup: proximal < medial < distal ($P < 0,05$). DMH: 1,2-dimetilhidrazina.

El grup control no presenta FCA en cap segment. Al segment proximal, només el grup 2 presenta FCA, trobant-ne 3,33 ± 2,33. Al segment medial, el recompte del grup 1 és de 15,7 ± 6,49 FCA, el del grup 2 és de 56,7 ± 11,6 FCA i el del grup 3 és de 48,3 ± 7,80 FCA. I, finalment, al segment distal del còlon, el nombre d'FCA comptats pel grup 1 és de 44,0 ± 12,5, pel grup 2 és de 168 ± 18,8 i pel grup 3 és de 176 ± 39,3.

També s'ha calculat la multiplicitat dels FCA que és la mitjana de CA que hi ha a cada FCA. La multiplicitat augmenta quan s'administren més dosis de carcinogen i a mesura que passa més temps després de l'última injecció intraperitoneal. És a dir, que les rates tractades amb 3 dosis de DMH tenen una major multiplicitat dels FCA; i d'aquestes, les que han viscut una setmana més encara incrementa més. Els resultats que es mostren a la Figura III.7. són referits a multiplicitat a tot el còlon. La multiplicitat del grup 1 és d'1,04 ± 0,02 CA/FCA, la del grup 2 és d'1,26 ± 0,04 CA/FCA i la del grup 3 és d'1,55 ± 0,08 CA/FCA. Atès que en el grup control no s'han trobat FCA, la multiplicitat és 0.

A la Figura III.8. es representa la multiplicitat a cada segment del còlon. El grup control no presenta multiplicitat ja que no té cap FCA. Al segment proximal el grup 2 té una multiplicitat d'1,00 ± 0,00 CA/FCA. Al segment medial, el grup 1 presenta una multiplicitat d'1,05 ± 0,04 CA/FCA, la del grup 2 és d'1,19 ± 0,09 CA/FCA i la del grup 3 és d'1,40 ± 0,28 CA/FCA. En el segment distal, la multiplicitat del grup 1 és d'1,04 ± 0,04 CA/FCA, la del grup 2 és d'1,30 ± 0,12 CA/FCA i la del grup 3 és d'1,58 ± 0,10 CA/FCA.

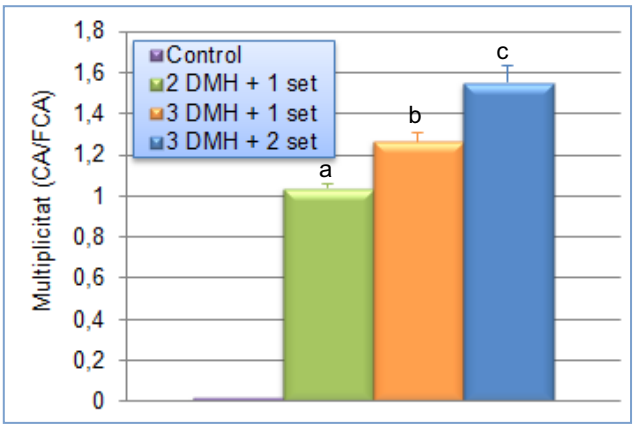

Figura III.7. Multiplicitat, representada com a criptes aberrants per cada focus (CA/FCA), a còlon sencer. Els resultats s'expressen com a mitjana ± error estàndard. Les mitjanes amb lletres distintes mostren diferències estadísticament significatives (P < 0,05). DMH: 1,2-dimetilhidrazina.

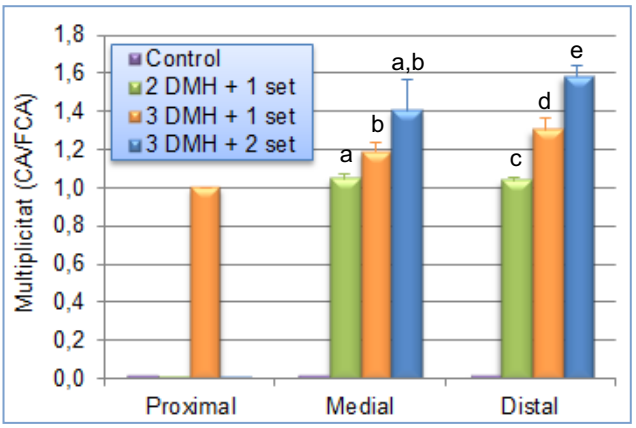

Figura III.8. Multiplicitat, representada com a criptes aberrants per cada focus (CA/FCA), a cada segment del còlon. Els resultats estan expressats com a mitjana ± error estàndard. Les mitjanes amb lletres distintes presenten diferències estadísticament significatives entre grups. Diferències entres els segments de cada grup: proximal < medial = distal (P < 0,05). DMH: 1,2-dimetilhidrazina.

2.1.3.5. Recompte de focus amb depleció de mucines

Després de la tinció HID-AB s'ha fet el recompte de CA però amb depleció de mucines. En cap cas, s'han trobat FDM al còlon de les rates control. El recompte total d'FDM, tal i com es pot observar a la Figura III.9., pel grup 1 és d'1,50 ± 0,50, pel grup 2 és de 7,00 ± 1,53 i pel grup 3 és de 8,33 ± 0,88. No s'han trobat FDM al grup control.

També s'ha trobat diferències quan el recompte es fa per segments, tal i com es pot veure a la Figura III.10. Les diferències entre segments no es veuen tan marcades com amb el recompte d'FCA. El grup control no presenta FDM en cap segment. En els grups tractats no es troben FDM al segment proximal a diferència del medial i distal. Al segment medial, el grup 1 no té FDM, el recompte del grup 2 és de 3,33 ± 0,67 FDM i el del grup 3

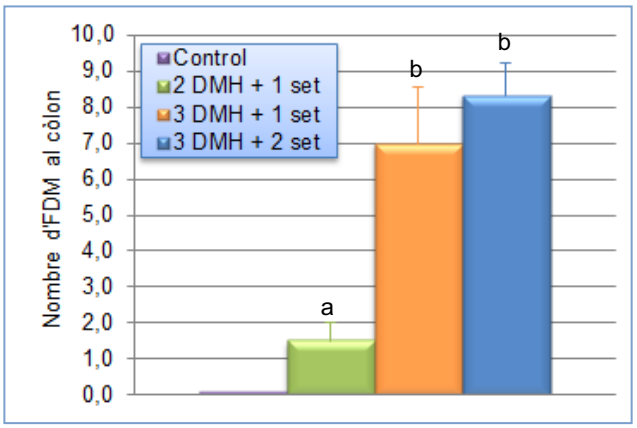

Figura III.9. Recompte total de focus amb depleció de mucines (FDM) a còlon sencer. El resultat s'expressa com a mitjana ± error estàndard. Les mitjanes amb lletres distintes presenten diferències estadísticament significatives (P < 0,05). DMH: 1,2-dimetilhidrazina.

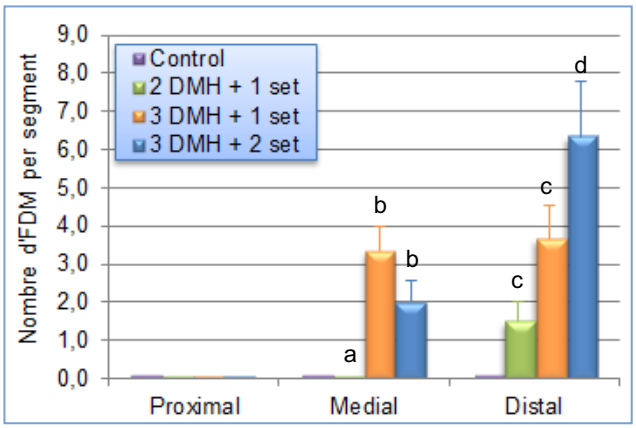

Figura III.10. Recompte focus amb depleció de mucines (FDM) a cada segment de còlon. El resultat s'expressa com a mitjana ± error estàndard. Les mitjanes amb lletres distintes presenten diferències estadísticament significatives entre grups. Diferències entre els segments, Grup 1: proximal = medial < distal; Grup 2: proximal < medial = distal; Grup 3: proximal < medial < distal (P < 0,05). DMH: 1,2-dimetilhidrazina.

és de 2,00 ± 0,58 FDM. Finalment, al segment distal del còlon, el nombre d'FDM és pel grup 1 d'1,50 ± 0,50, pel grup 2 és de 3,67 ± 0,88 i pel grup 3 és de 6,33 ± 1,45.

També s'ha tingut en compte el percentatge d'FDM que hi ha del total de FCA comptades en el còlon sencer. A la Figura III.11. es poden veure els resultats. El percentatge d'FCA que son FDM és de 2,21 ± 0,23 % al grup 1, de 3,06 ± 0,62 % al grup 2 i de 3,79 ± 0,28 % al grup 3.

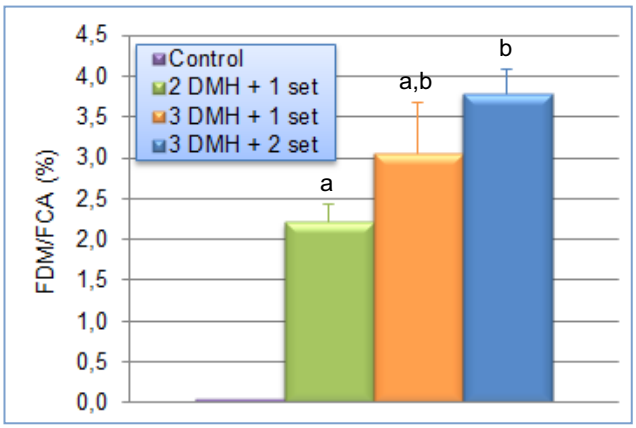

Figura III.11. Percentatge de focus amb depleció de mucines (FDM) respecte el total de focus de criptes aberrants (FCA) a còlon sencer. Els resultats s'expressen com a mitjana ± error estàndard. Les mitjanes amb lletres distintes mostren diferències estadísticament significatives (P < 0,05). DMH: 1,2-dimetilhidrazina.

Així com amb els FCA, també s'ha tingut en compte el nombre de CA que hi ha per cada FDM. A la Figura III.12. s'observen els resultats obtinguts a còlon sencer. La multiplicitat al grup 1 és d'1,00 ± 0,00 CA/FDM, al grup 2 és d'1,52 ± 0,19 CA/FDM i al grup 3 hi ha una multiplicitat d'1,94 ± 0,13 CA/FDM.

A la Figura III.13. es pot observar la multiplicitat a cada segment del còlon. Al segment proximal cap grup presenta FDM, per tant, no s'ha determinat la multiplicitat. Al segment medial, només els grups 2 i 3 presenten FDM i, per tant, la multiplicitat és d'1,17 ± 0,29 CA/FDM i d'1,78 ± 0,38 CA/FDM, respectivament. Al segment distal del còlon, el grup 1 presenta una multiplicitat d'1,00 ± 0,00 CA/FDM, el grup 2 té una multiplicitat d'1,85 ± 0,38 i el grup 3 una multiplicitat de 2,05 ± 0,33 CA/FDM.

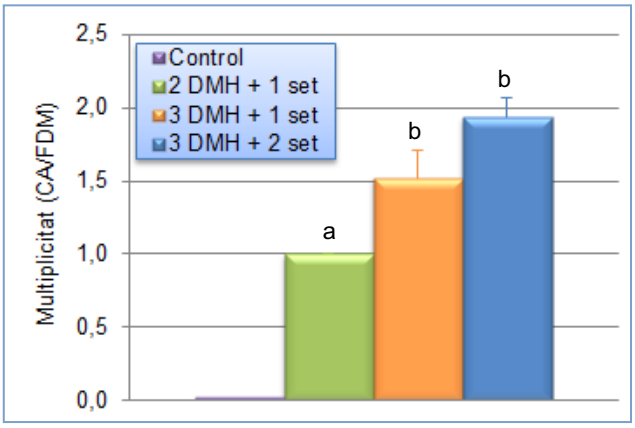

Figura III.12. Multiplicitat, representada com a criptes aberrants per cada focus (CA/FDM), a còlon sencer. Els resultats s'expressen com a mitjana ± error estàndard. Les mitjanes amb lletres distintes mostren diferències estadísticament significatives (P < 0,05). DMH: 1,2-dimetilhidrazina.

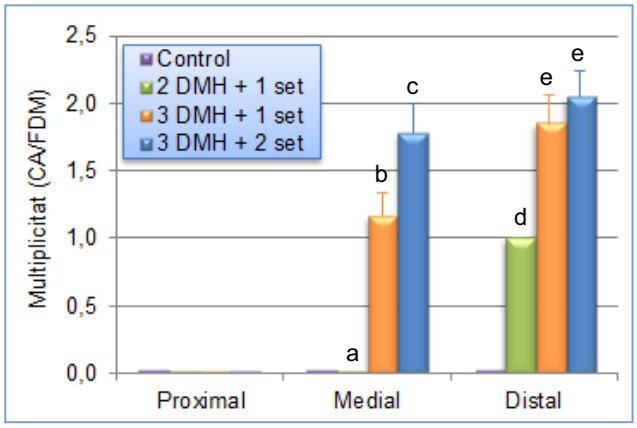

Figura III.13. Multiplicitat, representada com a criptes aberrants per cada focus (CA/FDM), a cada segment del còlon. Els resultats estan expressats com a mitjana ± error estàndard. Les mitjanes amb lletres distintes presenten diferències estadísticament significatives entre grups. Diferències entre els segments, Grup 1: proximal = medial < distal; Grup 2: proximal < medial < distal; Grup 3: proximal < medial = distal (P < 0,05). DMH: 1,2-dimetilhidrazina

2.1.4. Discussió

El càncer de còlon progressa en etapes, freqüentment caracteritzades per lesions intermèdies, amb mutacions i delecions en gens reguladors claus, que poden acabar evolucionant fins a un tumor. En el procés de la carcinogènesi s'ha identificat una sèrie de lesions preneoplàstiques que poden ajudar a la detecció dels carcinomes en estadis inicials. Si aquest procés de formació de carcinomes s'aplica a rosegadors, s'obté un model en animals d'experimentació que permet la possibilitat d'entendre millor la carcinogènesi. Així mateix possibilita l'ús d'aquest model en l'estudi de diferents compostos amb potencial anticancerigen (Wargovich *et al.*, 2000; Suh *et al.*, 2007) així com l'estudi de l'efecte que poden tenir diferents dietes en l'evolució del càncer (Verghese *et al.*, 2002; Raju i Bird, 2003).

S'han identificat diferents tipus de lesions preneoplàstiques en rosegadors. En primer terme, es van identificar els FCA (Bird, 1987). Aquestes lesions també es van trobar en humans (Pretlow *et al.*, 1991) i s'utilitzen per al cribratge de substàncies quimiopreventives però també per a l'avaluació del risc ambiental de diferents compostos. També es van identificar els FDM (Caderni *et al.*, 2003) que tenen un paper important en el desenvolupament de tumors. Aquests dos tipus de lesions preneoplàstiques es poden visualitzar a la superfície de la mucosa mitjançant diferents tincions. Per tant, la seva observació pot permetre la valoració del poder quimiopreventiu de diferents molècules d'una manera senzilla.

Les rates desenvolupen lesions preneoplàstiques en el còlon de rata en molt baixa freqüència de manera espontània (Wells *et al.*, 1938). En canvi, hi ha molts compostos que poden induir càncer de còlon en rosegadors, com per exemple la 2-amino-1-metil-6-fenilimidazo[4,5-b]piridina (Nakagama *et al.*, 2005) o la DMH. D'aquests els més emprats són la DMH o el seu metabòlit, l'AOM. En l'estudi que es presenta es va utilitzar la DMH per a la inducció de lesions preneoplàstiques a una dosi de 20 mg/kg de pes corporal de rata. Les rates es dividiren en 4 grups, un grup control que va rebre injeccions d'EDTA a pH 6,5, que era el solvent de la hidrazina, i tres grups que variaren de dosi total rebuda de carcinogen. El grup 1 va rebre dues injeccions i el grup 2 i 3 en van rebre tres. Tot i que aquests dos últims grups reberen les mateixes administracions, el temps d'espera després de l'última injecció va ser diferent, d'una i dues setmanes, respectivament.

Per tal d'establir quin número de dosis de carcinogen era el més adient per a l'estudi de l'eficàcia com a preventiu de càncer de còlon d'un compost, es va analitzar el número de criptes aberrants. En el present estudi s'observà com tres dosis de DMH provocà l'aparició de més del triple d'FCA que quan s'administraren dues dosis. Però, tot i que el

nombre total d'FCA depèn de la dosi, el seu recompte a mateixes dosis i mateix temps d'espera varia en funció dels investigadors. Quan s'administraren dues injeccions de 16 mg/kg d'AOM i s'esperaren 8 setmanes després de l'ultima injecció, el número de criptes aberrants va variar entre 150 i 300 FCA al còlon (Verghese *et al.*, 2002; Suh *et al.*, 2007). Per tant, el nombre d'FCA obtinguts en el present estudi va ser l'esperable i l'administració de tres dosis de 20 mg/kg es va considerar idònia per a l'estudi de l'efecte quimiopreventiu de diferents compostos. D'altra banda, Jackson i col·laboradors (1999) van observar que hi havia una relació directa entre el número de dosis de carcinogen administrat i el nombre de tumors que es produïen al còlon. Per tant, el fet que augmentant la dosi incrementés el nombre d'FCA i també el nombre de tumors, concordà amb l'afirmació que els FCA són lesions preneoplàstiques (Kinzler i Vogelstein, 1996).

En el present estudi, però, aquesta aparició de criptes aberrants no va ser proporcional a tot el còlon. Es va veure com apareixien més FCA a la part més distal del còlon que a la medial, sent molt baixa o nul·la la presència d'FCA a la part proximal. Aquesta regionalització ja s'havia observat amb anterioritat en altres estudis en rates tractades amb AOM (Williams *et al.*, 2007). Però també s'havia vist com aquesta distribució al llarg del còlon variava en funció del temps que s'esperava després de l'última injecció de carcinogen rebut (Bird, 1995). S'observà que si el temps d'espera era de 28 setmanes, al segment proximal era on apareixien més criptes aberrants. I si el temps d'espera s'escurçava fins a les 6 setmanes, el segment distal era el que mostrava major número d'FCA (Bird, 1995).

McLellan *et al.* (1991) van realitzar un estudi que mostrava com el temps afectava al número de CA per cada focus, és a dir, la multiplicitat. Aquesta multiplicitat augmentava quan més temps passava des de l'última injecció de carcinogen. Aquests resultats concorden amb els obtinguts en aquest estudi. El grup 3, a diferència del grup 2, es va mantenir una setmana més i, en conseqüència, la seva multiplicitat va ser major. També es va tenir en compte com aquesta variació de multiplicitat al llarg del temps es podria veure modificada amb la manipulació de la dieta en rosegadors (Hambly *et al.*, 1997). Per tant, és interessant saber que la multiplicitat pot ser un factor important a determinar en estudis de quimioprevenció perquè permetria valorar si un compost o una determinada dieta pot retardar, aturar o, fins i tot, impedir l'evolució de les CA.

L'augment de la multiplicitat observat en aquest estudi també es va veure quan es determinà la multiplicitat per a cada segment del còlon. La multiplicitat del grup que es va mantenir més temps després de l'última dosi de carcinogen, grup 3, tant a còlon medial com a còlon distal va ser superior a la multiplicitat obtinguda al grup que va rebre només

dues dosis, el grup 1. I la del grup 2 només va ser significativament diferent del grup 1 a còlon distal.

Els FCA s'han utilitzat com a marcadors de risc de càncer de còlon en estudis animals. Aquests focus exhibeixen diferents característiques preneoplàstiques com displàsia, proliferació anormal (McLellan *et al.*, 1991) i mutacions al gen *k-ras* (Vivona *et al.*, 1993). No obstant això, pocs FCA presents al còlon acaben evolucionant a tumors. A una dosi determinada el nombre de tumors és sempre més petit en relació amb els FCA totals trobats. És més, diversos estudis no troben correlació entre el nombre d'FCA i la formació eventual de tumors (Zheng *et al.*, 1999; Rao *et al.*, 1997). Això ha fet créixer l'interès d'identificar subgrups d'FCA que puguin ser més predictius de la tumorigènesi. Dos d'aquests possibles nous marcadors es basen en la producció de mucines de les cèl·lules de la mucosa colònica: els FCA productors de sialomucines (FPS) i els FDM. S'ha observat que els FCA que produeixen sialomucines presenten major velocitat de proliferació cel·lular, major grau de displàsia i un increment de la distorsió de l'obertura de la cripta que els FCA (Jenab *et al.*, 2001; Caderni *et al.*, 1995). Tenint en compte aquestes evidències, els FPS són un sistema millor de predicció del risc de càncer de còlon que el recompte total de FCA. Més recent és el descobriment dels FDM en el còlon de rates tractades amb AOM, que es caracteritzen per l'absència o escassa presència de mucines. Aquestes lesions són histològicament més displàstiques que els FPS, i apareixen en el mateix ordre de magnitud que els tumors, suggerint que aquests focus són precursors directes dels tumors (Caderni *et al.*, 2003). A més, en un estudi realitzat per Filipe (1975) de producció de mucines ja es va veure que en zones amb displàsia severa i carcinoma la depleció de mucines era habitual.

Aquesta displàsia dels FDM també es va corroborar per altres autors (Femia *et al.*, 2007). Aquests van realitzar un estudi en rates F344 a les quals van administrar un carcinogen per analitzar el tipus de mutacions que es produïen tant als FCA com als FDM i als tumors induïts. Van comprovar que la freqüència d'aparició de la mutació del gen *APC* en els FDM era la mateixa que la detectada en els tumors induïts. Però, en canvi, aquesta proporció no es veia reflectida en els FCA estudiats (Femia *et al.*, 2007). Això va reforçar la idea que els tumors i els FDM induïts amb carcinogen estan estretament correlacionats.

Per tant, posteriorment al recompte d'FCA, es va procedir a fer el recompte d'FDM. El nombre total d'FDM va ser molt inferior al d'FCA, menys del 4% dels FCA tenien depleció de mucines. Aquesta proporció tan petita ja va ser observada per Caderni *et al.* (2003) que administrant dues dosis de 15 mg/kg d'AOM i esperant 15 setmanes després de l'última injecció, observava una proporció inferior a un 3% d'FCA amb depleció de

mucines. De fet, aquesta baixa incidència la va relacionar amb la poca aparició de tumors en rates tractades amb la mateixa dosi de carcinogen. Això va portar a un major estudi dels FDM com a biomarcadors de la carcinogènesi de còlon de rata per part d'altres grups d'investigació (Yoshimi *et al.*, 2004; Pierre *et al.*, 2004). Cal destacar que no es van observar diferències en la proporció d'FCA amb depleció de mucines en el present estudi entre els diferents grups, mantenint-se constant encara que s'augmentessin les dosis administrades.

Segons els resultats obtinguts en l'estudi realitzat en el recompte d'FDM en tot el còlon, la seva presència també va dependre de la dosi administrada de DMH. Els grups que van rebre tres dosis de DMH tingueren més FDM que no el grup que va rebre 2 dosis. Aquests resultats concorden amb els resultats obtinguts per Femia *et al.* (2005). Tot i que entre els grups 2 i 3 no hi va haver diferències en el nombre d'FDM, a altres estudis es va observar un increment del nombre d'FDM quan, amb la mateixa dosi de carcinogen, el temps d'espera passà de 7 a 15 setmanes (Caderni *et al.*, 2003).

En el cas dels FDM també es va estudiar la seva distribució al llarg del còlon. Així com els FCA, a on aparegueren més FDM va ser a còlon distal, seguit del medial. Però aquesta distribució no es va veure tan marcada quan es va fer el recompte per segments dels FCA. Atès que els FDM aparegueren més a còlon distal, aquests resultats es podrien relacionar amb el fet que a la part més distal del còlon és on apareixen amb més freqüència els tumors tant en rates (Rodrigues *et al.*, 2002) com en ratolins (Jackson *et al.*, 1999) aportant més consistència a la relació directa que hi ha entre la formació d'FDM i de tumors.

Tot i la poca freqüència d'aparició dels FDM, també es va estudiar la multiplicitat que presentaren aquestes lesions preneoplàstiques i es va observar que la multiplicitat va ser major en els grups que reberen una dosi més de carcinogen. Això es compleix tant a còlon sencer com si es té en compte la distribució per segments. Així mateix, en l'estudi de Caderni (2003) s'observà que augmentant el temps d'espera després de l'última injecció de 7 a 15 setmanes augmentava també la multiplicitat d'aquestes lesions.

En resum, el recompte d'FCA i d'FDM en el còlon de rates tractades amb el carcinogen DMH sembla ser un mètode útil i reproduïble, així com fiable a l'hora de predir el risc de càncer còlon segons les dades obtingudes en el present estudi i les observades a la literatura. Així doncs, tres dosis de 20 mg/kg del carcinogen DMH és idoni per a la inducció de lesions preneoplàstiques, així com un temps d'espera després de l'última administració del carcinogen de dues setmanes o superior. El nombre d'FCA i FDM

obtinguts i la multiplicitat observada permeten l'avaluació de l'efecte quimiopreventiu de diferents fàrmacs i compostos naturals de la dieta.

Dels resultats obtinguts, es pot concloure que l'administració intraperitoneal de tres dosis de 20 mg/kg de DMH i un temps d'observació superior a dues setmanes és l'adient per a l'estudi de l'efecte quimiopreventiu de diferents fàrmacs i components de la dieta, donat que en aquestes condicions s'observa un major nombre de FCA i MDF.

trans-Resveratrol reduces precancerous colonic lesion in dimethylhydrazine-treated rats

J. Agric. Food Chem. 2010, 58, 8104-8110

2.2. Resum de l'article 2

Objectius: El *trans*-resveratrol s'ha descrit com un compost amb activitat antiproliferativa i pro-apoptòtica *in vitro*. Per tant, en aquest estudi es va avaluar l'efecte de l'administració oral de 60 mg/kg de *trans*-resveratrol durant 49 dies en l'aparició de lesions preneoplàstiques induïdes per DMH. A més es va quantificar el *trans*-resveratrol i els seus metabòlits a còlon.

Material i mètodes: Rates mascle Sprague-Dawley (n = 18) es van dividir en 3 grups experimentals. Un grup control administrat només amb solvents. Un grup DMH administrat per via intraperitoneal amb 20 mg/kg de DMH els dies 7, 14 i 21. Un grup resveratrol administrat diàriament per via oral amb 60 mg/kg durant 49 dies, que també va rebre les mateixes dosis de carcinogen. Durant l'experiment, es va controlar el pes corporal i el consum de pinso i d'aigua. Al final de l'estudi, es va extreure sang per punció cardíaca i contingut intestinal a còlon per a la determinació de *trans*-resveratrol i els seus metabòlits. També es va extreure el còlon i es va fixar amb formalina neutra tamponada al 10%. El còlon es va tenyir amb blau de metilè 0,2% per al recompte al microscopi òptic (20x) d'FCA i, posteriorment, es va fer la tinció HID-AB per al recompte d'FDM.

Resultats: El pes corporal així com el consum de pinso i d'aigua no es van veure afectats ni pel tractament amb carcinogen ni pel *trans*-resveratrol. Es va posar a punt un mètode per determinar el *trans*-resveratrol en contingut intestinal. Els resultats de la validació indicaren una recuperació del 98%, precisió (expressada en CV) del 13,5% i límit de detecció i quantificació de 16,5 i 20,6 pmol/g, respectivament. El mètode validat va permetre la quantificació del *trans*-resveratrol i els seus conjugats glucurònid i sulfat. També es va identificar i quantificar el dihidroresveratrol, sent el metabòlit majoritari en una concentració 446 vegades superior a la del compost pare. El tractament amb 60 mg/kg de *trans*-resveratrol va reduir els FCA en un 52%, així com el nombre total de CA en un 50%. Els FDM, que tot i ser menys nombrosos són lesions més displàstiques, també es van veure disminuïts en un 45% i les CA amb depleció de mucines en un 48%.

Conclusions: Després de l'administració oral de *trans*-resveratrol, part d'aquest polifenol i els seus metabòlits van arribar a còlon sent el dihidroresveratrol el metabòlit majoritari. Endemés, el *trans*-resveratrol administrat per via oral a una dosi de 60 mg/kg durant 49 dies va reduir les lesions preneoplàstiques induïdes per DMH a còlon sense efectes adversos aparents.

DOI:10.1021/jf100702x

JOURNAL OF AGRICULTURAL AND FOOD CHEMISTRY
ARTICLE

trans-Resveratrol Reduces Precancerous Colonic Lesions in Dimethylhydrazine-Treated Rats

Irene Alfaras, M. Emília Juan,* and Joana M. Planas

Departament de Fisiologia (Farmàcia) and Institut de Recerca en Nutrició i Seguretat Alimentària (INSA-UB), Universitat de Barcelona, Spain

trans-Resveratrol, a natural occurring polyphenol, has been described as an antiproliferative and proapoptotic agent in vitro. Here, we studied the effect of *trans*-resveratrol administered orally at a dose of 60 mg/kg for 49 days on early preneoplastic markers induced by the intraperitoneal injection of 1,2-dimethylhydrazine (20 mg/kg). We measured *trans*-resveratrol and its derivates by liquid−liquid extraction followed by high-performance liquid chromatography diode array detection analysis in colon contents. Dihydroresveratrol was the most abundant compound in the colon, followed by *trans*-resveratrol glucuronide and small amounts of *trans*-resveratrol and its sulfate. The administration of *trans*-resveratrol decreased aberrant crypt foci by 52%, and mucin depleted foci by 45% in colon. In conclusion, the correlation between the reduction of precancerous colonic lesions and the availability of *trans*-resveratrol in the colon provides a new insight into the therapeutical potential of this polyphenol and its metabolites.

KEYWORDS: Aberrant crypt foci; colon cancer; dihydroresveratrol; mucin-depleted foci; *trans*-resveratrol

INTRODUCTION

trans-Resveratrol (*trans*-3,4′,5-trihydroxystilbene) is synthesized by several plants in response to stress, injury, UV radiation, and fungal infection (*1*). This phytochemical, normally found in dietary products, has been described as a nutraceutic compound with beneficial effects in cancer prevention and treatment. In eliciting these actions, *trans*-resveratrol triggers a variety of cellular and molecular effectors that inhibit the growth of tumor cell lines derived from various human cancers (*2*). Animal and human studies have indicated that oral *trans*-resveratrol has low bioavailability, which may prevent the compound from reaching the target site at therapeutic concentrations in vivo (*1*). This limitation has been attributed to incomplete intestinal absorption (*3*), extensive intestinal metabolism (*4*), and the activity of ABC transporters (*5*). *trans*-Resveratrol enters the enterocyte by passive diffusion. It is metabolized, and its conjugates are secreted back to the intestinal lumen by the members of the ABC family, the Multidrug Resistance Protein 2 (MRP2) and Breast Cancer Resistance Protein (BCRP) (*5*). All of these processes increase the amount of *trans*-resveratrol metabolites reaching the large intestine. They thus favor its potential chemopreventive activity in colon cancer.

The antitumoral activity of *trans*-resveratrol in colon cancer has been studied in vitro (*2*). This phytochemical exerts a large number of effects that interferes with signaling pathways that control cell proliferation. *trans*-Resveratrol inhibits proliferation in colon cell cultures (*6*), which has been attributed to the induction of cell cycle arrest through the inhibition of CDK7 kinase activity (*7*) and to the increasing expression of cyclin A (*8*). In HT-29 cells, the apoptotic effect of *trans*-resveratrol is mediated partly by the intrinsic pathway, through the production of superoxide anions in mitochondria prior to the initiation of the caspase pathway (*6*, *9*). In addition, *trans*-resveratrol also triggers cell death through lysosomes and demonstrates a hierarchy of the proteolytic pathways involved in its cytotoxic mechanism in which lysosomal cathepsin D acts upstream of caspase activation (*10*). Moreover, this polyphenol has been reported to promote apoptosis through the endosplasmic reticulum (*11*) and the induction of CHOP/GADD153 gene expression, which has been acknowledged as a proapoptotic gene (*12*). In contrast, the effects of *trans*-resveratrol on colon cancer in vivo have received little attention (*13*, *14*). Although these studies provide evidence of the activity of *trans*-resveratrol in vivo, they were conducted considering tumors as an end point, without taking into account the early stages of carcinogenesis. Here, we attempt to evaluate the preventive activity of *trans*-resveratrol on the development of markers of colon carcinogenesis. Consequently, rats were given 60 mg/kg of *trans*-resveratrol orally for 49 days. The colon carcinogen 1,2-dimethylhydrazine (DMH) was injected intraperitoneally at days 7, 14, and 21. The chemopreventive activity of *trans*-resveratrol was evaluated by assessing the formation of aberrant crypt foci (ACF) and mucin-depleted foci (MDF) as preneoplastic markers. Moreover, the presence of *trans*-resveratrol and its metabolites in colon was measured. To this end, we developed a method consisting of liquid−liquid extraction followed by high-performance liquid chromatography diode array detection (HPLC-DAD) analysis. The correlation between the chemopreventive activity and the availability of *trans*-resveratrol in the colon provides new insight into the therapeutic potential of this polyphenol and its metabolites.

*To whom correspondence should be addressed. Tel: +34934024505. Fax: +34934035901. E-mail: mejuan@ub.edu.

 Published on Web 06/03/2010

MATERIALS AND METHODS

Chemicals and Reagents. *trans*-Resveratrol was purchased from Second Pharma Co., Ltd. (Shangyu, People's Republic of China), and dihydroresveratrol was from Biopharmalab S.L. (Alicante, Spain). Dose preparation, administration to rats, and sample treatment were performed in dim light to avoid photochemical isomerization of *trans*-resveratrol to the *cis* form. Acetonitrile and methanol were purchased from J. T. Baker (Deventer, Netherlands), and acetic acid was from Scharlau Chemie S.A. (Barcelona, Spain). All of these solvents were HPLC grade. Hydroxypropyl-β-cyclodextrin, β-glucuronidase type L-II (from *Patella vulgata*), and sulfatase type H-1 (from *Helix pomatia*) were from Sigma-Aldrich (St. Louis, MO). Water used in all experiments was passed through a Milli-Q water purification system (18 mΩ) (Millipore, Milan, Italy).

Rats and Diets. Male adult Sprague−Dawley rats (7 weeks old) were housed in cages (n = 3/cage) under controlled conditions of a 12 h light: dark cycle, at a temperature of 22 ± 3 °C and a relative humidity of 40−70%. Water and a standard solid diet (2014 Teklad Global 14%, Harlan, Spain) were consumed ad libitum. No traces of *trans*-resveratrol were detected in the commercial diet or in the plasma of control rats, analyzed following Juan et al. (*15*). Handling and killing of rats were in full accordance with the European Community guidelines for the care and management of laboratory rats. The studies were approved by the Ethics Committee of Animal Experimentation of the University of Barcelona (ref 2269/01). All rat manipulations were carried out in the morning to minimize the effects of circadian rhythm.

Experimental Design. After 1 week of acclimatization, rats were stratified by body weight and assigned to 1 of 3 experimental groups (n = 6 rats/group) such that there were no differences in mean initial weight. The experimental groups were as follows: control group (no test agent and no carcinogen), the DMH group (no test agent and DMH), and the resveratrol group (*trans*-resveratrol and DMH). Rats were orally administered by gavage at a constant volume of 10 mL/kg every day for 49 days. *trans*-Resveratrol was administered at a dose of 60 mg/kg considering this compound as a potential nutraceutical. Because of its low solubility in water, *trans*-resveratrol was dissolved in 20% hydroxypropyl-β-cyclodextrin (v/v). Rats in the control and DMH groups were given only the solvent during the same period. At days 7, 14, and 21, rats from DMH and resveratrol groups received an intraperitoneal injection of carcinogen (20 mg DMH/kg dissolved in EDTA 1 mmol/L, pH 6.5), and control animals received only the solvent at a constant volume of 1 mL/kg. Oral and intraperitoneal doses were adjusted according to rat weight to ensure a constant dose, and they were freshly prepared immediately before each administration.

Body weight and food and water consumption were monitored daily. The feed conversion efficiency (FCE) was calculated as the weekly body weight gain divided by the food consumption.

Sample Collection. At the end of the study, rats were deprived of food overnight and anesthetized with ketamine (90 mg/kg) and xylacine (10 mg/kg). Blood samples were collected by cardiac puncture and transferred as follows: 1 mL into EDTA-K_3 for hematology, 2 mL into a tube without anticoagulant for clinical chemistry, and 1 mL into EDTA-K_3 for *trans*-resveratrol determination. Serum for clinical chemistry and plasma for *trans*-resveratrol analysis were obtained after centrifugation of blood samples at 1500*g* (MEGAFUGE 1.0R, Heraeus, Boadilla, Spain) for 15 min at 4 °C.

A gross necropsy was performed. Subsequently, the brain, lungs, spleen, heart, liver, kidney, and testicle were excised and trimmed of any adherent tissue, and their wet weights were immediately recorded to avoid drying. Results are expressed as organ weight relative to 100 g of body weight (%).

The colon was removed, and the contents were collected and stored at −20 °C for extraction and subsequent analysis of *trans*-resveratrol. The colon was then washed in phosphate-buffered solution (PBS) (pH 7.4) and trimmed of adherent mesenteric tissue, and its wet weight was recorded. The colon was divided into three equal segments: proximal (close to the cecum), medial, and distal (close to the rectum). Each segment was opened along the longitudinal median and pinned flat onto a polystyrene board for the ACF assay.

Hematology and Clinical Chemistry. Complete and differential cell counts were performed using a Cell-Dyn blood analyzer (Abbott Diagnostics Division, Santa Clara, CA). Biochemical analyses of serum were performed with a Roche/Hitachi 747 clinical analyzer from Roche Diagnostics GmbH (Mannheim, Germany).

Determination of *trans*-Resveratrol and Its Metabolites in Plasma. *trans*-Resveratrol and glucuronide and sulfate conjugates concentrations were determined using the method of Juan et al. (*15*) in plasma samples 24 h after the last oral administration.

Quantification of *trans*-Resveratrol and Its Metabolites in Colon Content. Colon content samples were defrosted at room temperature and weighed. To extract *trans*-resveratrol, 10 mL of 80% methanol with 2.5% acetic acid and 10 μL of 15% ascorbic acid were added to 1 g of colon sample. The mixture was agitated with constant stirring for 30 min at 60 °C. Then, samples were transferred to a centrifuge tube, and the content remaining in the beaker was collected with an additional 2 mL of acidified methanol. The homogenates were centrifuged at 33000*g* (Centrikon H-401, Kontron Hermle Instruments, Italy) for 30 min at 4 °C. The supernatant was transferred to a clean tube, and the residue was extracted once again, by the same procedure. The organic solvent of the supernatant was evaporated with a Concentrator 5301 (Eppendorf Iberica, S.L., San Sebastian de los Reyes, Spain) at 45 °C to a final volume of 500 μL.

The determination of *trans*-resveratrol and its metabolites by HPLC analysis was carried out following Juan et al. (*15*) but with a different gradient elution program. The execution was performed as follows: 0−5 min, 15% B; 7 min, 20% B; 10 min, 21% B; 20 min, 22% B; 30 min, 30% B; 35 min, 35% B; 40 min, 40% B; 45 min, 50% B; 50 min, 70% B; 55−60 min, 100% B; and 62 min, 15% B. There was a 5 min delay prior to the injection of the next sample to ensure re-equilibration of the column.

The chromatograms were obtained at 306 and 276 nm, which correspond to the maximum absorbance of *trans*-resveratrol and dihydroresveratrol, respectively. Authentic standards of *trans*-resveratrol and dihydroresveratrol were used for the construction of calibration curves. The chromatographic peaks were further identified by spectroscopic analysis with diode array-UV detection from 220 to 400 nm. The results of the analyses are expressed as nmol/L of plasma and nmol/g of colonic content.

The identity of the peaks detected in colon content was confirmed by mass spectrometry. An Agilent series 1100 HPLC instrument with an API 3000 triple quadrupole mass spectrometer (Applied Biosystems, PE Sciex, Concord, Ontario, Canada) equipped with a Turbo IonSpray source in negative-ion mode was used for HPLC-MS analysis. The ion spray voltage was 3500 V, using nitrogen as the nebulizer gas (10 arbitrary units) and curtain gas (15 arbitrary units). The detection conditions were optimized with a standard solution of *trans*-resveratrol and dihydroresveratrol in the presence of LC mobile phase, as follows: declustering potential, −70 V; focusing potential, −200 V; drying gas (N_2) heated to 400 °C and introduced at a flow rate of 5000 cm^3/min. Mass spectra were acquired in the 100−500 m/z range.

Validation of the Method To Quantify *trans*-Resveratrol in Colon Content. The method was validated according to The United States Pharmacopoeia (*16*). Approximately 1 g of blank colon content was spiked with 5 nmol of *trans*-resveratrol and agitated in the vortex for 2 min before being processed as indicated above. Precision was determined by assaying six samples at 5 nmol/g and was expressed as the experimental coefficient of variation (CV). Recovery was measured by spiking blank samples with a final concentration of 5 nmol/g (n = 6). Finally, the limit of detection (LOD) and the limit of quantification (LOQ) were calculated by measuring the analytical background response of six blanks of colon content. Signal-to-noise ratios of 3:1 and 10:1 were used for the LOD and LOQ, respectively.

ACF. Aberrant crypts (AC) and ACF were evaluated using a modification of a method previously described (*17*). Briefly, the intestine was fixed in 10% buffered formalin, pH 7.4 (Sigma-Aldrich), for a minimum of 24 h. The fixed segments were washed in PBS. Colon segments were stained in a 0.2% methylene blue solution for 8−10 min, and the excess of dye was rinsed off with PBS. Each segment was placed mucosal side up on a microscopic slide and examined by light microscope at 20× magnification (model CHS; Olympus Optical Co., Ltd., Hamburg, Germany). ACF were identified as described elsewhere (*17*). The number of ACF and AC in each focus was counted. The scores were checked by an observer who was blinded to treatment groups. All of the images of the mucosal surface were captured with KAPPA Image Base Control 2.6 (KAPPA opto-electronics GmbH, Gleichen, Germany).

Mucin-Depleted Foci. After ACF determination, colons were kept in 10% buffered formalin, pH 7.4, at −4 °C and later processed with the high-iron diamine Alcian blue staining (HID-AB) at pH 2.5 for the visualization of mucin production. Segments were washed in PBS and then dyed in a high-iron diamine solution for 18−24 h protected from the light. Then, segments were washed and stained for 5 min with 1% alcian blue in 3% acetic acid, washed again, and finally stained for 2 min in neutral red (1 g of neutral red dissolved in 1 L of mQ water with 2 mL of 1% acetic acid). The HID-AB-stained colons were placed mucosal side up in slides and observed under a light microscope at 20× magnification. The total number of MDF and number of mucin-depleted aberrant crypts (MDAC) per focus in colon were determined following Caderni et al. (*18*): absence or little production of mucins, distortion of the opening of the lumen as compared with normal surrounding crypts, and elevation of the lesion above the surface of the colon. The scores were determined by an observer blinded to the experiment. Images of the mucosal surface were captured with KAPPA Image Base Control 2.6.

Statistical Analysis. Results are presented as the means ± standard errors of the mean (SEMs). All data evaluation and analyses were done by GraphPad Prism 4 (GraphPad Software, Inc., La Joya, CA). Organs, colon weight, and hematological and clinical biochemistry were compared using one-way analysis of variance (ANOVA), followed by Bonferroni's posthoc test. When the normality test was significant, as evaluated by the Kolmogorov−Smirnov test, differences between means were assessed instead by the nonparametric Kruskal−Wallis test. Significant differences of body weight, FCE, the number ACF per segment, and the number of AC per ACF were analyzed by two-way ANOVA followed by Bonferroni's posthoc test. The total number of AC, ACF, MDF, and MDAC was compared using Student's unpaired *t* test. The *F* test was performed to check that samples had equal variances. For all tests, $P < 0.05$ was considered significant.

RESULTS

Body Weight, Food, and Water Consumption. No mortality or adverse effects occurred during the experiment. Stool consistency was firm (pelleted) throughout the study, with no visible differences between groups. Body weight was not affected by the administration of DMH or *trans*-resveratrol with respect to the control group. Thus, the body weight of the control animals increased from 235 ± 16 g on day 1 to 376 ± 39 g on day 49. The DMH group increased from 232 ± 13 g on day 1 to 353 ± 29 g on day 49, and the resveratrol group increased from 235 ± 20 g on day 1 to 354 ± 34 g on day 49. There were no significant differences in food or water consumption between the three groups. Feed conversion efficiency (**Figure 1**) was highest during the first week, decreased during the second and third week, and remained constant thereafter, with no significant differences between groups.

Gross Necropsy. At the end of the study, a postmortem examination showed no evidence of gross abnormality or toxicity in any group. The examination of the vital organs carried out during the autopsy did not show macroscopic differences in size, color, or texture in any of the groups studied. The final relative weights of liver, kidney, heart, brain, lungs, testicles, spleen, and colon were not different among groups.

Hematology and Clinical Chemistry. The results of the hematologic tests carried out at the end of the study did not show any differences among control, DMH, or resveratrol groups. The erythrocyte, leukocyte, and platelets results were comparable to those obtained previously (*19*). The clinical chemistry variables were also evaluated. No differences between groups were observed in glucose or protein concentrations. Serum cholesterol, triglycerides, and high-density lipoproteins were not affected by the oral administration of 60 mg/kg of *trans*-resveratrol or DMH treatment. The hepatic integrity was maintained throughout the experiment as indicated with ALT and AST, which did not differ between groups. Renal function and the plasma levels of electrolytes were within reference values.

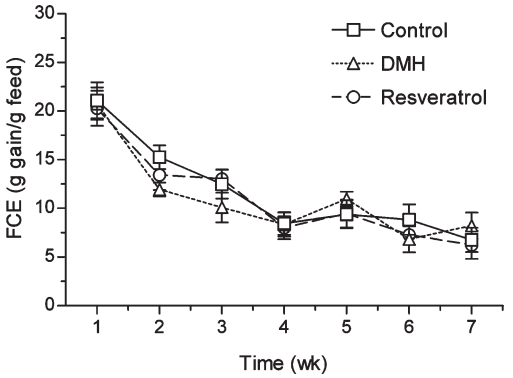

Figure 1. FCE of male Sprague−Dawley rats of control (no test agent and no carcinogen), DMH (no test agent and 20 mg/kg DMH once a week for 3 weeks), and resveratrol groups (60 mg/kg *trans*-resveratrol and 20 mg/kg DMH once a week for 3 weeks). Results are expressed as means ± SEMs, $n = 6$. No differences between groups are found. Differences over time: control group, 1 week = 2 weeks > 3 weeks = 4 weeks = 5 weeks = 6 weeks = 7 weeks; 2 weeks = 3 weeks = 5 weeks; DMH group, 1 week > 2 weeks = 3 weeks = 4 weeks = 5 weeks = 6 weeks = 7 weeks; and *trans*-resveratrol group, 1 week > 2 weeks = 3 weeks = 5 weeks > 4 weeks = 6 weeks = 7 weeks; 3 weeks = 6 weeks; 4 weeks = 5 weeks = 6 weeks = 7 weeks, $p < 0.05$.

Determination of *trans*-Resveratrol and Its Metabolites in Plasma. Free *trans*-resveratrol was the main compound present in plasma 24 h after the last administration, with concentrations of 43.2 ± 10.8 nmol/L. *trans*-Resveratrol glucuronide was identified in plasma of only two of the six *trans*-resveratrol-treated rats, at a concentration of 37.8 ± 13.8 nmol/L. No traces of sulfate conjugate were found.

Validation of the Method To Quantify *trans*-Resveratrol in Colon Content. The extraction of *trans*-resveratrol and its metabolites in colon content was attempted using different solvents. When ethanol, ethyl acetate, and methanol (80%, v/v) without acidification were evaluated, the recovery was lower than that obtained when methanol was mixed with acetic acid (2.5%). The mean total recovery was 98.3 ± 11.3%, which indicates that *trans*-resveratrol was quantitatively extracted by this method. The precision expressed as CV was 13.5%, which is less than the recommended value of 20% (*20*). The sensitivity was adequate to measure *trans*-resveratrol in colonic content samples with an LOD of 16.5 pmol/g and LOQ of 20.6 pmol/g. The chromatographic gradient elution, which was modified from a previous method (*15*), allowed a good separation of *trans*-resveratrol and its glucuronide and sulfate conjugates from interference peaks with detection at 306 nm. Moreover, the method allowed the identification and quantification of dihydroresveratrol at 276 nm.

Quantification of *trans*-Resveratrol and Its Metabolites in Colon Content. The method developed allowed the separation and identification of *trans*-resveratrol (peak 1) and its glucuronide and sulfate conjugates (peaks 2 and 3, respectively) (**Figure 2**). The identity of the peaks was confirmed by MS. *trans*-Resveratrol glucuronide was characterized by the deprotonated molecular ion $(M - H)^-$ at m/z 403 (**Figure 2C**), whereas the resveratrol fragment was observed at m/z 227. The sulfate conjugate showed a deprotonated molecular ion $(M - H)^-$ at m/z 307 (**Figure 2C**) and also the resveratrol fragment at m/z 227. The method also allowed identification of another metabolite, dihydroresveratrol, resulting from the reduction of the double bond (**Figure 3**). This compound eluted at 28 min, which was barely 1 min after *trans*-resveratrol, but it had a different spectrum and maximum of absorbance (λ_{max} 276 nm) (**Figure 3A**). Dihydroresveratrol was further identified

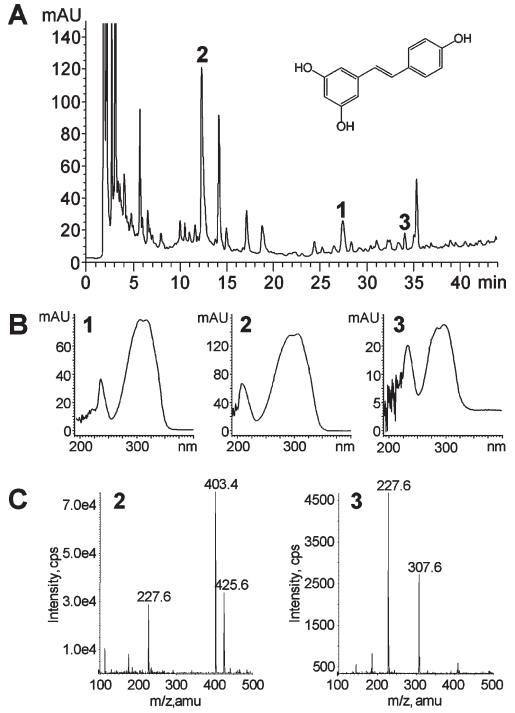

Figure 2. HPLC chromatogram and mass spectra of *trans*-resveratrol obtained in colonic content from rats of the resveratrol group, 24 h after the last oral administration of 60 mg/kg. (**A**) HPLC chromatogram at 306 nm. Peaks of (1) *trans*-resveratrol and its conjugates, (2) glucuronide, and (3) sulfate are indicated. (**B**) UV spectrum obtained by diode array detection of (1) *trans*-resveratrol, (2) glucuronide, and (3) sulfate. (**C**) Full-scan product ion mass spectra of (2) glucuronide and (3) sulfate.

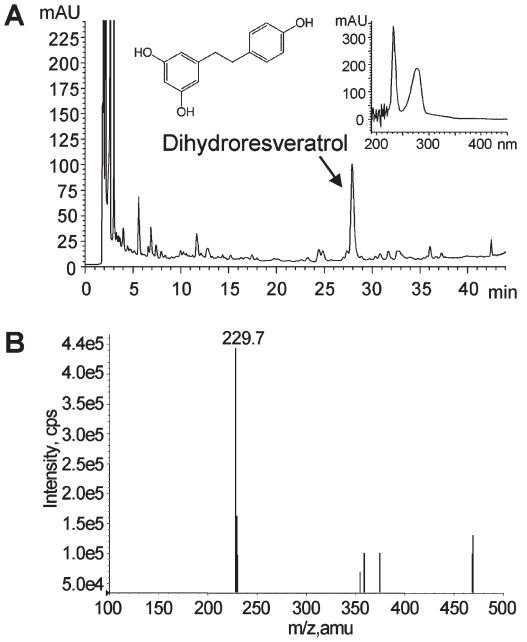

Figure 3. HPLC chromatogram and mass spectra of dihydroresveratrol obtained in colonic content from rats of the resveratrol group, 24 h after the last oral administration of 60 mg/kg. (**A**) HPLC chromatogram at 276 nm. Inserts depict the chemical structure of dihydroresveratol and its UV spectrum obtained by diode array detection. (**B**) Full-scan product ion mass spectra of dihydroresveratrol.

by MS, which gave a deprotonated molecular ion $(M - H)^-$ at m/z 229 (**Figure 3B**).

trans-Resveratrol was detected in the colon content of rats treated with 60 mg/kg, 24 h after the last administration, at a concentration of 0.68 ± 0.24 nmol/g. The most abundant metabolite in colon was dihydroresveratrol, with a concentration of 303.0 ± 34.7 nmol/g, 446-fold that of the parent compound. The glucuronide and sulfate conjugates of *trans*-resveratrol were also detected, at concentrations of 3.40 ± 1.29 and 0.44 ± 0.23 nmol/g, respectively.

ACF. Control rats showed no microscopically observable changes in colon morphology. DMH-injected rats developed ACF (**Figure 4**) with the absence of lesions in the proximal colon followed by a few ACF in the medial segment and more in the distal colon, in all groups (**Table 1**). *trans*-Resveratrol treatment inhibited the number of ACF by 58 ($p < 0.01$) and 48% ($p < 0.001$) in the medial and distal segments, respectively. Crypt multiplicity (number of AC per ACF) was also counted (**Figure 4I**) and showed the same pattern, more singlets than 2, 3, or ≥4 AC in both groups. However, rats treated with *trans*-resveratrol had fewer foci with 1 ($p < 0.001$), 2 ($p < 0.01$), and 3 crypts being inhibited by 53, 49, and 64%, respectively. *trans*-Resveratrol treatment also decreased the number of total AC (**Table 1**) present in colon by 50% ($p < 0.01$).

Mucin-Depleted Foci. MDF were observed in the DMH-treated groups (**Figure 4**). The daily oral administration of 60 mg/kg of *trans*-resveratrol reduced the number of MDF by 45% ($p < 0.05$) (**Figure 4H**), with 5.00 ± 0.01 MDF in the DMH group and 2.75 ± 0.75 MDF in the resveratrol group. *trans*-Resveratrol treatment reduced the number of MDF lesions by 36 and 53% in the medial and distal segment, respectively (**Table 1**). The number of foci with 1, 2, 3, and ≥4 AC did not differ between groups, but there was a reduction of 48% in the total number of MDAC ($p < 0.05$) in the resveratrol group with respect to the DMH group (**Table 1**).

DISCUSSION

Colorectal cancer is one of the leading causes of death in both men and women in Western countries, and it is usually lethal when diagnosed at later stages of progression (*21*). Environmental aspects are believed to be involved in colon carcinogenesis, including diet. Up to 80% of sporadic colorectal cancers are therefore potentially preventable (*22*). Diet and lifestyle are most likely related to colon cancer etiology through the overconsumption of energy, coupled with inadequate intake of protective substances, including micronutrients, dietary fiber, and a variety of phytochemicals (*23*). For this reason, the present study aims to evaluate the effect of *trans*-resveratrol on the development of early markers of colon carcinogenesis in DMH-treated rats and measure the concentrations of this polyphenol and its metabolites in colon content.

Our results show that the method presented is suitable for the extraction, identification, and quantification of the target substance and its metabolites, given that we obtained a recovery of 98%, good precision, and adequate sensitivity. Once the method was established, it was applied to the samples of colon content obtained 24 h after the last oral administration of 60 mg/kg of *trans*-resveratrol. Our results showed that this compound reached the colon together with its metabolites. The most abundant compound was dihydroresveratrol followed by resveratrol glucuronide and minor amounts of *trans*-resveratrol and its sulfate conjugate. The conjugates come from the metabolism in the enterocyte and subsequent extrusion back to the intestinal lumen (*4*, *5*). Moreover, enterohepatic circulation may affect the concentration of these compounds in the colon (*24*). Although these conjugates are believed to be pharmacologically inactive and excreted in urine and bile, deconjugation has been reported to

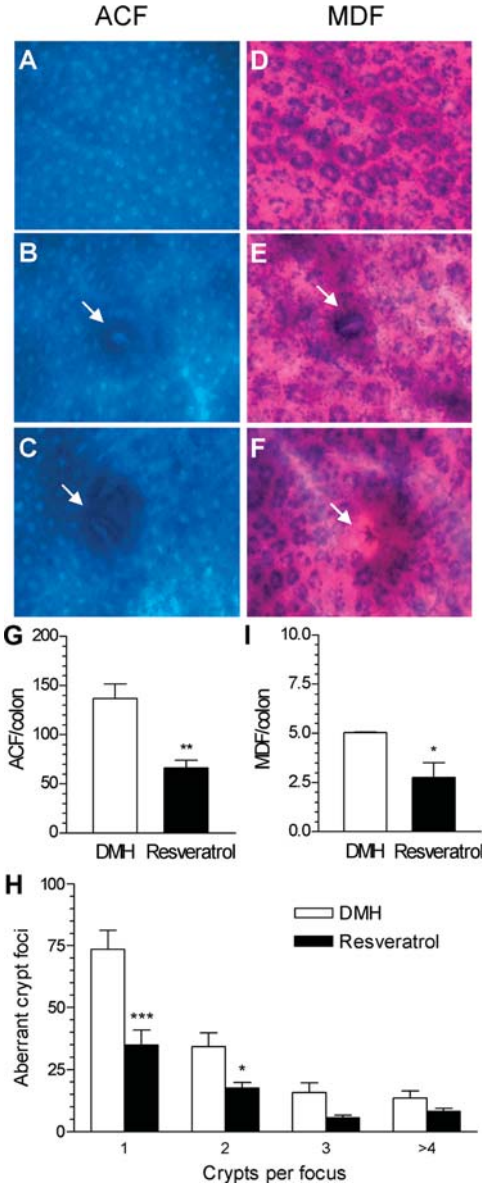

Figure 4. Preneoplastic lesions ACF (**A**−**C**) and MDF (**D**−**F**) observed under a light microscope after staining of the colon with methylene blue or HID-AB, respectively. Images show the whole mount colon of control rats (**A** and **D**) and DMH-treated animals depicting a topographic view of ACF with 1 crypt (**B**) and more than 3 crypts (**C**), a mucinous ACF (**E**), and a mucin-depleted foci (**F**). Effects of *trans*-resveratrol on the total number of ACF (**G**), crypt multiplicity of ACF (**H**), and total number of mucin-depleted foci (**I**). Rats were orally administered with 60 mg/kg *trans*-resveratrol for 49 days. DMH (20 mg/kg) was injected intraperitoneally at days 7, 14, and 21. Results are expressed as means + SEMs ($n = 6$); *$p < 0.05$, **$p < 0.01$, and ***$p < 0.001$ vs DMH group. Differences in the number of ACs per focus (**H**): DMH group, 1 AC/ACF > 2 AC/ACF > 3 AC/ACF = >4 AC/ACF; resveratrol group, 1 AC/ACF > 2 AC/ACF = 3 AC/ACF = >4 AC/ACF, $p < 0.05$.

occur in the gut, releasing the parent compound (*25*, *26*). Consequently, the glucuronide and sulfate conjugates of *trans*-resveratrol could act as colon-specific prodrugs, as shown for sulfate-conjugated methylprednisolone and prednisolone. The latter had been developed to release the corresponding glucocorticoid in the cecum for the treatment of inflammatory bowel disease (*26*).

The method also permitted the detection of dihydroresveratrol, a metabolite of *trans*-resveratrol, which is formed by

Table 1. Effect of *trans*-Resveratrol in the Occurrence of Preneoplastic Lesions in Colon Induced by DMH[a]

	DMH group	resveratrol group
ACF/proximal	0	0
ACF/medial	52.8 ± 13.3	22.2 ± 3.94**
ACF/distal	84.2 ± 8.82	44.0 ± 9.48***
AC/colon	218 ± 28.9	110 ± 13.8**
MDF/proximal	0	0
MDF/medial	2.33 ± 0.88	1.50 ± 0.29
MDF/distal	2.67 ± 0.88	1.25 ± 0.75
MDAC/colon	10.7 ± 0.33	5.50 ± 1.67*

[a] Values are means ± SEMs, $n = 6$. * Significantly different from DMH group, $p < 0.05$. ** $p < 0.01$. *** $p < 0.001$.

the reduction of the stilbenic double bond. This compound is scarcely known, and its presence has been reported only in urine but not in plasma (*27*, *28*). In humans, it was detected as dihydroresveratrol glucuronide and sulfate (*27*) and in rats as dihydroresveratrol and its sulfate conjugate (*28*). These authors attributed the presence of dihydroresveratrol to the activity of the intestinal microflora and posterior absorption. That hypothesis is consistent with our results, since when intestinal perfusions were performed in the absence of bacteria only resveratrol glucuronide and sulfate were found (*5*). A recent study identified dihydroresveratrol as a metabolite produced by *E. lenta* and *B. uniformis*, both of which have been isolated from human feces (*29*). All of these findings support the involvement of the intestinal flora in the synthesis of this metabolite. The biological activity of dihydroresveratrol is hardly known, although it has been reported to possess less antioxidant activity and less ability to inhibit DNA synthesis (*30*). However, it has a slightly stronger effect than *trans*-resveratrol in cell growth inhibition assays (*31*).

In the present study, we evaluate the potential chemopreventive activity of *trans*-resveratrol on colon cancer in the DMH rat model, where carcinogenesis develops through a multistep process as it does in humans. ACF have been identified in humans at high risk and are widely used as a surrogate marker of colon cancer (*32*). Prior to the performance of our study, we optimized the experimental conditions (data not shown). Therefore, we assayed two and three subcutaneous injections of DMH (20 mg/kg, 1 week apart) and different observation periods to validate the appearance of ACF. Our results showed that three subcutaneous injections followed by an observation period of 4 weeks proved to be appropriate for the screening of potentially chemopreventive agents. Under our experimental conditions, *trans*-resveratrol and/or its metabolites reduced the number of preneoplastic lesions, since ACF were inhibited by 52% and the total number of AC by 50%. Furthermore, MDF were described in carcinogen-treated rodents (*18*) and in humans at high risk of colon cancer (*32*). MDF are characterized by harboring mutations that show Wnt signaling activation like in colon tumors, suggesting that these lesions are precancerous (*32*). In our experimental condition, the number of MDF was reduced by 50%, thus remarking the protecting activity exerted by *trans*-resveratrol in the colon mucosa. Because *trans*-resveratrol was administered 1 week prior to the first exposure to DMH, the present results demonstrated that *trans*-resveratrol acts as an efficient agent inhibiting cancer initiation.

The potential cancer chemopreventive activity of *trans*-resveratrol in vivo has been examined only in long-term studies (*13*, *14*, *33*−*35*). The effect of *trans*-resveratrol on azoxymethane-induced colon carcinogenesis was assessed in F344 rats. This phytochemical was administered in drinking water at a dose of 200 μg/kg for 100 days, beginning 10 days before the administration of the carcinogen (*33*).

trans-Resveratrol reduced the growth of colorectal ACF modulating the expression of bax and p21, both involved in the regulation of cell proliferation and apoptosis (*33*). Sengottuvelan et al. also assessed the anticarcinogenic activity of 8 mg/kg of *trans*-resveratrol in a model of colon carcinogenesis induced by DMH, but these were long-term experiments that lasted 30 weeks (*14*, *34*, *35*). Their results showed that in rats, *trans*-resveratrol markedly reduced the number of DMH-induced ACF and incidence and size of tumors, possibly through the modulation of antioxidant defense status and activities of carcinogen-detoxifying enzymes (*14*, *34*, *35*). In Apc^{Min} mice, which are used as a model of human familial adenomatous polyposis, *trans*-resveratrol administered in drinking water at a dose of 15 mg/kg for 7 weeks prevented the formation of colon tumors and reduced the formation of small intestinal tumor by 70% by down-regulating genes that are directly involved in cell cycle progression such as cyclin D1, D2, and DP-1 and in the inhibition of the carcinogenic process and tumor expansion (*13*). It is noteworthy that using the same animal model where *trans*-resveratrol was administered in the diet at 4, 20, or 90 mg/kg for 7 weeks in Apc^{Min}, there were no effects in colon tumorigenesis (*36*). Those results are in accordance with the ones obtained by Sale et al. (*37*), who only found a decrease on the number of adenomas when doses of 280 mg/kg were used. The effect of the higher dose of *trans*-resveratrol was associated with inhibition of COX enzymes and interference with prostaglandin E_2 generation (*37*).

Our findings showed that *trans*-resveratrol given orally significantly reduced DMH-induced colon preneoplastic lesions without any apparent adverse effects. For chemopreventive purposes, daily, long-term ingestion is necessary, so safety was a prime consideration. Our results indicate that in terms of body growth, *trans*-resveratrol is well-tolerated by animals, as shown previously (*19*). Moreover, the gross necropsy revealed a normal appearance of the vital organs without the presence of pathological lesions. These results were substantiated by the results of the hematological and clinical chemistry studies, which indicated that *trans*-resveratrol is nontoxic (*19*).

In conclusion, these results indicate that following the oral administration of 60 mg/kg of *trans*-resveratrol, some of this polyphenol and its metabolites reached the colon. It inhibited ACF formation and mucin-depleted foci. The present findings support the hypothesis that *trans*-resveratrol contributes to the prevention of colon carcinogenesis and provides an insight into the extensive metabolism that this polyphenol undergoes in the intestine.

ABBREVIATIONS USED

AC, aberrant crypt; ACF, aberrant crypt foci; BCRP, Breast Cancer Resistance Protein; DMH, 1,2-dimethylhydrazine; FCE, food conversion efficiency; MDAC, mucin-depleted aberrant crypt; MDF, mucin-depleted foci; MRP2, Multidrug Resistance Protein 2.

LITERATURE CITED

(1) Baur, J. A.; Sinclair, D. A. Therapeutic potential of resveratrol: the in vivo evidence. *Nat. Rev. Drug Discovery* **2006**, *5*, 493–506.

(2) Bishayee, A. Cancer prevention and treatment with resveratrol: From rodent studies to clinical trials. *Cancer Prev. Res.* (*Philadelphia, PA*) **2009**, *2*, 409–418.

(3) Kuhnle, G.; Spencer, J. P.; Chowrimootoo, G.; Schroeter, H.; et al. Resveratrol is absorbed in the small intestine as resveratrol glucuronide. *Biochem. Biophys. Res. Commun.* **2000**, *272*, 212–217.

(4) Sabolovic, N.; Humbert, A. C.; Radominska-Pandya, A.; Magdalou, J. Resveratrol is efficiently glucuronidated by UDP-glucuronosyltransferases in the human gastrointestinal tract and in Caco-2 cells. *Biopharm. Drug Dispos.* **2006**, *27*, 181–189.

(5) Juan, M. E.; González-Pons, E.; Planas, J. M. Multidrug resistance proteins restrain the intestinal absorption of *trans*-resveratrol. *J. Nutr.* **2010**, *140*, 489–495.

(6) Juan, M. E.; Wenzel, U.; Daniel, H.; Planas, J. M. Resveratrol induces apoptosis through ROS-dependent mitochondria pathway in HT-29 human colorectal carcinoma cells. *J. Agric. Food Chem.* **2008**, *56*, 4813–4818.

(7) Liang, Y. C.; Tsai, S. H.; Chen, L.; Lin-Shiau, S. Y.; Lin, J. K. Resveratrol-induced G2 arrest through the inhibition of CDK7 and p34CDC2 kinases in colon carcinoma HT29 cells. *Biochem. Pharmacol.* **2003**, *65*, 1053–1060.

(8) Colin, D.; Gimazane, A.; Lizard, G.; Izard, J. C.; et al. Effects of resveratrol analogs on cell cycle progression, cell cycle associated proteins and 5-fluorouracil sensitivity in human derived colon cancer cells. *Int. J. Cancer* **2009**, *124*, 2780–2788.

(9) Hwang, J. T.; Kwak, D. W.; Lin, S. K.; Kim, H. M.; et al. Resveratrol induces apoptosis in chemoresistant cancer cells via modulation of AMPK signaling pathway. *Ann. N.Y. Acad. Sci.* **2007**, *1095*, 441–448.

(10) Trincheri, N. F.; Nicotra, G.; Follo, C.; Castino, R.; Isidoro, C. Resveratrol induces cell death in colorectal cancer cells by a novel pathway involving lysosomal cathepsin D. *Carcinogenesis* **2007**, *28*, 922–931.

(11) Park, J. W.; Woo, K. J.; Lee, J. T.; Lim, J. H.; et al. Resveratrol induces pro-apoptotic endoplasmic reticulum stress in human colon cancer cells. *Oncol. Rep.* **2007**, *18*, 1269–1273.

(12) Woo, K. J.; Lee, T. J.; Lee, S. H.; Lee, J. M.; et al. Elevated gadd153/chop expression during resveratrol-induced apoptosis in human colon cancer cells. *Biochem. Pharmacol.* **2007**, *73*, 68–76.

(13) Schneider, Y.; Duranton, B.; Gossé, F.; Schleiffer, R.; et al. Resveratrol inhibits intestinal tumorigenesis and modulates host-defense-related gene expression in an animal model of human familial adenomatous polyposis. *Nutr. Cancer* **2001**, *39*, 102–107.

(14) Sengottuvelan, M.; Viswanathan, P.; Nalini, N. Chemopreventive effect of *trans*-resveratrol, a phytoalexin against colonic aberrant crypt foci and cell proliferation in 1,2-dimethylhydrazine induced colon carcinogenesis. *Carcinogenesis* **2006**, *27*, 1038–1046.

(15) Juan, M. E.; Maijó, M.; Planas, J. M. Quantification of *trans*-resveratrol and its metabolites in rat plasma and tissues by HPLC. *J. Pharm. Biomed. Anal.* **2010**, *51*, 391–398.

(16) Validation of compendial methods. In *The United States Pharmacopeia and The National Formulary*, USP32-NF27; The United States Pharmacopeial Convention: Rockville, MD, 2009; pp. 733−736.

(17) Bird, R. P. Observation and quantification of aberrant crypts in the murie colon treated with a colon carcinogen: Preliminary findings. *Cancer Lett.* **1987**, *37*, 147–151.

(18) Caderni, G.; Femia, A. P.; Giannini, A.; Favuzza, A.; et al. Identification of mucin-depleted foci in the unsectioned colon of azoxymethane-treated rats: Correlation with carcinogenesis. *Cancer Res.* **2003**, *63*, 2388–2392.

(19) Juan, M. E.; Vinardell, M. P.; Planas, J. M. The daily oral administration of high doses of *trans*-resveratrol to rats for 28 days is not harmful. *J. Nutr.* **2002**, *132*, 257–260.

(20) Bansal, S.; DeStefano, A. Key elements of bioanalytical method validation for small molecules. *AAPS J.* **2007**, *9*, E109–E114.

(21) Ferlay, J.; Autier, P.; Boniol, M.; Heanue, M.; et al. Estimates of the cancer incidence and mortality in Europe in 2006. *Ann. Oncol.* **2007**, *18*, 581–592.

(22) Cummings, J. H.; Bingham, S. A. Diet and the prevention of cancer. *BMJ* **1998**, *317*, 1636–1640.

(23) Watson, A. J. An overview of apoptosis and the prevention of colorectal cancer. *Crit. Rev. Oncol. Hematol.* **2006**, *57*, 107–121.

(24) Marier, J. F.; Vachon, P.; Gritsas, A.; Zhang, J.; et al. Metabolism and disposition of resveratrol in rats: Extent of absorption, glucuronidation, and enterohepatic recirculation evidenced by a linked-rat model. *J. Pharmacol. Exp. Ther.* **2002**, *302*, 369–373.

(25) Sakamoto, H.; Yokota, H.; Kibe, R.; Sayama, Y.; Yuasa, A. Excretion of bisphenol A-glucuronide into the small intestine and deconjugation in the cecum of the rat. *Biochim. Biophys. Acta* **2002**, *1573*, 171–176.

(26) Kong, H.; Kim, Y.; Lee, Y.; Choi, B. Sulfate-conjugated methylprednisolone: Evaluation as a colon-specific methylprednisolone

prodrug and comparison with sulfate-conjugated prednisolone and dexamethasone. *J. Drug Target* **2009**, *17*, 159–167.
(27) Walle, T.; Hsieh, F.; DeLegge, M. H.; Oatis, J. E., Jr.; Walle, U. K. High absorption but very low bioavailability of oral resveratrol in humans. *Drug Metab. Dispos.* **2004**, *32*, 1377–1382.
(28) Wang, D.; Hang, T.; Wu, C.; Liu, W. Identification of the major metabolites of resveratrol in rat urine by HPLC-MS/MS. *J. Chromatogr., B: Anal. Technol. Biomed. Life Sci.* **2005**, *829*, 97–106.
(29) Jung, C. M.; Heinze, T. M.; Schnackenberg, L. K.; Mullis, L. B.; et al. Interaction of dietary resveratrol with animal-associated bacteria. *FEMS Microbiol. Lett.* **2009**, *297*, 266–273.
(30) Stivala, L. A.; Savio, M.; Carafoli, F.; Perucca, P.; et al. Specific structural determinants are responsible for the antioxidant activity and the cell cycle effects of resveratrol. *J. Biol. Chem.* **2001**, *276*, 22586–22594.
(31) Cardile, V.; Lombardo, L.; Spatafora, C.; Tringali, C. Chemoenzymatic synthesis and cell-growth inhibition activity of resveratrol analogues. *Bioorg. Chem.* **2005**, *33*, 22–33.
(32) Femia, A. P.; Caderni, G. Rodent models of colon carcinogenesis for the study of chemopreventive activity of natural products. *Planta Med.* **2008**, *74*, 1602–1607.
(33) Tessitore, L.; Davit, A.; Sarotto, I.; Caderni, G. Resveratrol depresses the growth of colorectal aberrant crypt foci by affecting bax and p21(CIP) expression. *Carcinogenesis* **2000**, *21*, 1619–1922.
(34) Sengottuvelan, M.; Deeptha, K.; Nalini, N. Influence of dietary resveratrol on early and late molecular markers of 1,2-dimethylhydrazine-induced colon carcinogenesis. *Nutrition* **2009**, *25*, 1169–1176.
(35) Sengottuvelan, M.; Nalini, N. Dietary supplementation of resveratrol suppresses colonic tumour incidence in 1,2-dimethylhydrazine-treated rats by modulating biotransforming enzymes and aberrant crypt foci development. *Br. J. Nutr.* **2006**, *96*, 145–153.
(36) Ziegler, C. C.; Rainwater, L.; Whelan, J.; McEntee, M. F. Dietary resveratrol does not affect intestinal tumorigenesis in Apc(Min/+) mice. *J. Nutr.* **2004**, *134*, 5–10.
(37) Sale, S.; Tunstall, R. G.; Ruparelia, K. C.; Potter, G. A.; et al. Comparison of the effects of the chemopreventive agent resveratrol and its synthetic analog trans 3,4,5,4′-tetramethoxystilbene (DMU-212) on adenoma development in the Apc(Min+) mouse and cyclooxygenase-2 in human-derived colon cancer cells. *Int. J. Cancer* **2005**, *115*, 194–201.

Received for review February 19, 2010. Revised manuscript received May 14, 2010. Accepted May 23, 2010. Supported by the Ministerio de Ciencia y Tecnología Grants AGL2005-05728 and AGL2009-12866 and the Generalitat de Catalunya Grants 2005-SGR-00632 and 2009-SGR-00471. We thank the staff of the Clinical Analysis department of CAP Just Oliveras (Hospitalet de Llobregat, Spain) for excellent technical assistance.

Resultats ~ Capítol 3

CAPÍTOL 3. ESTUDI DE L'EFECTE DEL *trans*-RESVERATROL EN UN MODEL DE COLITIS ESPONTÀNIA EN RATOLÍ

Els resultats obtinguts han donat lloc a la següent comunicació a congressos:

- *Efecto del trans-resveratrol en un modelo de colitis espontánea en ratones mdr1a*$^{-/-}$
  Alfaras, I., Juan, M.E., Planas, J.M.

  Presentada com a pòster en el congrés:

  XXXIII Congreso de la Sociedad Española de Bioquímica y Biología Molecular (SEBBM)
  Còrdova, 14 - 17 de setembre de 2010

3.1. Introducció

La malaltia inflamatòria intestinal (MII), la qual inclou la colitis ulcerosa i la malaltia de Crohn, és un trastorn inflamatori crònic de l'intestí en el que els pacients pateixen sagnat rectal, diarrea severa, dolor abdominal, febre i pèrdua de pes (Koboziev *et al.*, 2010). A la malaltia de Crohn es pot veure afectada qualsevol part de l'intestí, tot i que majoritàriament les lesions estan localitzades a la part terminal de l'ili i/o principi del còlon. La colitis ulcerosa, en canvi, comença des del recte i s'estén cap a les parts més proximals del còlon (D'Haens, 2010). L'origen d'aquesta malaltia és idiopàtic, malgrat que es creu que està causada per la influència de diversos gens en combinació amb un conjunt de factors mediambientals (Xavier i Podolsky, 2007).

El *multidrug resistance protein* 1 (*MDR1*) és un gen que codifica la P-gp en els éssers humans però que ve codificada per 2 gens diferents en ratolí, *Mdr1a* i *Mdr1b*. Aquesta proteïna és un transportador de membrana que es creu que juga un paper important en el metabolisme del colesterol, en la regulació de la diferenciació cel·lular, la proliferació i la supervivència cel·lular entre d'altres (Wilk *et al.*, 2005). Aquest transportador ha estat molt estudiat com a mediador en la resistència a fàrmacs associat a diferents tipus de càncers. En el teixit sa, la seva expressió està involucrada en processos que afecten la biodisponibilitat i subseqüent resposta dels fàrmacs (Annese *et al.*, 2006). L'evidència més notable de la importància fisiològica de la P-gp en el tracte gastrointestinal ve donada per la descripció d'un model en ratolins que no expressen aquesta proteïna (ratolins *Mdr1a*$^{-/-}$) (Annese *et al.*, 2006). En ratolins, la pèrdua d'aquest mecanisme d'efluxió de xenobiòtics comporta el desenvolupament espontani d'inflamació intestinal amb moltes similituds amb la colitis humana (Collett *et al.*, 2008). Els ratolins *Mdr1a*$^{-/-}$ no mostren cap immunodeficiència primària i, per tant, el defecte està associat directament als canvis en la funció de la barrera epitelial i/o en la resposta a la flora bacteriana (Ho *et al.*, 2003; Collett *et al.*, 2008). Hi ha un engruiximent de la mucosa i evidències d'infiltrat de cèl·lules inflamatòries a la *lamina propria*. Els abscessos a les criptes i les ulceracions que s'estenen al llarg de la mucosa intestinal humana també apareixen en la malaltia espontània d'aquests ratolins (Wilk *et al.*, 2005).

Nombrosos estudis dels efectes del *trans*-resveratrol indiquen que és un potent antiinflamatori (Gautam i Jachak, 2009). El *trans*-resveratrol realitza la seva activitat antiinflamatòria mitjançant la inhibició de la cascada de l'NF-κB disminuint la transcripció de l'ADN així com disminueix l'expressió de citocines inflamatòries (Bisht *et al.*, 2010). Per tant, en aquest estudi es va voler avaluar l'efecte de 60 mg/kg de *trans*-resveratrol administrats via oral un cop al dia durant 21 dies en un model de colitis espontània severa en ratolins *Mdr1a*$^{-/-}$.

3.2. Material i mètodes

3.2.1. Preparació de la solució de *trans*-resveratrol

El *trans*-resveratrol pur es va obtenir de Second Pharma Co., Ltd. (Shangyu, P.R. China). Totes les activitats experimentals que implicaren la manipulació de *trans*-resveratrol es van realitzar sota llum vermella per evitar la isomerització fotoquímica de la forma *trans*- a la *cis*-. El *trans*-resveratrol és parcialment soluble en aigua, per aquest motiu es va utilitzar la 2-hidroxipropil-β-ciclodextrina (ref. 332607, Sigma-Aldrich, St. Louis, EUA) a una concentració final del 20% (v/v) com a solvent. En primer lloc es va preparar una solució mare de ciclodextrina al 40%, que es mantingué en una ampolla de vidre topazi a 4ºC. Per poder solubilitzar el *trans*-resveratrol es va dissoldre en la meitat del volum final amb ciclodextrina al 40%. Un cop es solubilitzà completament es va afegir la quantitat suficient d'aigua mQ per obtenir una solució final de ciclodextrina al 20%. Les solucions de *trans*-resveratrol es van preparar sempre just abans de ser administrades.

3.2.2. Animals d'experimentació

S'utilitzaren ratolins femella *Mdr1a*$^{-/-}$ (FVB.129P2-*Abcb1a*^{tm1Bor}N7) i com a control els ratolins consanguinis no modificats genèticament (FVB). Els animals es van mantenir en condicions lliures de patògens (SPF, acrònim anglès de *Specific Pathogen Free*), amb temperatura (22 ± 3ºC) i humitat (50 ± 10%) controlades i amb cicles de llum-foscor de 12 hores al servei d'estabulari animal del Parc Científic de Barcelona. A l'edat de 12 setmanes es traslladaren a l'estabulari de la Facultat de Farmàcia de la Universitat de Barcelona, sota les mateixes condicions de temperatura, humitat i cicles de llum-foscor però en condicions no SPF. Els animals van rebre una dieta control (Harlan, Espanya) i aigua *ad libitum*.

3.2.3. Tractament

S'establiren els següents grups experimentals:

- *Wild-type* Control (n = 9): ratolins no modificats genèticament administrats amb solvent.
- *Mdr1a*$^{-/-}$ Control (n = 7): ratolins que no expressen la proteïna MDR1A administrats amb solvent.
- *Wild-type* RSV (n = 13): ratolins no modificats genèticament administrats amb 60 mg/kg de *trans*-resveratrol.
- *Mdr1a*$^{-/-}$ RSV (n = 13): ratolins que no expressen la proteïna MDR1A tractats amb 60 mg/kg de *trans*-resveratrol.

Els 4 grups experimentals s'administraren per via oral mitjançant una sonda intragástrica durant 21 dies. El volum administrat va ser de 10 mL/kg, que es va ajustar segons el pes corporal de l'animal.

Durant tot el procés es va controlar el pes corporal així com el consum d'aigua i de pinso. L'administració dels ratolins es realitzà a primera hora del matí. La manipulació dels animals així com el sacrifici es va dur a terme segons els procediments autoritzats pel Comitè Ètic d'Experimentació Animals de la Universitat de Barcelona i seguint les recomanacions de la Federation of European Laboratory Animal Science Associations (1995).

3.2.4. Obtenció de mostres

Els ratolins s'anestesiaren amb xilacina (Rompun® Bayer Leverkusen, Alemanya) i ketamina (Imalgene® 500 Rhône Mérieux, Lyon, França), a una dosi de 0,1% i 0,01% volum/pes corporal. Es va realitzar una laparotomia i es va extreure l'intestí prim i el còlon. Es rasparen les mucoses del jejú i l'ili i es pesaren. Es va mesurar el pes humit del còlon i, posteriorment, es van tallar dos trossos de 5 mm cadascun de la part més distal (pròxima al recte) que es disposaren en uns cassets d'histologia.

3.2.5. Estudi histopatològic del còlon

El teixit disposat en els cassets es va mantenir en paraformaldehid al 4% (en una proporció de 40:1 de paraformaldehid:teixit). La preparació en blocs de parafina i el seu posterior estudi histopatològic es va realitzar al Servei d'Anatomia Patològica de l'Hospital Universitari Vall d'Hebron. Es va avaluar la presència d'inflamació de la làmina pròpia, criptitis, abscessos a la cripta, úlceres, inflamació transmural, depleció de moc i fibrosi. La valoració de les lesions es va fer de 0 (teixit que no presenta lesions) a 3 (màxima puntuació per a una lesió).

3.2.6. Tractament de les dades

Tots els resultats s'expressen com a mitjana i error estàndard. L'anàlisi estadística es va dur a terme amb el programa GraphPad Prism 4.03. L'evolució del pes corporal al llarg del temps es va analitzar amb una ANOVA de 2 factors seguit del test de Bonferroni. La resta de dades s'analitzaren mitjançant una ANOVA d'1 factor seguit del test de Bonferroni. Els valors de $P < 0,05$ es consideraren com a diferències estadísticament significatives.

3.3. Resultats

3.3.1. Pes corporal

A l'inici de l'experiment el pes dels ratolins *Mdr1a*$^{-/-}$ va ser un 11% inferior al dels ratolins *wild-type* (Figura III.14.). Després de 21 dies, el pes corporal del ratolins *Mdr1a*$^{-/-}$ Control i *Mdr1a*$^{-/-}$ RSV va ser un 13% i un 15% inferior, respectivament, en comparació als ratolins *wild-type* Control (P < 0,001). El tractament amb *trans*-resveratrol no va afectar el pes dels ratolins *wild-type* ni dels *Mdr1a*$^{-/-}$, respecte els seus controls.

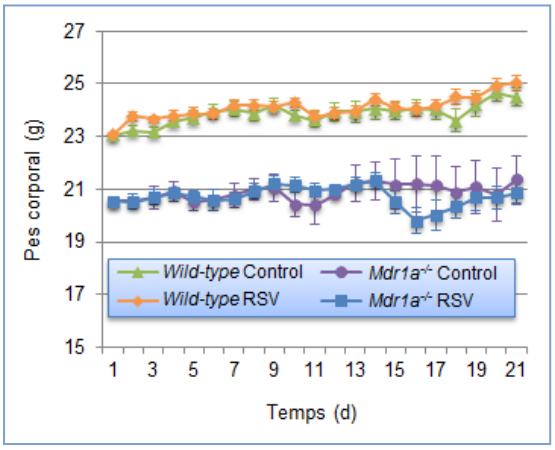

Figura III.14. Evolució del pes corporal. Els resultats s'expressen com a mitjana ± error estàndard (n = 7-13). Diferències significatives entre els grups *wild-type* i els grups *Mdr1a*$^{-/-}$ (P > 0,01).

3.3.2. Consum de pinso i aigua

En relació al consum de pinso (Figura III.15.), es va observar que els animals *wild-type* i *Mdr1a*$^{-/-}$ administrats amb *trans*-resveratrol menjaven un 22% i un 32% menys de pinso al dia, respectivament, que els ratolins no administrats amb el polifenol (P < 0,001). En canvi, el consum d'aigua per rata i dia va ser inferior en els ratolins no modificats genèticament FVB, respecte els *Mdr1a*$^{-/-}$ (Figura III.16.). Els ratolins *Mdr1a*$^{-/-}$ Control van beure un 44% més d'aigua al dia que els *wild-type* Control (P < 0,01) i els *Mdr1a*$^{-/-}$ tractats un 39% més d'aigua al dia que els *wild-type* RSV (P < 0,01).

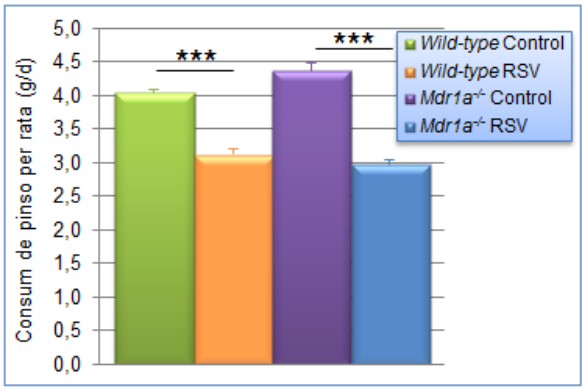

Figura III.15. Consum de pinso per rata i dia. Els resultats s'expressen com a mitjana + error estàndard (n = 7-13). ***P > 0,001.

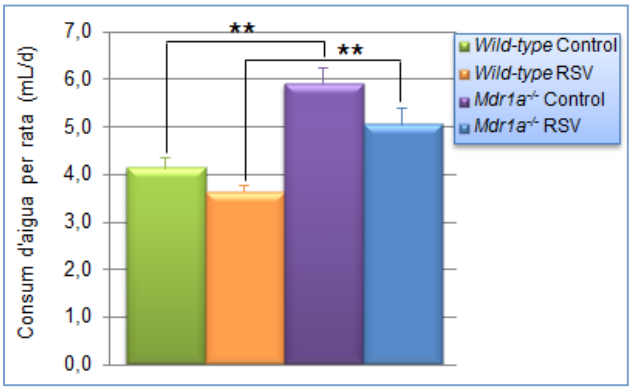

Figura III.16. Consum d'aigua per rata i dia. Els resultats s'expressen com a mitjana + error estàndard (n = 7-13). **P > 0,01.

3.3.3. Pes de les mucoses de jejú i ili i pes del còlon

Els pesos de les mucoses del jejú i l'ili no van mostrar diferències entre ratolins *wild-type* o ratolins *Mdr1a*$^{-/-}$. Els ratolins amb colitis i administrats amb *trans*-resveratrol van mostrar el pes de la mucosa més elevat que el dels ratolins *wild-type*, tant en el cas dels control com dels RSV. El pes del còlon dels animals *Mdr1a*$^{-/-}$ Control que presentaren colitis espontània era un 200% més elevat que el dels *wild-type* Control i el pes del còlon dels *Mdr1a*$^{-/-}$ tractats amb *trans*-resveratrol un 206% més que el dels *wild-type* RSV, indicant inflamació en ambdós casos (Figura III.17.). No obstant, el tractament amb *trans*-resveratrol no va disminuir el pes del còlon dels animals que presentaven colitis i no va modificar el dels ratolins sans.

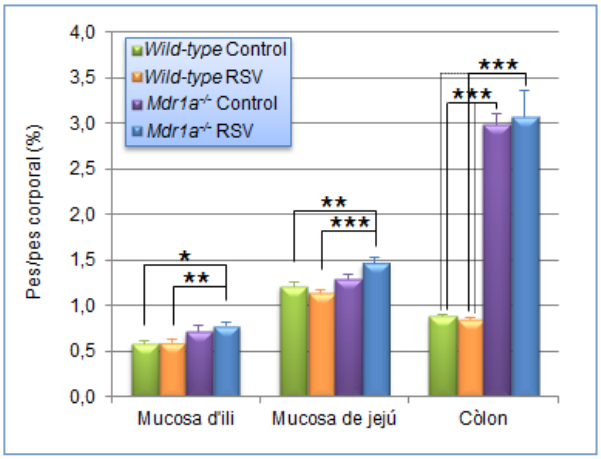

Figura III.17. Pes de les mucoses de jejú i ili i pes del còlon normalitzat pel pes corporal. Els resultats s'expressen com a mitjana + error estàndard (n = 7-13). **P* < 0,05; ***P* < 0,01; ****P* < 0,001.

3.3.4. Estudi histopatològic del còlon

L'estudi histopatològic no mostrà cap efecte a conseqüència del tractament amb *trans*-resveratrol. La valoració obtinguda en l'estudi de les lesions al còlon va ser de 10,9 ± 1,49 en els ratolins *Mdr1a*$^{-/-}$ Control i d'11,6 ± 1,48 en els ratolins *Mdr1a*$^{-/-}$ RSV. En canvi, no es van observar lesions en els animals no modificats genèticament (Figura III.18.).

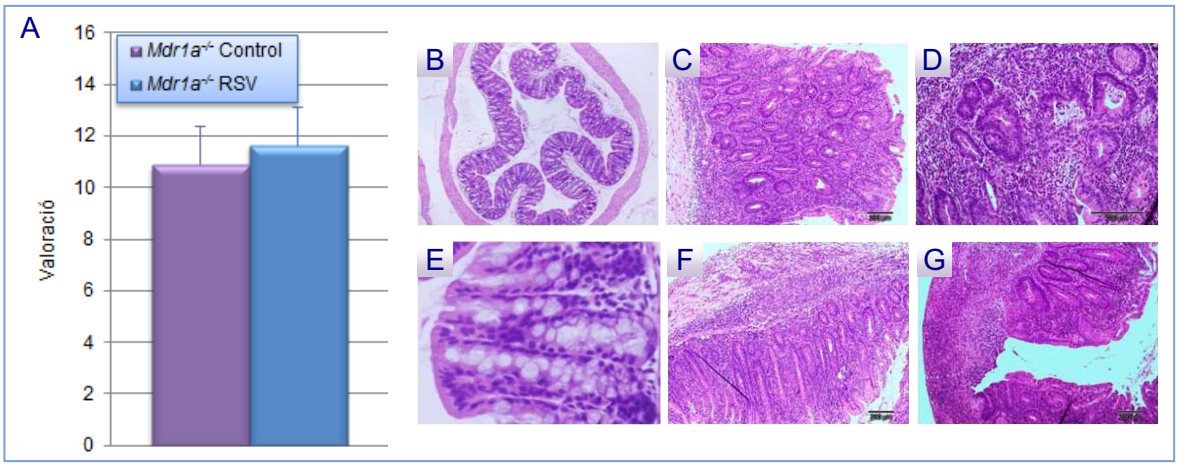

Figura III.18. Estudi histopatològic del còlon. A) Valoració de les lesions observades en l'estudi histopatològic del còlon. Els resultats s'expressen com a mitjana + error estàndard (n = 7-13). No s'observen diferències significatives. B-G) Imatges representatives del còlon dels ratolins *wild-type* i *Mdr1a*$^{-/-}$. B i E) Còlon sa. C i D) Abscessos a les criptes. F) Infiltració. G) Ulceració.

3.4. Discussió

El model emprat per a l'estudi de l'efecte del *trans*-resveratrol sobre la colitis és un model instaurat del qual no es coneixen bé les causes que provoquen el desenvolupament de la malaltia (Collett *et al.*, 2008). El desenvolupament de la MII que es produeix als ratolins *Mdr1a*$^{-/-}$ es va estudiar a diferents laboratoris i sembla tenir moltes similituds a la colitis humana (Collet *et al.*, 2008). La rellevància d'aquest model de patogènesi de la MII humana ve també recolzada pel fet que en algunes poblacions les variants al·lèliques del gen *MDR* vinculades a una disminució de l'activitat de la P-gp al teixit intestinal estan associades a un augment de la predisposició a patir colitis ulcerosa (Ho *et al.*, 2006). No obstant, els canvis moleculars pels quals la deficiència de la P-gp i la flora intestinal combinades porten a la inflamació colònica són desconegudes. Els ratolins *Mdr1a*$^{-/-}$ no mostren deficiència immunitària primària, per tant, la malaltia està associada directament amb canvis en la funció de la barrera epitelial i/o la resposta de les bactèries comensals (Collet *et al.*, 2008).

En la present tesi, es van utilitzar ratolins femella M*dr1a*$^{-/-}$ de 13 setmanes d'edat que van créixer sota condicions SPF fins a la setmana 12. El manteniment d'aquests ratolins sota aquestes condicions ja provoca l'inici d'una inflamació intestinal espontània que inclou creixement cel·lular epitelial anòmal i infiltració leucocitària a la mucosa (Panwala *et al.*, 1998), tot i que les femelles desenvolupen la malaltia més lentament que els mascles (Resta-Lenert *et al.*, 2005). Però, altrament, els animals van estar una setmana en condicions normals d'estabulació, ja que s'ha demostrat que la colitis dels ratolins M*dr1a*$^{-/-}$ comença abans, és més severa i té més prevalença quan estan en condicions convencionals i no SPF (Resta-Lenert *et al.*, 2005).

Mitjançant aquests ratolins que no expressen la P-gp, es va fer un estudi de l'efecte d'un tractament diari amb *trans*-resveratrol. Es va observar que els animals malalts tenien un pes inferior i ingerien menys pinso. Aquest efecte també es va observar en altres models de colitis com ara la colitis induïda per l'àcid 2,4,6-trinitrobenzè sulfònic (TNBS) mitjançant una instil·lació a l'anus (Martín *et al.*, 2006) o la colitis induïda per sulfat de dextran sòdic (DSS) (Larrosa *et al.*, 2009; Sanchez-Fidalgo *et al.*, 2010; Singh *et al.*, 2010). El tractament amb *trans*-resveratrol en aquests models va revertir la pèrdua de pes en la majoria dels casos, no obstant, s'ha de tenir en compte que es tracta de models d'inducció de colitis aguda i no crònica com en el model emprat.

La inflamació intestinal és una via fenotípica característica a moltes malalties i el tret causant de la MII. Per aquesta raó, també es va avaluar el pes de l'intestí prim i del còlon com a marcador d'inflamació. Es va detectar un increment en el pes del jejú, de l'ili i del

còlon d'aquells animals que desenvolupen espontàniament una colitis, el qual indicà un estat inflamatori avançat que no es va poder revertir amb el tractament amb el polifenol.

La manca d'efecte en el pes de les mucoses de l'intestí prim i el còlon també es va reflectir en l'estudi histopatològic que es va realitzar a diferents talls d'intestí. La valoració de l'estat inflamatori en l'estudi histopatològic no es va veure afectat pel tractament amb *trans*-resveratrol. No obstant, altres estudis mostraren un efecte d'aquest polifenol en els estudis histopatològics del còlon (Yao *et al.*, 2010; Cui *et al.*, 2010), tot i que la inducció de la colitis en aquests casos era concomitant a l'administració del compost.

Altres estudis *in vivo* revelaren un efecte antiinflamatori per part del *trans*-resveratrol mitjançant la disminució de les citocines proinflamatòries, com ara la IL-8, l'interferó α (IFNα) i el TNFα (Martin *et al.*, 2006; Yao *et al.*, 2010; Singh *et al.*, 2010), i augmentant les antiinflamatòries, com la interleucina IL-10 (Sanchez-Fidalgo *et al.*, 2010). També el tractament amb aquest polifenol va ser capaç de reduir diferents enzims implicats en la inflamació com la iNOS (Youn *et al.*, 2009) o la COX-2 (Martin *et al.*, 2006; Larrosa *et al.*, 2009; Singh *et al.*, 2010). També es va observar que regulava el sistema antioxidant, reduint la peroxidació lipídica i la mieloperoxidasa i augmentant la superòxid dismutasa i la glutatió peroxidasa (Yao *et al.*, 2010).

Tal i com s'ha dit prèviament, aquest efecte antiinflamatori no es va observar en l'estudi presentat. Aquesta manca d'efectivitat pot ser deguda a l'estat avançat de la malaltia intrínseca d'aquests ratolins modificats genèticament. No obstant, quan la colitis és induïda per agents químics el *trans*-resveratrol té uns efectes protectors vers la inflamació del còlon. En conclusió, el tractament amb una dosis de 60 mg/kg de *trans*-resveratrol no millora la colitis espontània en estat avançat que es desenvolupa als ratolins *Mdr1a*$^{-/-}$.

Resultats ~ Capítol 4

CAPÍTOL 4. AVALUACIÓ DE LA PARTICIPACIÓ DE LES PROTEÏNES ABC INVOLUCRADES EN LA RESISTÈNCIA A FÀRMACS EN L'ABSORCIÓ I DISTRIBUCIÓ DEL *trans*-RESVERATROL.

Aquest capítol es troba desglossat en dos apartats. Els resultats del primer es troben recollits a l'article 3. El segon apartat està redactat en català en format d'article i inclou els nivells plasmàtics del *trans*-resveratrol i els seus conjugats en ratolins que no expressen el transportador MDR1A i ratolins no modificats genèticament.

Article 3:

Involvement of breast cancer resistance protein (BCRP1/ABCG2) in the bioavailability and tissue distribution of trans-resveratrol in knockout mice.

Alfaras, I., Pérez, M., Juan, M.E., Merino, G., Prieto, J.G., Planas, J.M., Alvarez, A.I.

J. Agric. Food Chem. 2010, 58, 4523-4528

Els resultats obtinguts han donat lloc a les següents comunicacions a congressos:

- *Implicación de BCRP en la eliminación intestinal y la distribucion tisular del trans-resveratrol y sus formas conjugadas*

  Perez, M., Alfaras, I., Juan, M.E., Merino, G., Prieto, J.G., Planas, J.M., Alvarez, A.I.

  Presentada com a pòster en el congrés:

  XXXI Congreso de la Sociedad Española de Bioquímica y Biología Molecular

  Bilbao, 10 - 13 de setembre de 2008

- *Involvement of breast cancer resistance protein on the bioavailability of trans-resveratrol in knockout mice.*

  Alfaras, I., Perez, M., Juan, M.E., Merino, G., Prieto, J.G., Alvarez, A.I., Planas, J.M.

  Presentada com a pòster en el congrés:

  5th International Meeting, Advances in Antioxidants (Trace Elements, Vitamins and Polyphenols): Molecular mechanisms, nutritional and Clinical Aspects

  Monastir – Sousse, Tunísia, 11 - 15 d'octubre de 2008

- *Plasmatic concentrations of trans-resveratrol in P-glycoprotein knockout mice and wild-type FVB.*
  Alfaras, I., Juan, M.E., Pérez-Bosque, A., Moretó, M., Planas, J.M.

  Presentada com a pòster en el congrés:

  4th International Conference on Polyphenols and Health (ICPH2009)
  Harrogate, Anglaterra, 7 - 11 de desembre de 2009

Involvement of Breast Cancer Resistance Protein (BCRP1/ABCG2) in the bioavailability and tissue distribution of *trans*-resveratrol in knockout mice

J. Agric. Food Chem. 2010, 58, 4523-4528

4.1. Resum de l'article

Objectius: Estudis amb tècniques de perfusió en intestí indiquen que el *trans*-resveratrol és absorbit per difusió passiva, metabolitzat a les cèl·lules intestinals en glucurònid i sulfat els quals són excretats al lumen intestinal a través de les proteïnes MRP2 i BCRP. Donada la importància que va presentar la proteïna BCRP en l'efluxió dels conjugats del *trans*-resveratrol es va estudiar en ratolins que no expressen aquest transportador (*Mdr1a*$^{-/-}$) la biodisponibilitat i la distribució en teixits d'aquest polifenol.

Material i mètodes: S'utilitzaren ratolins mascle *Mdr1a*$^{-/-}$ i consanguinis no modificats genèticament (FVB) com a controls, que van ser administrats amb una única dosis de 60 mg/kg de *trans*-resveratrol. Es va extreure sang als 5, 10 i 30 minuts. Els animals es van sacrificar als 10 i 30 minuts i es va obtenir el contingut intestinal, l'intestí prim, el cervell, el cor, el fetge, els ronyons i els pulmons. Les concentracions plasmàtiques de *trans*-resveratrol i els seus conjugats es van determinar seguint un mètode d'extracció en fase sòlida. Es va determinar el *trans*-resveratrol i els seus conjugats glucurònid i sulfat a la sang, el cervell, el fetge, el cor, els ronyons i els pulmons segons el descrit a Juan *et al.* (2010b).

L'extracció del polifenol i els seus conjugats de l'intestí prim es va fer amb metanol al 80% i àcid acètic al 2,5% agitant durant 2 minuts i deixant reposar 24 hores a 4ºC. Després de centrifugar, el sobrenedant es va recollir i evaporar fins a 400 µL que s'analitzaren per HPLC. La determinació a contingut intestinal es va realitzar mitjançant dues extraccions seguides mantenint el contingut intestinal en agitació constant a 60ºC durant 30 minuts amb metanol al 80% i àcid acètic al 2,5%. Després de centrifugar, els sobrenedants es van evaporar fins a 400 µL que es van analitzar per HPLC. La fase mòbil utilitzada a l'HPLC estava formada per un solvent A, àcid acètic al 3%, i un solvent B que consistia en el 20% de solvent A i el 80% d'acetonitril. Els cromatogrames es van obtenir a la longitud d'ona de 306 nm, màxim d'absorbància del *trans*-resveratrol.

Resultats: Les determinacions realitzades mostraren una elevada influència de la proteïna transportadora BCRP1 en la biodisponibilitat del *trans*-resveratrol. A l'intestí prim es va observar una disminució de les concentracions de glucurònid i sulfat als 30 minuts del 68% i del 87%, respectivament. A contingut intestinal també es va produir una reducció del glucurònid d'un 34% i d'un 71% a 10 i 30 minuts, respectivament, i el sulfat va disminuir un 95% i un 97%, respectivament. A plasma, l'àrea sota la corba (AUC) del

resveratrol es va reduir en un 44% mentre que la del glucurònid i la del sulfat van augmentar un 34% i un 392%, respectivament. En ronyons i pulmons s'observà una acumulació de *trans*-resveratrol i conjugats en els ratolins *Bcrp1*$^{-/-}$. En canvi, a fetge les concentracions de *trans*-resveratrol i glucurònid van ser similars en ambdós tipus de ratolins, tot i que el sulfat va augmentar en els *Bcrp1*$^{-/-}$.

Conclusions: En conclusió, la proteïna transportadora BCRP1 està implicada en la biodisponibilitat i la distribució en teixits del *trans*-resveratrol i els seus conjugats sent l'intestí, els ronyons i els pulmons els òrgans més afectats.

JOURNAL OF AGRICULTURAL AND FOOD CHEMISTRY
ARTICLE

J. Agric. Food Chem. 2010, 58, 4523–4528 4523
DOI:10.1021/jf9042858

Involvement of Breast Cancer Resistance Protein (BCRP1/ABCG2) in the Bioavailability and Tissue Distribution of *trans*-Resveratrol in Knockout Mice

Irene Alfaras,[†] Míriam Pérez,[‡] Maria Emília Juan,[†] Gracia Merino,[§] Julio Gabriel Prieto,[‡] Joana Maria Planas,[†] and Ana Isabel Álvarez*,[‡]

[†]Grup de Fisiologia i Nutrició Experimental, Departament de Fisiologia (Farmàcia) and Institut de Recerca en Nutrició i Seguretat Alimentària (INSA), Universitat de Barcelona, Av. Joan XXIII s/n, E-08028 Barcelona, Spain, [‡]Departamento de Ciencias Biomédicas, Área de Fisiología, Universidad de León, Campus Vegazana s/n, E-24071 León, Spain, and [§]Instituto de Sanidad Animal y Desarrollo Ganadero, Universidad de León, Campus Vegazana, E-24071 León, Spain

trans-Resveratrol undergoes extensive metabolism in the intestinal cells, which leads to the formation of glucuronide and sulfate conjugates. Given the important role of the breast cancer resistance protein (ABCG2/BCRP) in the efflux of conjugated forms, the present study investigates the bioavailability and tissue distribution of *trans*-resveratrol and its metabolites after the oral administration of 60 mg/kg in Bcrp1$^{-/-}$ mice. *trans*-Resveratrol and its metabolites were measured in intestinal content, plasma and tissues by HPLC. At 30 min after administration, intestinal content showed decreases of 71% and 97% of resveratrol glucuronide and sulfate, respectively, in Bcrp1$^{-/-}$, indicating a lower efflux from the enterocytes. Furthermore, the area under plasma concentration curves (AUC) of these metabolites increased by 34% and 392%, respectively, whereas a decrease in the AUC of *trans*-resveratrol was found. In conclusion, Bcrp1 plays an important role in the efflux of resveratrol conjugates, contributing to their bioavailability, tissue distribution and elimination.

KEYWORDS: Bioavailability; Bcrp1$^{-/-}$ mice; distribution; HPLC-DAD; *trans*-resveratrol

INTRODUCTION

The breast cancer resistance protein (BCRP/ABCG2) and its murine homologue Bcrp1 belong to the ATP binding cassette (ABC) transmembrane drug transporter family. BCRP is constitutively expressed in healthy tissues, including the intestine, liver, blood−brain barrier, breast and placenta, as well as in tumors, where it is one mechanism contributing to multidrug resistance (*1*). Its location on the apical membrane of epithelial cells of the intestine suggests its strategic function as a protective efflux pump that increases the elimination of ingested xenobiotics and drugs (*2*). In the liver, this transporter has been found in the canalicular membrane, hepatocytes, bile duct, reactive bile ductules and blood vessel endothelium (*3*), thus playing a role in the biliary excretion of drugs, xenobiotics and metabolites (*1*). In kidney, BCRP was located in the brush border membrane of proximal tubules (*4*), suggesting its possible involvement in renal drug excretion. Overall, BCRP favors the excretion of endogenous and exogenous compounds into bile, feces and urine, and dramatically influences the pharmacokinetics of many drugs and dietary bioactive compounds (*1*).

trans-Resveratrol (*trans*-3,4′,5-trihydroxystilbene) is a polyphenol present in grapes, red wine, peanuts and various berries (*5*). This naturally occurring molecule, known as a phytoalexin, is synthesized by plants in response to stress, injury, UV radiation and fungal infections. *trans*-Resveratrol holds a wide range of pharmacological properties (*6*) with no harmful effects (*7*). Numerous biochemical and molecular actions seem to contribute to *trans*-resveratrol effects in different human disease models. The health-protecting properties of this phytoalexin include cardioprotective (*8*), neuroprotective (*9*), spermatogenesis-enhancing (*10*), antiaging (*11*) and cancer chemopreventive actions (*12*). However, these beneficial effects may be affected by its low oral bioavailability, as shown in studies on both laboratory animals and humans (*5*).

Recently, we studied the intestinal absorption of this polyphenol, using an *in vivo* perfusion technique in Sprague−Dawley rats (*13*). Our results showed that, although *trans*-resveratrol quickly enters the enterocyte, it is highly metabolized to glucuronide and sulfate, which are secreted back to the intestinal lumen through multidrug resistance protein 2 (MRP2) and BCRP. All these processes contributed to the limited intestinal net absorption of this polyphenol. Given that BCRP is involved in the intestinal secretion of *trans*-resveratrol conjugates, the present study investigates the bioavailability and tissue distribution of *trans*-resveratrol after the oral administration of 60 mg/kg in a knockout mouse model for this transporter. Transgenic rodent models in which specific proteins are deleted provide a powerful tool for examining the complex processes involved in the bioavailability of *trans*-resveratrol.

*Corresponding author. Tel: +34987291265. Fax: +34987291267. E-mail: aialvf@unileon.es.

Published on Web 03/16/2010

MATERIALS AND METHODS

Chemicals. *trans*-Resveratrol was chemically pure and purchased from Second Pharma Co., Ltd. (Shangyu, P. R. China). All laboratory procedures involving the manipulation of *trans*-resveratrol were performed in dim light to avoid its photochemical isomerization to the *cis* form. Acetonitrile and methanol were from J. T. Baker (Deventer, Netherlands) and acetic acid from Scharlau Chemie S.A. (Barcelona, Spain). β-Glucuronidase (type L-II, *Patella vulgata*) and sulfatase (type H-1, *Helix pomatia*) were from Sigma-Aldrich (St. Louis, MO). All these solvents were HPLC grade. Other chemicals used were analytical grade and obtained from Sigma-Aldrich. Water used in all experiments was passed through a Milli-Q water purification system (18 MΩ) (Millipore, Milan, Italy).

Animal Experiments. Mice were housed and handled according to procedures approved by the Research Committee of Animal Use of the University of León (Spain) and performed according to the "Principles of Laboratory Animal Care" and the European guidelines described in EC Directive 86/609. The animals used in the experiments were Bcrp1$^{-/-}$ and wild-type mice (9−14 wk), all of >99% FVB genetic background. The Bcrp1$^{-/-}$ mice were kindly supplied by Dr. A. H. Schinkel from The Netherlands Cancer Institute. Animals were kept in a temperature-controlled environment with a 12 h light/12 h dark cycle. They received a standard rodent diet (Panlab SA, Barcelona, Spain) and water was available *ad libitum*.

trans-Resveratrol was administered intragastrically by oral gavage feeding in overnight fasted mice, as an aqueous solution of 20% hydroxypropyl β-cyclodextrin at the single dose of 60 mg/kg at a constant volume of 10 mL/kg. Blood samples were taken at 5, 10, and 30 min and placed in tubes containing EDTA-K2 as anticoagulant. Plasma was immediately obtained by centrifugation at 1500*g* for 15 min at 4 °C, immediately frozen in liquid nitrogen and kept at −80 °C until analysis.

For the tissue distribution study of *trans*-resveratrol, a group of 4 mice were killed at 10 min and another at 30 min by cervical dislocation. Small intestine was removed, and the intestinal content was collected. Subsequently, brain, heart, liver, kidney and lungs were rapidly excised and washed with NaCl 0.9% to remove residual blood containing *trans*-resveratrol and its metabolites. Tissues were wiped with filter paper, weighed, immediately frozen in liquid nitrogen and kept at −80 °C until analysis.

Determination of *trans*-Resveratrol and Its Metabolites in Intestinal Content. Intestinal content samples were defrosted at room temperature, and 10 mL of 80% methanol, with 2.5% acetic acid and 10 μL of 15% ascorbic acid as antioxidant, was added. The mixture was shaken with constant stirring for 30 min at 60 °C. Then, samples were transferred to a centrifuge tube and the remaining content in the beaker was gathered with an additional 2 mL of acidified methanol. The homogenates were centrifuged at 33000*g* (Centrikon H-401, Kontron Hermle Instruments, Italy) for 30 min at 4 °C. The supernatant was transferred to a clean tube, and the residue was extracted one more time following the same procedure. The organic solvent of the supernatant was evaporated with a Concentrator 5301 (Eppendorf Iberica S.L., San Sebastián de los Reyes, Spain) at 45 °C to a final volume of 400 μL, which was then placed in a sealed amber vial for HPLC analysis.

Determination of *trans*-Resveratrol and Its Metabolites in Tissues. The defrosted small intestine was placed in a conical tube, and 4 mL of methanol (80%, v/v) acidified with acetic acid (2.5%, v/v) and 10 μL of ascorbic acid (15%, v/v), as antioxidant, was added to the same tube. The entire tissue was stirred for 2 min and kept overnight at 4 °C. After this, the intestine was stirred again for 2 min and centrifuged at 1500*g* for 30 min at 4 °C (Megafuge 1.0R, Heraeus, Boadilla, Spain). The supernatant was placed in a clean tube. The organic solvent of the supernatant was evaporated to a final volume of 400 μL, and placed in a sealed amber vial for HPLC analysis.

The other tissues were finely minced with scissors and placed in a homogenizer vessel, following the validated method described elsewhere (*14*). Briefly, methanol acidified with acetic acid and 10 μL of ascorbic acid was added, and tissues were subsequently homogenized. The homogenization process was adjusted to each tissue. Brain and testes were placed in 3 mL of acidified methanol and ground by a manual glass homogenizer with 30 strokes. An additional 1 mL was used to collect the residues in the glass vase and was added to the initial 3 mL. However, liver, lungs and kidney were homogenized with 6 short pulses of a Polytron tissue homogenizer (Kinematica AG, Lucerne, Switzerland) using 2 mL of acidified methanol. The homogenizer was cleaned twice with 1 mL of acidified methanol, which was added to the 2 mL, making a final volume of 4 mL.

Homogenized samples were transferred to a 10 mL conical glass tube and processed in the vortex for 5 min prior to centrifugation at 1500*g* for 30 min at 4 °C. The supernatant was placed in a clean tube. The residue was extracted twice more with 4 mL of acidified methanol by vigorous shaking in the vortex for 5 min, followed by centrifugation at 3000*g* for 30 min at 4 °C. The organic solvent of the supernatants was evaporated to a final volume of 400 μL and subsequently placed in a sealed amber vial for HPLC analysis.

Determination of *trans*-Resveratrol and Its Metabolites in Plasma. Resveratrol was extracted from plasma samples on a reversed-phase C18 Sep-Pak Classic Cartridge for manual operation (WAT051910, Waters, Milford, MA), using a method described previously (*14*). Briefly, plasma was acidified with acetic acid (30 μL/mL of plasma), stirred in the vortex for 2 min, and slowly loaded onto the cartridge, which was rinsed with water (10 mL/mL of plasma). *trans*-Resveratrol and metabolites contained in the cartridge were eluted with 4 mL of methanol. Ten microliters of ascorbic acid at 15% was added to the eluted liquid, which was evaporated to a final volume of 400 μL. Finally, this was placed in a sealed amber vial for HPLC analysis.

HPLC Analyses. An Agilent model 1100 (Agilent Technologies, Palo Alto, CA) gradient liquid chromatograph equipped with an automatic injector, a Synergi Fusion-RP 80A (250 × 4.6 mm; 4 μm) (Phenomenex, Torrance, CA) with a C18 guard column cartridge, and a diode array UV−visible detector coupled to a ChemStation were used. The temperature of the column was kept at 40 °C. The flow rate was 1.5 mL/min, and injection volume was 100 μL. The mobile phase consisted of two phases: phase A was a 3% acetic acid solution, and phase B was a mixture of phase A:acetonitrile (20:80, v/v). The gradient elution differed, depending on the samples. Plasma: min 0 with 22% solvent B to min 2; 2−6 min, linear gradient from 22 to 30% B; 6−14 min, linear from 30 to 50% B; 14−18 min, increasing to 60% B; 18−25 min, linear from 60 to 100% B; followed by washing and reconditioning the column. Tissue samples and intestinal content: 0−5 min, 15% B; 7 min, 20% B; 10 min, 21% B; 20 min, 22% B; 30 min, 30% B; 35 min, 35% B; 40 min, 40% B; 45 min, 50% B; 50 min, 70% B; 55−60 min, 100% B; 62 min, 15% B. There was a 5 min delay prior to the injection of the next sample to ensure re-equilibration of the column.

The chromatograms were obtained according to the retention time, with detection at 306 nm (**Figure 1**), at which the absorbance of *trans*-resveratrol reaches a maximum. Resveratrol was initially identified using comparative retention times of pure standard and photodiode array spectra (from 200 to 400 nm). The identity of all peaks was confirmed by HPLC−MS (**Figure 1**). *trans*-Resveratrol was quantified by using standard curves constructed after spiking relevant concentrations of it in the appropriate sample matrix, either plasma or homogenized tissues. The curves were characterized by regression coefficients of $R^2 = 0.99$ or above. *trans*-Resveratrol glucuronide and sulfate were quantified after hydrolysis by means of enzyme treatment, as already described (*14*).

Statistical Analysis. All data are given as means ± SEM. Tissue concentrations were analyzed by 1-way ANOVA followed by Bonferroni's *post hoc* test. Statistical differences of plasma concentrations were compared by means of 2-way ANOVA. When the effects were significant, differences between means were assessed with Bonferroni's *post hoc* test. Differences were considered statistically significant when $p < 0.05$.

RESULTS

***trans*-Resveratrol and Resveratrol Glucuronide and Sulfate Concentration in Small Intestine.** No differences were observed in the concentrations of *trans*-resveratrol in the small intestine of wild-type or Bcrp1$^{-/-}$ mice (**Table 1**). The glucuronide and sulfate conjugates were detected at 10 min in wild-type and Bcrp1$^{-/-}$ animals, with no differences between groups. However, at 30 min, the concentrations of *trans*-resveratrol glucuronide and sulfate were inhibited by 68% ($p < 0.05$) and 87% ($p < 0.001$), respectively, in Bcrp1$^{-/-}$ and wild-type mice.

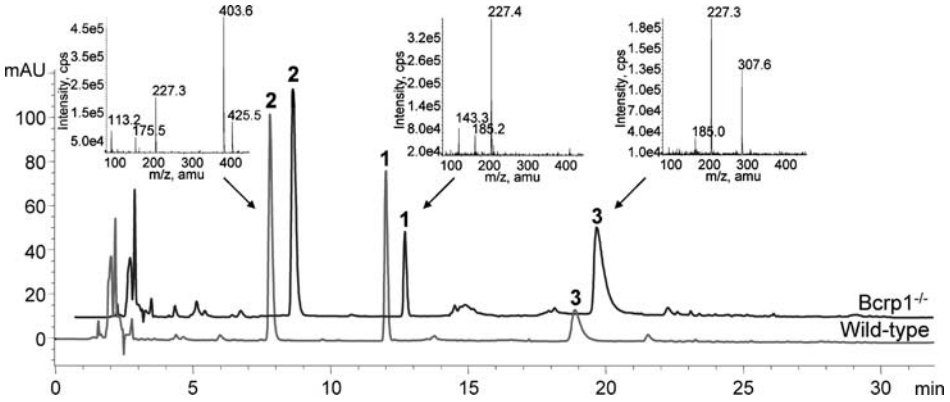

Figure 1. HPLC chromatograms at 306 nm from plasma of wild-type and Bcrp1$^{-/-}$ mice, 30 min after the oral administration of 60 mg/kg *trans*-resveratrol. Peak 1, *trans*-resveratrol; peak 2, *trans*-resveratrol glucuronide; peak 3, *trans*-resveratrol sulfate. The insets depict the full-scan product ion mass spectra of *trans*-resveratrol (1), *trans*-resveratrol glucuronide (2) and *trans*-resveratrol sulfate (3).

Table 1. Concentrations of *trans*-Resveratrol and Glucuronide and Sulfate Conjugates in Tissues and Intestinal Content of Wild-Type and Bcrp1$^{-/-}$ Mice after the Oral Administration of 60 mg/kg of *trans*-Resveratrol[a]

	trans-resveratrol		glucuronide		sulfate	
	wild-type	Bcrp1$^{-/-}$	wild-type	Bcrp1$^{-/-}$	wild-type	Bcrp1$^{-/-}$
			Small Intestine, nmol/g tissue			
10 min	314 ± 38	313 ± 74	198 ± 20	148 ± 66	35.2 ± 9.8	20.4 ± 2.3
30 min	436 ± 66	236 ± 33	345 ± 42	109 ± 25*	119 ± 11$^{\Phi}$	15.9 ± 0.6***
			Intestinal Content, nmol/g content			
10 min	1370 ± 207	1622 ± 563	215 ± 35	142 ± 17	170 ± 34	9.4 ± 4.2*
30 min	5424 ± 806$^{\Phi}$	1394 ± 458**	553 ± 15.1$^{\Phi}$	160 ± 13***	781 ± 49$^{\Phi}$	23.3 ± 7.0***
			Liver, nmol/g tissue			
10 min	5.6 ± 1.4	8.7 ± 0.9	30.2 ± 3.0	31.3 ± 5.8	9.0 ± 1.2	23.1 ± 3.5**
30 min	5.2 ± 1.3	3.6 ± 0.4$^{\varphi}$	32.1 ± 5.4	20.7 ± 3.6	12.6 ± 2.8	13.0 ± 1.3$^{\varphi}$
			Kidney, nmol/g tissue			
10 min	5.7 ± 1.2	16.1 ± 3.6**	99.6 ± 15.5	199.5 ± 13.7**	11.4 ± 2.1	31.0 ± 18.3
30 min	0.8 ± 0.4	3.2 ± 0.8$^{\Phi}$	3.0 ± 0.4$^{\theta}$	98.2 ± 19.1$^{**\theta}$	4.6 ± 1.9	3.2 ± 1.1
			Lung, nmol/g tissue			
10 min	4.8 ± 2.5	6.3 ± 2.4	9.3 ± 1.8	19.4 ± 2.0**	nd[b]	1.0 ± 0.8
30 min	2.1 ± 0.8	12.2 ± 2.2*	10.6 ± 2.9	11.6 ± 1.2$^{\varphi}$	nd	1.7 ± 0.5
			Heart, nmol/g tissue			
10 min	3.5 ± 1.2	3.2 ± 0.5	5.5 ± 1.2	12.1 ± 1.0**	nd	nd
30 min	2.5 ± 0.9	0.8 ± 0.0	12.0 ± 2.0$^{\varphi}$	13.7 ± 1.0	nd	nd
			Brain, nmol/g tissue			
10 min	0.43 ± 0.11	1.25 ± 0.56	0.54 ± 0.14	0.88 ± 0.16	0.01 ± 0.01	0.09 ± 0.03
30 min	0.82 ± 0.10	0.28 ± 0.05	1.28 ± 0.29	1.87 ± 0.75	0.36$^{\varphi}$	0.19 ± 0.12

[a] Results are expressed as the mean ± SEM (n = 3−4). Bcrp1$^{-/-}$ vs wild-type: *p < 0.05, **p < 0.01, ***p < 0.001. Thirty minutes vs 10 min: $^{\varphi}p$ < 0.05, $^{\theta}p$ < 0.01, $^{\Phi}p$ < 0.001. [b] Not detected.

***trans*-Resveratrol and Resveratrol Glucuronide and Sulfate Concentration in Intestinal Content.** After 10 min of the oral administration in wild-type mice, glucuronide and sulfate conjugates were found in intestinal content in concentrations of 215 ± 34 and 170 ± 34 nmol/g, respectively (**Table 1**). At 30 min, the efflux of conjugates increased by 157% (p < 0.001) and 360% (p < 0.001) for the *trans*-resveratrol glucuronide and sulfate, respectively.

trans-Resveratrol glucuronide was 34% and 71% (p < 0.001) lower in Bcrp1$^{-/-}$ mice than in wild-type animals, at 10 and 30 min, respectively. *trans*-Resveratrol sulfate was reduced by 95% (p < 0.05) and 97% (p < 0.001) at 10 and 30 min, respectively.

Plasma Concentrations of *trans*-Resveratrol and Conjugates. After the oral administration of 60 mg/kg of *trans*-resveratrol, blood was withdrawn at different times: 5, 10, and 30 min (**Figure 2**). In wild-type mice, this polyphenol was detected at 5 min at concentrations of 7.3 ± 2.1 μM, which were maintained until 10 min (7.4 ± 1.3 μM). From this time point, the plasma levels decreased to 6.0 ± 1.5 μM at 30 min. *trans*-Resveratrol glucuronide was the most abundant compound in plasma, and was already detected at 5 min, in a concentration 5-fold higher (p < 0.001) than in the parent compound. The concentration of glucuronide increased over time with values of 57.4 ± 5.9 and

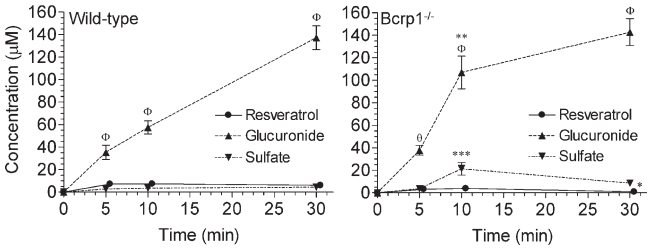

Figure 2. Plasma concentrations after the oral administration of 60 mg/kg of *trans*-resveratrol in wild-type and Bcrp1$^{-/-}$ mice. Values are represented as means ± SEM ($n = 4$). Bcrp1$^{-/-}$ vs wild-type: $^{*}p < 0.05$, $^{**}p < 0.01$, $^{***}p < 0.001$. Conjugates vs *trans*-resveratrol: $^{\theta}p < 0.01$, $^{\Phi}p < 0.001$. Statistical analysis at different times: In wild-type mice, *trans*-resveratrol and sulfate, 5 = 10 = 30 min; glucuronide, 5 = 10 < 30 min. In Bcrp1$^{-/-}$ mice, *trans*-resveratrol, 5 = 10 = 30 min; glucuronide, 5 < 10 < 30 min; sulfate, 5 = 30 < 10 min; $p < 0.05$.

137 ± 10 μM at 10 and 30 min, which were 8 ($p < 0.001$) and 23 ($p < 0.001$) times the *trans*-resveratrol levels. The sulfate conjugate was also present in plasma of wild-type mice, ranging from 2.8 ± 0.2 μM at 5 min to 4.4 ± 0.8 μM at 30 min.

In Bcrp1$^{-/-}$ mice, the plasma concentrations of *trans*-resveratrol at 5 and 10 min were 3.2 ± 1.0 μM and 4.0 ± 1.8 μM, respectively. At 30 min, the plasma levels were 1.0 ± 0.2 μM, which was 6-fold lower ($p < 0.05$) than the values observed in wild-type animals. *trans*-Resveratrol glucuronide was also the main metabolite found in plasma of mice lacking Bcrp1. At 5 min, the glucuronide was 37.8 ± 4.3 μM; at 10 min, it reached 107 ± 14 μM. The plasma concentration of *trans*-resveratrol glucuronide was 143 ± 12 μM at 30 min, 148 times higher ($p < 0.001$) than that of *trans*-resveratrol. The absence of Bcrp1 influenced the plasma levels of *trans*-resveratrol sulfate. The plasma levels of *trans*-resveratrol sulfate in Bcrp1$^{-/-}$ mice were 3.7 ± 0.7 μM at 5 min, and reached a maximum at 10 min with values of 21.4 ± 5.5 μM, which were 5 times higher ($p < 0.001$) than *trans*-resveratrol alone. At 30 min, the concentration of the sulfate conjugate dropped to 8.6 ± 1.4 μM.

We also determined the area under plasma concentration curves (AUC) for *trans*-resveratrol and its conjugates. The results showed a decrease of 44% in the AUC for *trans*-resveratrol in Bcrp1$^{-/-}$ mice. Conversely, the AUC of glucuronide and sulfate increased by 34% and 392%, respectively.

Tissue Distribution of *trans*-Resveratrol and Resveratrol Glucuronide and Sulfate. The concentrations of *trans*-resveratrol and its metabolites were also examined in the liver, kidney, lung, heart and brain of wild-type and Bcrp1$^{-/-}$ mice. Liver concentrations of *trans*-resveratrol and its glucuronide were similar in wild-type and knockout mice (**Table 1**). The absence of Bcrp1 mainly affected the sulfate content at 10 min, with a concentration 2.6-fold higher in Bcrp1$^{-/-}$ mice ($p < 0.01$).

The organs with the greatest differences between wild-type and Bcrp1$^{-/-}$ mice were kidney and lung (**Table 1**). In kidney, *trans*-resveratrol at 10 min was 3-fold higher ($p < 0.01$) in Bcrp1$^{-/-}$ mice than in wild-type ones. The glucuronide conjugate was 2-fold (10 min) and 32.7-fold (30 min) higher in kidney of Bcrp1$^{-/-}$ mice than in wild-type ones ($p < 0.01$). No differences between animals were observed for the sulfate conjugate, either at 10 or at 30 min.

trans-Resveratrol and its glucuronide and sulfate conjugates were also found in lung (**Table 1**), although the concentrations of these compounds were lower than those in liver or kidney. The concentrations of *trans*-resveratrol were similar in Bcrp1$^{-/-}$ and wild-type mice at 10 min. However, at 30 min the concentration of this compound was 6-fold higher ($p < 0.05$) in Bcrp1$^{-/-}$ than in wild-type mice. At 10 min, glucuronide was 2.1-fold higher in Bcrp1$^{-/-}$ mice ($p < 0.01$). No differences in glucuronide concentrations were observed at 30 min. It is worth mentioning that the sulfate conjugate was only detected in mice lacking Bcrp1.

In heart, no differences between wild-type and Bcrp1$^{-/-}$ mice were observed in the concentration of *trans*-resveratrol (**Table 1**). However, in knockout mice, the glucuronide conjugate was double ($p < 0.01$) that in wild-type mice. The sulfate conjugate was not detected in any group.

The lowest concentrations of *trans*-resveratrol and its glucuronide were measured in the brain (**Table 1**). In wild-type mice the sulfate conjugate was barely detected at 10 min and decreased with time, so that at 30 min it was only present in one mouse brain in a concentration of 0.36 nmol/g.

DISCUSSION

The use of genetically modified mice that lack expression of the transporter Bcrp1 (knockout) has proved a useful tool in studying the *in vivo* function of this efflux pump (*15*). The present study attempts to identify the contribution of this protein to the bioavailability and tissue distribution of *trans*-resveratrol and its conjugates. In a previous study, we established that *trans*-resveratrol was absorbed by simple diffusion and conjugated quickly inside the enterocyte to glucuronide and sulfate. Part of these conjugates was secreted back to the intestinal lumen through Mrp2 and Bcrp1 (*13*). In the present study, the concentrations of *trans*-resveratrol and its metabolites were assessed 10 and 30 min after the oral administration of 60 mg/kg in the intestinal content, small intestine, plasma, liver, kidney, lung, heart and brain in wild-type and Bcrp1$^{-/-}$ mice.

The rapid and extensive metabolism that *trans*-resveratrol undergoes in the enterocytes was clearly seen 10 min after oral administration of 60 mg/kg, since the glucuronide and sulfate conjugates were found in the intestinal tissue as well as in the luminal content in both groups. A significant reduction of the efflux toward the intestinal content was observed in Bcrp1$^{-/-}$ mice, in which secretion of the glucuronide conjugate was inhibited by 70% and the sulfate by 95% more than in wild-type mice. Results here demonstrate that Bcrp1 is predominantly responsible for the intestinal excretion of sulfate conjugates and, to a lesser extent, of glucuronide. Our data corroborate previous findings in Bcrp1$^{-/-}$ mice for 4-methylumbelliferone and its conjugates (*16*) and for minoxidil and its sulfate (*17*). In our experiments, the efflux of both metabolites was not completely halted in Bcrp1$^{-/-}$ mice because the conjugates of *trans*-resveratrol are also substrates of Mrp2, as previously shown in rats (*13*, *18*). The decreased concentrations of glucuronide and sulfate conjugates in the luminal content of Bcrp1$^{-/-}$ mice could not be attributed to changes in the level of conjugating enzymes secondary to the absence of transporters in knockout mice, because no changes in intestinal UDP-glucuronosyltransferase or sulfotransferases were reported in them (*17*).

The analysis of the luminal content revealed that *trans*-resveratrol concentration was higher in wild-type mice than in Bcrp1$^{-/-}$ mice at 30 min. This result cannot be explained by active transport of intact *trans*-resveratrol from the enterocyte, since this compound is not transported by BCRP at physiological pH, as studied in MDCKII cells overexpressing human BCRP (*19*). Moreover, *in vivo* perfusion in rat jejunum using Ko143 as BCRP inhibitor showed that *trans*-resveratrol was not secreted back to the intestinal lumen (*13*). A reasonable explanation could be an intestinal absorption rate of *trans*-resveratrol that is different in wild-type and knockout animals. The lower concentration of *trans*-resveratrol in the luminal content and enterocytes in knockout vs wild-type mice could be due to a major gradient of

concentration of this compound from the lumen to the blood in Bcrp1$^{-/-}$ mice. Moreover, the contribution of enterohepatic circulation cannot be ruled out in wild-type mice, in which the luminal content of *trans*-resveratrol and its conjugates was higher than in knockout ones (*20*).

We also evaluated the plasma levels of *trans*-resveratrol after the oral administration of 60 mg/kg. The higher AUC, observed for *trans*-resveratrol conjugates, is consistent with the fact that these compounds are transported by Bcrp1. The same pattern has been described for other substrates transported by this protein (*17*, *21*). It is worth mentioning that the greater increase of AUC in Bcrp1$^{-/-}$ mice corresponds to resveratrol sulfate, which implies greater affinity of Bcrp1 for this substrate, as pointed out by other authors (*17*, *22*). Moreover, the fact that the AUC of *trans*-resveratrol in knockout mice does not increase indicates that it is not transported by Bcrp1 (*13*). The pattern of plasma concentrations of *trans*-resveratrol and its metabolites is quite similar to that described by van de Wetering et al. (*23*) in wild-type mice. However, important differences were found between our results and van de Wetering's results in plasma from Bcrp1$^{-/-}$ mice. First, van de Wetering et al. (*23*) failed to detect *trans*-resveratrol in plasma. Second, they identified a third metabolite corresponding to *trans*-resveratrol disulfate, which is absent in our samples. These discrepancies may be attributed to the different extraction methods and chromatographic conditions used to determine *trans*-resveratrol from plasma samples.

In the liver, Bcrp1 has been described as mediating the biliary excretion of drugs and its metabolites. No differences between groups for *trans*-resveratrol and its glucuronide were observed. The fact that the glucuronide conjugate did not accumulate in liver could be attributed to the involvement of Mrp2 in its efflux, as previously seen in rats (*18*). In Bcrp1$^{-/-}$ mice, the concentration of *trans*-resveratrol sulfate was higher at 10 min, probably due to the greater affinity of Bcrp1 for sulfates than for glucuronide conjugates (*22*). Moreover, the higher level of *trans*-resveratrol sulfate in Bcrp1$^{-/-}$ mice mirrored the plasma peak observed at this time point.

Kidney was the organ with the highest concentration of *trans*-resveratrol and its conjugates in Bcrp1$^{-/-}$ mice. It is precisely this organ in which the expression of Bcrp1 mRNA has been reported to be the highest (*24*). The absence of Bcrp1 from the apical membrane of the tubular cells leads to the accumulation of the conjugates in the kidney. Our results are consistent with the findings of the Borst group (*23*), who pointed to a decrease in the excretion of resveratrol conjugates in urine of mice with absence of Bcrp1.

The presence of *trans*-resveratrol and its conjugates in lungs has been previously reported in mice and rats (*14*, *26*, *27*). It should be noted that *trans*-resveratrol sulfate was not detected in wild-type mice, whereas it was present in Bcrp1$^{-/-}$ mice, thus confirming the high affinity of this transporter for *trans*-resveratrol sulfate. The concentrations of *trans*-resveratrol in heart have been determined before in rats (*28*) and mice (*26*), but conjugates were not taken into account in those studies. *trans*-Resveratrol glucuronide appeared the only detectable conjugate in this organ, in which it was found in higher amounts than the parent compound was.

The tissue distribution of *trans*-resveratrol was also evaluated in the brain, since Bcrp1 is known to be present in the blood−brain barrier, restricting the penetration of different compounds (*15*). Our results show that this polyphenol is able to cross the blood−brain barrier, although its concentration is lower than that found in other tissues. These data corroborate previous observations in mice and rats (*14*, *26*, *27*). The contribution of Bcrp1 is small, since there is a similar amount of glucuronide and sulfate in knockout and wild-type mice.

In conclusion, the bioavailability and tissue distribution of *trans*-resveratrol is the result of a complex interaction of transporters and enzyme activities in the different tissues. Our results emphasize the role of Bcrp1 in the distribution of *trans*-resveratrol and its conjugates. The most affected organs are the small intestine, kidney and the lungs, with higher amounts in Bcrp1$^{-/-}$ mice. It is worthy of note that Bcrp1 is responsible for the extrusion of the conjugates of *trans*-resveratrol from the enterocytes to the intestinal lumen, which favors high concentrations of these compounds throughout the intestine. Since the conjugates could be converted back to the parent compound (*25*) or even the conjugated compounds could have beneficial effects similar to *trans*-resveratrol's effect (*5*), our results support the suitability of the use of *trans*-resveratrol in therapy for colon cancer (*29*) or intestinal bowel disease (*30*).

ABBREVIATIONS USED

AUC, area under the plasma concentration curve; BCRP/ABCG2, breast cancer resistance protein; ABC, ATP binding cassette; MRP2/ABCC2, multidrug resistance protein 2.

ACKNOWLEDGMENT

The authors thank A. H. Schinkel (The Netherlands Cancer Institute, Amsterdam, The Netherlands), who provided Bcrp1$^{-/-}$ mice.

LITERATURE CITED

(1) Robey, R. W.; To, K. K.; Polgar, O.; Dohse, M.; Fetsch, P.; Dean, M.; Bates, S. E. ABCG2: a perspective. *Adv. Drug Delivery Rev.* **2009**, *61*, 3–13.

(2) Gutmann, H.; Hruz, P.; Zimmermann, C.; Beglinger, C.; Drewe, J. Distribution of breast cancer resistance protein (BCRP/ABCG2) mRNA expression along the human GI tract. *Biochem. Pharmacol.* **2005**, *70*, 695–699.

(3) Fetsch, P. A.; Abati, A.; Litman, T.; Morisaki, K.; Honjo, Y.; Mittal, K.; Bates, S. E. Localization of the ABCG2 mitoxantrone resistance-associated protein in normal tissues. *Cancer Lett.* **2006**, *235*, 84–92.

(4) Huls, M.; Brown, C. D.; Windass, A. S.; Sayer, R.; van den Heuvel, J. J.; Heemskerk, S.; Russel, F. G.; Masereeuw, R. The breast cancer resistance protein transporter ABCG2 is expressed in the human kidney proximal tubule apical membrane. *Kidney Int.* **2008**, *73*, 220–225.

(5) Baur, J. A.; Sinclair, D. A. Therapeutic potential of resveratrol: the in vivo evidence. *Nat. Rev. Drug Discovery* **2006**, *5*, 493–506.

(6) Pervaiz, S.; Holme, A. L.; Aggarwal, B. B.; Anekonda, T. S.; Baur, J. A.; Gojkovic-Bukarica, L.; Ragione, F. D.; Kim, A. L.; Pirola, L.; Saiko, P. Resveratrol: its biologic targets and functional activity. *Antioxid. Redox Signaling* **2009**, *11*, 2851–2897.

(7) Juan, M. E.; Vinardell, M. P.; Planas, J. M. The daily oral administration of high doses of *trans*-resveratrol to rats for 28 days is not harmful. *J. Nutr.* **2002**, *132*, 257–260.

(8) Penumathsa, S. V.; Maulik, N. Resveratrol: a promising agent in promoting cardioprotection against coronary heart disease. *Can. J. Physiol. Pharmacol.* **2009**, *87*, 275–286.

(9) Pallàs, M.; Casadesús, G.; Smith, M. A.; Coto-Montes, A.; Pelegrí, C.; Vilaplana, J.; Camins, A. Resveratrol and neurodegenerative diseases: activation of SIRT1 as the potential pathway towards neuroprotection. *Curr. Neurovasc. Res.* **2009**, *6*, 70–81.

(10) Juan, M. E.; González-Pons, E.; Munuera, T.; Ballester, J.; Rodríguez-Gil, J. E.; Planas, J. M. *trans*-Resveratrol, a natural antioxidant from grapes, increases sperm output in healthy rats. *J. Nutr.* **2005**, *135*, 757–760.

(11) Pearson, K. J.; Baur, J. A.; Lewis, K. N.; Peshkin, L.; Price, N. L.; Labinskyy, N.; Swindell, W. R.; Kamara, D.; Minor, R. K.; Perez, E.; Jamieson, H. A.; Zhang, Y.; Dunn, S. R.; Sharma, K.; Pleshko,

N.; Woollett, L. A.; Csiszar, A.; Ikeno, Y.; Le Couteur, D.; Elliott, P. J.; Becker, K. G.; Navas, P.; Ingram, D. K.; Wolf, N. S.; Ungvari, Z.; Sinclair, D. A.; de Cabo, R. Resveratrol delays age-related deterioration and mimics transcriptional aspects of dietary restriction without extending life span. *Cell Metab*. **2008**, *8*, 157–168.

(12) Bishayee, A. Cancer prevention and treatment with resveratrol: from rodent studies to clinical trials. *Cancer Prev. Res*. **2009**, *2*, 409–418.

(13) Juan, M. E.; González-Pons, E.; Planas, J. M. Multidrug resistance proteins restrain the intestinal absorption of *trans*-resveratrol. *J. Nutr*. **2010**, 140. doi:10.3945/jn.109.114959.

(14) Juan, M. E.; Maijó, M.; Planas, J. M. Quantification of *trans*-resveratrol and its metabolites in rat plasma and tissues by HPLC. *J. Pharm. Biomed. Anal*. **2010**, *51*, 391–398.

(15) Vlaming, M. L.; Lagas, J. S.; Schinkel, A. H. Physiological and pharmacological roles of ABCG2 (BCRP): recent findings in Abcg2 knockout mice. *Adv. Drug Delivery Rev*. **2009**, *61*, 14–25.

(16) Adachi, Y.; Suzuki, H.; Schinkel, A. H.; Sugiyama, Y. Role of breast cancer resistance protein (Bcrp1/Abcg2) in the extrusion of glucuronide and sulfate conjugates from enterocytes to intestinal lumen. *Mol. Pharmacol*. **2005**, *67*, 923–928.

(17) Enokizono, J.; Kusuhara, H.; Sugiyama, Y. Regional expression and activity of breast cancer resistance protein (Bcrp/Abcg2) in mouse intestine: overlapping distribution with sulfotransferases. *Drug Metab. Dispos*. **2007**, *35*, 922–928.

(18) Maier-Salamon, A.; Hagenauer, B.; Reznicek, G.; Szekeres, T.; Thalhammer, T.; Jäger, W. Metabolism and disposition of resveratrol in the isolated perfused rat liver: role of Mrp2 in the biliary excretion of glucuronides. *J. Pharm. Sci*. **2008**, *97*, 1615–1628.

(19) Breedveld, P.; Pluim, D.; Cipriani, G.; Dahlhaus, F.; van Eijndhoven, M. A.; de Wolf, C. J.; Kuil, A.; Beijnen, J. H.; Scheffer, G. L.; Jansen, G.; Borst, P.; Schellens, J. H. The effect of low pH on breast cancer resistance protein (ABCG2)-mediated transport of methotrexate, 7-hydroxymethotrexate, methotrexate diglutamate, folic acid, mitoxantrone, topotecan, and resveratrol in in vitro drug transport models. *Mol. Pharmacol*. **2007**, *71*, 240–249.

(20) Marier, J. F.; Vachon, P.; Gritsas, A.; Zhang, J.; Moreau, J. P.; Ducharme, M. P. Metabolism and disposition of resveratrol in rats: extent of absorption, glucuronidation, and enterohepatic recirculation evidenced by a linked-rat model. *J. Pharmacol. Exp. Ther*. **2002**, *302*, 369–373.

(21) Van Herwaarden, A. E.; Jonker, J. W.; Wagenaar, E.; Brinkhuis, R. F.; Schellens, J. H.; Beijnen, J. H.; Schinkel, A. H. The breast cancer resistance protein (Bcrp1/Abcg2) restricts exposure to the dietary carcinogen 2-amino-1-methyl-6-phenylimidazo(4,5-b)pyridine. *Cancer Res*. **2003**, *63*, 6447–6452.

(22) Zamek-Gliszczynski, M. J.; Nezasa, K.; Tian, X.; Kalvass, J. C.; Patel, N. J.; Raub, T. J.; Brouwer, K. L. The important role of Bcrp (Abcg2) in the biliary excretion of sulfate and glucuronide metabolites of acetaminophen, 4-methylumbelliferone, and harmol in mice. *Mol. Pharmacol*. **2006**, *70*, 2127–2133.

(23) van de Wetering, K.; Burkon, A.; Feddema, W.; Bot, A.; de Jonge, H.; Somoza, V.; Borst, P. Intestinal breast cancer resistance protein (BCRP)/Bcrp1 and multidrug resistance protein 3 (MRP3)/Mrp3 are involved in the pharmacokinetics of resveratrol. *Mol. Pharmacol*. **2009**, *75*, 876–885.

(24) Tanaka, Y.; Slitt, A. L.; Leazer, T. M.; Maher, J. M.; Klaassen, C. D. Tissue distribution and hormonal regulation of the breast cancer resistance protein (Bcrp/Abcg2) in rats and mice. *Biochem. Biophys. Res. Commun*. **2005**, *326*, 181–187.

(25) Mizuno, N.; Takahashi, T.; Kusuhara, H.; Schuetz, J. D.; Niwa, T.; Sugiyama, Y. Evaluation of the role of breast cancer resistance protein (BCRP/ABCG2) and multidrug resistance-associated protein 4 (MRP4/ABCC4) in the urinary excretion of sulfate and glucuronide metabolites of edaravone (MCI-186; 3-methyl-1-phenyl-2-pyrazolin-5-one). *Drug Metab. Dispos*. **2007**, *35*, 2045–2052.

(26) Vitrac, X.; Desmoulière, A.; Brouillaud, B.; Krisa, S.; Deffieux, G.; Barthe, N.; Rosenbaum, J.; Mérillon, J. M. Distribution of (14C)-*trans*-resveratrol, a cancer chemopreventive polyphenol, in mouse tissues after oral administration. *Life Sci*. **2003**, *72*, 2219–2233.

(27) Sale, S.; Verschoyle, R. D.; Boocock, D.; Jones, D. J.; Wilsher, N.; Ruparelia, K. C.; Potter, G. A.; Farmer, P. B.; Steward, W. P.; Gescher, A. J. Pharmacokinetics in mice and growth-inhibitory properties of the putative cancer chemopreventive agent resveratrol and the synthetic analogue trans 3,4,5,4′-tetramethoxystilbene. *Br. J. Cancer* **2004**, *90*, 736–744.

(28) Abd El-Mohsen, M.; Bayele, H.; Kuhnle, G.; Gibson, G.; Debnam, E.; Srai, S. K.; Rice-Evans, C.; Spencer, J. P. Distribution of (3H)*trans*-resveratrol in rat tissues following oral administration. *Br. J. Nutr*. **2006**, *96*, 62–70.

(29) Sengottuvelan, M.; Deeptha, K.; Nalini, N. Influence of dietary resveratrol on early and late molecular markers of 1,2-dimethylhydrazine-induced colon carcinogenesis. *Nutrition* **2009**, *25*, 1169–1176.

(30) Larrosa, M.; Yañéz-Gascón, M. J.; Selma, M. V.; González-Sarrías, A.; Toti, S.; Cerón, J. J.; Tomás-Barberán, F.; Dolara, P.; Espín, J. C. Effect of a low dose of dietary resveratrol on colon microbiota, inflammation and tissue damage in a DSS-induced colitis rat model. *J. Agric. Food Chem*. **2009**, *57*, 2211–2220.

Received for review December 4, 2009. Revised manuscript received March 5, 2010. Accepted March 5, 2010. Supported by grants AGL2005-05728, AGL2006-13186 and the "Ramon y Cajal" Programme of Spain's Ministry of Science and Technology and grant 2009-SGR-471 from the Generalitat (Autonomous Government) of Catalonia, Spain. The group is a member of the Network for Cooperative Research on Membrane Transport Proteins (REIT) (Grant BFU2007-30688-E/BFI).

4.2. Estudi de la biodisponibilitat del *trans*-resveratrol i els seus conjugats en ratolins que no expressen el transportador Mdr1a i ratolins no modificats genèticament

4.2.1. Introducció

La P-gp és el primer transportador de xenobiòtics transmembrana conegut de la família de les proteïnes ABC (Kannan *et al.*, 2009). Aquesta proteïna és el producte del gen humà *MDR1* i va ser identificat inicialment com una proteïna que donava resistència als fàrmacs en diferents cèl·lules tumorals (Stanley *et al.*, 2009). Posteriorment, es va localitzar aquesta proteïna en teixits normals, suggerint una funció fisiològica per aquest transportador. Estudis de localització i farmacocinètica demostraren que la P-gp pot transportar substrats fora de les cèl·lules, a l'espai luminal, ja que està àmpliament expressada a la membrana apical de cèl·lules epitelials de diferents òrgans com ronyó, fetge i intestí (Kannan *et al.*, 2009).

En rosegadors, a diferència del que passa en humans, la P-gp està codificat per 2 gens diferents, *Mdr1a* i *Mdr1b* (Wilk *et al.*, 2005). L'expressió d'*Mdr1a* s'ha trobat a cèl·lules epitelials intestinals, a cèl·lules T $CD8^+$, a algunes cèl·lules T $CD4^+$, a altres cèl·lules hematopoètiques com cèl·lules mononuclears de sang perifèrica, macròfags, cèl·lules NK (acrònim anglès de *Natural killer*) i cèl·lules dendrítiques, i a la part luminal de l'endoteli dels capil·lars sanguinis del cervell (Wilk *et al.*, 2005). En canvi, *Mdr1b* es troba predominantment a la glàndula adrenal, l'ovari i a l'úter de dones embarassades (Schinkel *et al.*, 1995). Per tant, la biodisponibilitat de xenobiòtics es pot estudiar en ratolins que no expressen *Mdr1a* (ratolins $Mdr1a^{-/-}$) ja que les cèl·lules epitelials intestinals dels ratolins contenen sobretot *Mdr1a* i no *Mdr1b* (Ho *et al.*, 2003).

En rosegadors, l'epiteli intestinal està molt involucrat en el procés metabòlic del *trans*-resveratrol (Juan *et al.*, 2010a), donant lloc a conjugats glucurònid i sulfat els quals utilitzen transportadors de la família ABC per a creuar les membranes. Recentment, s'ha demostrat que els transportadors MRP2 i BCRP estan implicats en la secreció des de l'enteròcit al lumen intestinal tant del glucurònid com del sulfat de *trans*-resveratrol (Juan *et al.*, 2010a). A més, la biodisponibilitat i la distribució en teixits d'aquest polifenol i els seus conjugats es troba modificada en ratolins $Bcrp1^{-/-}$ (Apartat 4.1. - Alfaras *et al.*, 2010). Per tant, es va estudiar la biodisponibilitat oral del *trans*-resveratrol i els seus conjugats glucurònid i sulfat després de l'administració oral de 60 mg/kg en ratolins $Mdr1a^{-/-}$ i *wild-type*.

4.2.2. Material i mètodes

4.2.2.1. Reactius i substàncies utilitzades

El *trans*-resveratrol pur es va obtenir de Second Pharma Co., Ltd. (Shangyu, P.R. China). Totes les activitats experimentals que implicaren la manipulació de *trans*-resveratrol es realitzaren sota llum vermella per evitar la isomerització fotoquímica a la forma *cis*-. L'acetonitril i el metanoles van adquirir de J.T. Baker (Deventer, Holanda) i l'àcid acètic de Scharlau Chemie S.A. (Barcelona, Espanya). Tots els solvents tingueren puresa HPLC. La 2-hidroxipropil-β-ciclodextrina (ref. 332607) i altres reactius utilitzats es van obtenir a Sigma-Aldrich (St. Louis, EUA). L'aigua utilitzada en tots els experiments va passar a través d'un sistema de purificació d'aigua Milli-Q (18 MΩ) (Millipore, Milan, Itàlia).

4.2.2.2. Animals d'experimentació

S'utilitzaren ratolins mascle *Mdr1a*$^{-/-}$ (FVB.129P2-*Abcb1a*^{tm1Bor}N7) i els ratolins consanguinis no modificats genèticament (FVB, *wild-type*) com a controls. Els animals es mantingueren sota condicions SPF, temperatura (22 ± 3ºC) i humitat (50 ± 10%) controlades i amb cicles de llum-foscor de 12 hores al servei d'estabulari animal del Parc Científic de Barcelona. A l'edat de 12 setmanes van ser traslladats a l'estabulari de la Facultat de Farmàcia de la Universitat de Barcelona, sota les mateixes condicions de temperatura i humitat i cicles de llum-foscor però condicions no SPF. Els animals van rebre una dieta control per ratolí (Harlan, Espanya) i aigua *ad libitum*.

Els experiments es realitzaren sempre a primera hora del matí, per minimitzar els efectes de qualsevol ritme circadiari i amb els animals sotmesos a dejuni previ. La manipulació dels animals al llarg de tot el tractament, així com el seu sacrifici, es va dur a terme segons els procediments autoritzats pel Comitè ètic d'Experimentació Animal de la Universitat de Barcelona i seguint les recomanacions de la Federation of European Laboratory Animal Science Associations (1995).

4.2.2.3. Obtenció de les mostres

Els ratolins control i els *Mdr1a*$^{-/-}$ van rebre per via oral mitjançant una sonda intragàstrica, una dosi única de *trans*-resveratrol de 60 mg/kg dissolt en 2-hidroxipropil-β-ciclodextrina al 20% (v/v). Els animals s'anestesiaren amb ketamina i xilacina (0,1% i 0,01% volum/pes corporal, respectivament). Un cop es va comprovar que el ratolí no tenia reflexes, es va procedir a la punció cardíaca amb agulles 21G i amb xeringa de 2,5 mL. Els temps d'extracció de la mostra van ser 10, 15 i 30 min (n=4/grup i temps experimental).

La sang es va recollir en tubs d'extracció que contenien EDTA-K3 com anticoagulant i es mantingueren a 4ºC fins al seu anàlisi.

4.2.2.4. Determinació de *trans*-resveratrol i els seus conjugats a plasma

Les mostres de sang obtingudes es centrifugaren a 1500×*g* i 4ºC durant 15 minuts. Posteriorment, se separà el plasma de les cèl·lules, que es recollí amb un tub cònic de vidre i es mesurà el volum de plasma obtingut. A continuació s'afegí un volum d'àcid acètic, a una relació de 15 µL d'àcid acètic per 500 µL de plasma, per tal de mantenir els grups hidroxil del *trans*-resveratrol en forma no ionitzada. Seguidament s'agità 2 minuts al vòrtex.

La determinació del *trans*-resveratrol del plasma es va realitzar emprant un mètode d'extracció en fase sòlida (Juan *et al.*, 2010b) utilitzant un cartutx C18 de fase reversa (Sep-Pack®, Waters, Milford, EUA). El procediment analític per l'extracció va ser, primerament, l'activació del cartutx fent passar 4 mL de metanol i 10 mL d'aigua mQ. A continuació es van passar les mostres de plasma, molt lentament, pel cartutx per tal que el *trans*-resveratrol s'adsorbís. Seguidament es rentà el cartutx amb aigua mQ a una relació de 10 mL d'aigua mQ per 1 mL de plasma. Finalment, el *trans*-resveratrol retingut al cartutx s'eluí amb 4 mL de metanol.

Un cop extret el *trans*-resveratrol amb el metanol es van afegir 10 µL d'àcid ascòrbic per evitar l'oxidació del polifenol i es portà a evaporar al concentrador 5301 (Eppendorf Ibèrica S.L., San Sebastián de los Reyes, Espanya). Un cop finalitzada l'evaporació es va mesurar el volum final obtingut i es va posar en un vial topazi per al posterior anàlisi per HPLC.

4.2.2.5. Anàlisis cromatogràfiques

El *trans*-resveratrol i els seus conjugats es determinaren mitjançant HPLC. L'aparell utilitzat va ser un cromatògraf Agilent Technologies 1100 (Agilent Technologies, Palo Alto, CA), equipat amb un injector automàtic, una columna Synergi Fusion-RP 80A (250 × 4.6 mm; 4 µm) (Phenomenex, Torrance, CA), una precolumna C18 i un detector diode array UV-visible acoblat a un ordinador amb software que controlava l'instrument (ChemStation, for LC3D, Agilent Technologies 1999-2000). La temperatura de la columna es mantingué a 40ºC. El flux va ser d'1,5 mL/min i el volum d'injecció de 100 µL.

La fase mòbil utilitzada constava de dues fases A i B. La Fase A estava formada per un 97% d'aigua mQ i un 3% d'àcid acètic, mentre que la Fase B contenia un 20% de Fase A i un 80% d'acetonitril. El gradient d'elució d'aquesta fase mòbil per a la determinació del *trans*-resveratrol i els seus conjugats en plasma es troba descrit en la taula III.2.

Temps (min)	Fase A (%)	Fase B (%)
0	78	22
6	70	30
14	50	50
18	40	60
25	0	100
30	0	100
32	78	22

Taula III.2. Gradient d'elució per a mostres de plasma.

Els cromatogrames s'obtingueren mitjançant la detecció per UV-diode-array a 306 nm que correspon a la màxima absorbància del *trans*-resveratrol. La identificació del *trans*-resveratrol es va fer comparant el temps de retenció amb el de l'estàndard i el seu espectre d'absorbància (des de 200 a 400 nm).

La identitat dels pics es va confirmar per HPLC acoblat a MS. L'equip constava d'un HPLC model Agilent series 1100 combinat amb un espectròmetre de masses model API 3000 triple quadrupol (Applied Biosystems, PE Sciex, Concord, Ontario, Canada) equipat amb una font d'ionització Turbo IonSpray^{TM} (electrospray assistit per turbo nebulització). Les determinacions es van fer en mode negatiu. El voltatge de la font d'ionització va ser 3500 V, mitjançant el nitrogen com a gas nebulitzador (10 unitats arbitràries) i gas cortina (15 unitats arbitràries). El gas turbo, també nitrogen, estava a una temperatura de 400°C i es va introduir a un flux de 5000 cm^3/min. Les condicions de detecció es van optimitzar amb una solució estàndard de *trans*-resveratrol en presència de fase mòbil utilitzant, finalment, un potencial de ruptura de -70 V i un potencial d'enfocament dels ions de -200 V. L'adquisició de dades es va realitzar fent un escombratge complert de masses entre 100 i 500 *m/z*.

4.2.2.6. Tractament de les dades

Tots els resultats s'expressen com a mitjana ± error estàndard. L'anàlisi estadística es va dur a terme amb el programa GraphPad Prism 4.03. Les diferencies entre les concentracions plasmàtiques de *trans*-resveratrol s'analitzaren mitjançant la prova de la *t* de Student. Els valors $P < 0,05$ van ser considerats com a diferències estadísticament significatives.

4.2.3. Resultats

Es va analitzar el plasma extret als 10, 15 i 30 minuts després de l'administració oral de 60 mg/kg de *trans*-resveratrol a ratolins amb manca de P-gp i ratolins no modificats

genèticament. El cromatograma característic obtingut en analitzar les mostres de plasma així com els espectres d'absorbància es representen a la figura III.19. Tal com es pot observar, les mostres de plasma, tant dels ratolins *Mdr1a*$^{-/-}$ com dels control, es caracteritzaren per presentar un pic corresponent al *trans*-resvertrol que va eluir als 12,8 min, així com els seus conjugats glucurònid i sulfat amb temps de retenció de 7,5 i 16,5 min, respectivament.

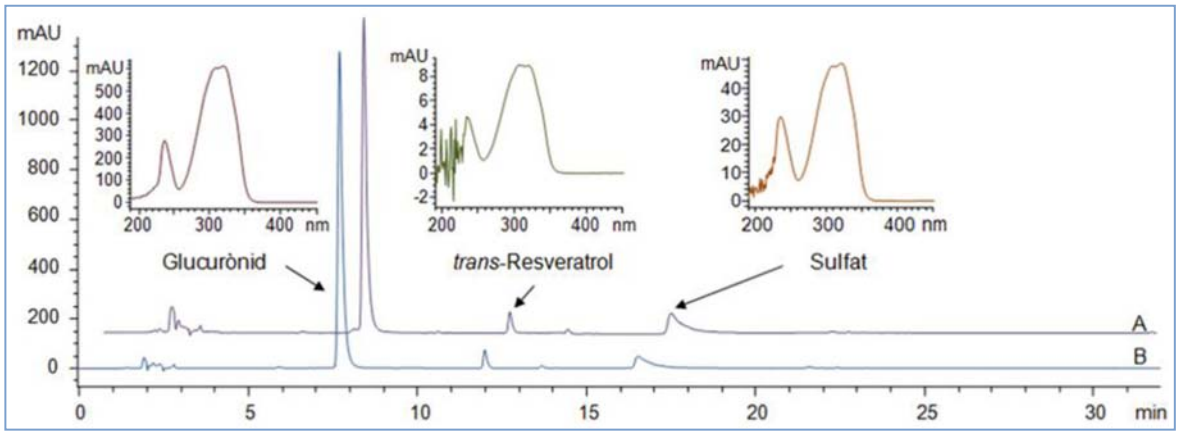

Figura III.19. Cromatogrames característics d'una mostra de plasma després de l'administració oral de 60 mg/kg de *trans*-resveratrol a ratolins amb manca de glicoproteïna P (A) i ratolins no modificats genèticament (B). També estan representats els espectres d'absorbància del *trans*-resveratrol i els dels seus conjugats glucurònid i sulfat.

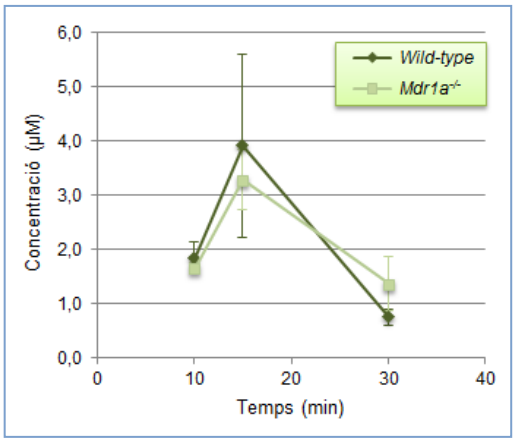

Figura III.20. Concentracions plasmàtiques de *trans*-resveratrol 10, 15 i 30 minuts després de l'administració de 60 mg/kg de *trans*-resveratrol a ratolins. Valors representats com a mitjana ± error estàndard. Diferències al llarg del temps, *Wild-type*: 10' = 15' < 30'; 15' = 30'; *Mdr1a*$^{-/-}$: 10' = 15' < 30'; 10' = 30' (P < 0,05).

Les concentracions obtingudes de *trans*-resveratrol a plasma en ratolins *Mdr1a*$^{-/-}$ i en els control es mostren a la figura III.20. En els ratolins no modificats genèticament, les concentracions de *trans*-resveratrol van ser 1,84 ± 0,30 µM als 10 minuts, 3,91 ± 1,69 µM als 15 minuts i 0,75 ± 0,15 µM als 30 minuts després de l'administració del *trans*-resveratrol. Les concentracions del polifenol en els ratolins amb manca de P-gp van ser 1,65 ± 0,10 µM als 10 minuts, 3,29 ± 0,56 µM als 15 minuts i 1,37 ± 0,49 µM als 30 minuts i no mostraren diferències significatives amb les observades als ratolins control.

El conjugat majoritari va ser el glucurònid tant als ratolins modificats genèticament com als que no expressen la P-gp i no s'observaren diferències significatives entre els 2 grups de ratolins (Figura III.21.). Als ratolins control, les concentracions de glucurònid van ser 51,7 ± 14,7 µM als 10 minuts, 53,9 ± 11,2 µM als 15 minuts i 57,9 ± 5,8 µM als 30 minuts.

Als ratolins que no expressen P-gp, les concentracions observades van ser 31,8 ± 8,3 µM, 45,6 ± 5,7 µM i 60,8 ± 4,4 µM als 10, 15 i 30 minuts, respectivament.

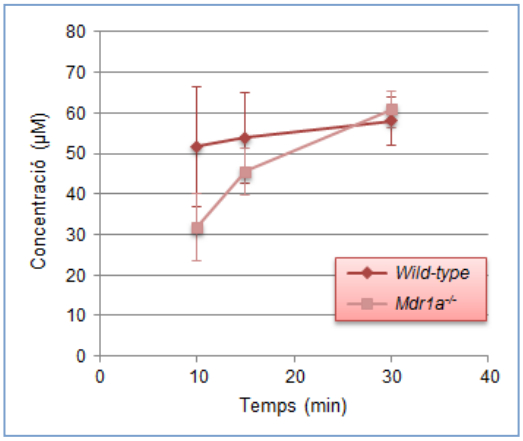

Figura III.21. Concentracions plasmàtiques de glucurònid 10, 15 i 30 minuts després de l'administració de 60 mg/kg de *trans*-resveratrol a ratolins. Valors representats com a mitjana ± error estàndard. No hi ha diferències entre els grups. Diferències al llarg del temps, *Wild-type*: 10' = 15' = 30'; *Mdr1a*$^{-/-}$: 10' = 15' < 30'; 15' = 30' (P < 0,05).

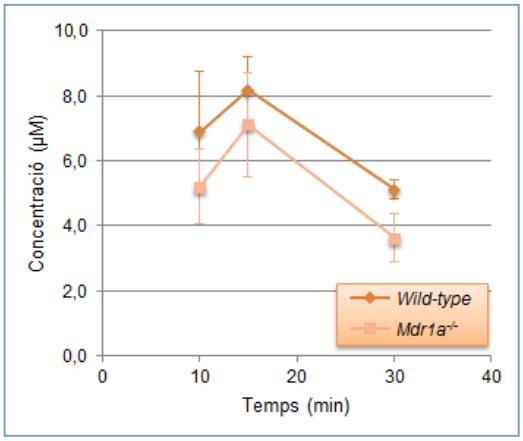

Figura III.22. Concentracions plasmàtiques de sulfat 10, 15 i 30 minuts després de l'administració de 60 mg/kg de *trans*-resveratrol a ratolins. Valors representats com a mitjana ± error estàndard. No hi ha diferències entre els grups. Diferències al llarg del temps, *Wild-type*: 10' = 15' < 30'; 10' = 30'; *Mdr1a*$^{-/-}$: 10' = 15' = 30' (P < 0,05).

El sulfat de *trans*-resveratrol també es va trobar en concentracions més elevades que el compost pare, tot i que no hi va haver diferències entre els grups experimentals (Figura III.22.). Als ratolins no modificats genèticament, les concentracions de sulfat a plasma van ser 6,88 ± 1,86 µM als 10 minuts, 8,17 ± 1,03 µM als 15 minuts i 5,12 ± 0,30 µM als 30 minuts. Les mesures realitzades als ratolins amb manca de P-gp varen ser 5,20 ± 1,15 µM, 7,11 ± 1,60 µM i 3,64 ± 0,73 µM als 10, 15 i 30 minuts de l'administració, respectivament.

4.2.4. Discussió

La P-gp o proteïna MDR1 és un transportador poliespecífic amb la capacitat d'acceptar xenobiòtics de diferents grandàries i estructures i, a més, té múltiples llocs d'unió per a aquests compostos (Klaassen i Aleksunes, 2010). Juntament amb els enzims que conformen el metabolisme de fase I i II, l'expressió de la P-gp constitueix un mecanisme de protecció contra xenobiòtics potencialment tòxics (Fromm, 2004). La P-gp es troba expressada a la membrana apical dels enteròcits a on transporta xenobiòtics des de l'interior de la cèl·lula cap a la lumen intestinal i, així, aconsegueix disminuir l'absorció d'aquests compostos quan són administrats oralment (Klaasen i Aleksunes, 2010). En rosegadors, la P-gp humana és codificada pels gens *Mdr1a* i *Mdr1b*, l'expressió dels quals difereix en la seva localització (Schinkel *et al.*, 1995). Atès que en les cèl·lules epitelials de l'intestí dels ratolins es troba majoritàriament la proteïna MDR1A i gairebé no es troba la MDR1B, els ratolins *Mdr1a*$^{-/-}$ poden ser utilitzats en l'estudi de la

biodisponibilitat oral de xenobiòtics (Schinkel *et al.*, 1995). Per aquesta raó, en aquest estudi es va avaluar mitjançant ratolins que no expressen el gen *Mdr1a* la implicació de la P-gp en la biodisponibilitat oral del *trans*-resveratrol i els seus conjugats glucurònid i sulfat.

Els substrats de la P-gp són bàsicament compostos hidrofòbics, la majoria dels quals poden travessar la bicapa lípidica per difusió passiva (Murakami i Takano, 2008). En estudis realitzats amb cèl·lules Caco-2, es va observar que la velocitat de transport del *trans*-resveratrol era directament proporcional al polifenol inicialment administrat i, per tant, es va concloure que el *trans*-resveratrol entra a les cèl·lules també per difusió passiva (Henry *et al.*, 2005; Maier-Salamon *et al.*, 2006). Mitjançant un mètode *in vivo* de perfusió intestinal en rates es va arribar a les mateixes conclusions (Juan *et al.*, 2010a). L'ús d'inhibidors específics per a la P-gp, com ara verapamil i ciclosporina, va permetre rebutjar que el *trans*-resveratrol o els seus conjugats fossin substrats d'aquesta proteïna transportadora (Juan *et al.*, 2010a). Així com en els estudis previs, les concentracions de *trans*-resveratrol obtingudes en els ratolins no modificats genèticament i els que no expressen *Mdr1a* van ser iguals i, per tant, es va descartar la implicació de la P-gp en la biodisponibilitat oral del polifenol.

Un cop dintre dels enteròcits, el *trans*-resveratrol pateix metabolisme de fase II formant els conjugats glucurònid i sulfat. Mitjançant l'ús d'inhibidors específics es va veure que aquests conjugats eren retornats en part al lumen intestinal pels transportadors BCRP1 i MRP2 però sense la implicació de la P-gp (Juan *et al.*, 2010a). Posteriorment, es va demostrar la implicació de la proteïna BCRP1 *in vivo* mitjançant ratolins que no expressen aquesta proteïna (resultats presentats al Capítol 3 de la present tesi, apartat 3.4.1., Alfaras *et al.*, 2010). En aquest estudi, es va demostrar que la biodisponibilitat oral del *trans*-resveratrol i els seus conjugats no es va veia afectada per la implicació de la P-gp ja que les concentracions de *trans*-resveratrol i els seus conjugats no es van alterar per la manca del transportador.

Mitjançant ratolins *Mdr1a/b*$^{-/-}$, el transport de conjugats com el glucurònid i el sulfat també havia estat estudiat prèviament en bilis i fetge (Zamek-Gliszczynski *et al.*, 2006). El transport de glucurònid i sulfat de compostos com acetaminofen, harmol i 4-metilumbeliferil a nivell biliar es realitzà mitjançant la BCRP i la MRP2. En canvi, la P-gp no va tenir un paper rellevant en el transport biliar d'aquests metabòlits de fase II (Zamek-Gliszczynski *et al.*, 2006). Aquests resultats estan en concordança amb els resultats obtinguts per al glucurònid i sulfat de *trans*-resveratrol en aquest estudi ja que els nivells plasmàtics d'ambdós conjugats no es van veure modificats per l'absència de la proteïna transportadora.

En conclusió, els resultats obtinguts després de l'administració d'una dosi única de 60 mg/kg en ratolins *Mdr1a*$^{-/-}$ indicaren que l'absència de P-gp no va afectar la biodisponibilitat ni del *trans*-resveratrol ni dels seus conjugats confirmant que aquests compostos no són específics del transportador.

Resultats ~ Capítol 5

CAPÍTOL 5. DESENVOLUPAMENT D'UN MODEL FARMACOCINÈTIC DEL *trans*-RESVERATROL SEGUINT UNA APROXIMACIÓ POBLACIONAL.

Els resultats presentats en el capítol es troben recollits a l'article 4:

Population pharmacokinetic modeling of trans-resveratrol and its glucuronide and sulfate conjugates after oral and intravenous administration in rats.
Colom, H., Alfaras, I., Maijó, M., Juan, M.E., Planas, J.M.
Pharm. Res. 2011, 28, 1606-1621

Els resultats obtinguts han donat lloc a les següents comunicacions a congressos:

- *Population pharmacokinetic study of trans-resveratrol after single intravenous and oral administration in rats*
  Colom, H., Juan, M.E., Maijó, M., Alfaras, I., Planas, J.M.

  Presentada com a pòster en el congrés:

  10th European Nutrition Conference
  Paris, França, 10 – 13 de juliol de 2007

  Publicat en *Ann. Nutr. Metab.* 51, 210, 2007

- *Population pharmacokinetics of trans-resveratrol and its metabolites after intravenous administration in rats*
  Colom, H., Juan, M.E., Maijó, M., Alfaras, I., Fernández-Campos, F., Planas, J.M.

  Presentada com a pòster en el congrés:

  6th World Meeting on Pharmaceutics, Biopharmaceutics and Pharmaceutical Technology
  Barcelona, 7 - 10 d'abril de 2008

- *Population pharmacokinetics of trans-resveratrol and its metabolites in rats*
  Colom, H., Alfaras, I., Maijó, M., Juan, M.E., Planas, J.M.

  Presentada com a pòster en el congrés:

  III Jornadas de Modelización y Simulación en Biomedicina
  Barcelona, 26 - 27 novembre de 2009

- *Population pharmacokinetic study of trans-resveratrol and its metabolites after intravenous and oral administrations of 2, 10 and 20 mg/kg in rats*
  Alfaras, I., Colom, H, Maijo, M., Juan, M.E., Planas, J.M.

  Presentada com a pòster en el congrés:

  4th International Conference on Polyphenols and Health (ICPH2009)
  Harrogate, Anglaterra, 7 - 11 de desembre de 2009

Population pharmacokinetic modeling of *trans*-resveratrol and its glucuronide and sulfate conjugates after oral and intravenous administration in rats

Pharm. Res. 2011, 28, 1606-1621

5.1. Resum de l'article 4

Objectius: La farmacocinètica del *trans*-resveratrol ha estat descrita des d'un punt de vista clàssic i sense incloure els metabòlits d'aquest polifenol. Per aquesta raó, es va desenvolupar un model farmacocinètic que analitza simultàniament el *trans*-resveratrol i els seus conjugats des d'una aproximació poblacional a partir de les concentracions plasmàtiques obtingudes en rata.

Material i mètodes: Rates mascle Sprague-Dawley es van administrar per via intravenosa o via oral amb 2, 10 i 20 mg/kg de *trans*-resveratrol. Els temps d'extracció de les mostres es trobava dins del rang de 0 a 25 hores. Les mostres de sang es van processar i analitzar segons el mètode descrit per Juan *et al.* (2010b). Es va utilitzar la metodologia del modelatge no lineal d'efectes mixtes mitjançant el programa NONMEM versió 6.2. El model es va validar emprant la tècnica de la comprovació visual predictiva corregida per les prediccions típiques del model (pcVPC, acrònim anglès de *prediction-corrected visual predictive check*). Posteriorment, la capacitat predictiva del model s'avaluà amb simulacions després de l'administració intravenosa de 15 mg/kg que es van comparar amb dades externes obtingudes sota les mateixes condicions experimentals.

Resultats: Es va desenvolupar un model estructural bàsic que vinculà els models bicompartimentals del *trans*-resveratrol, el glucurònid i el sulfat. La conversió del *trans*-resveratrol en els seus conjugats es va donar per un procés d'ordre 1, en canvi, els conjugats glucurònid i sulfat s'eliminaren mitjançant un procés d'ordre 1 i una cinètica de Michaelis-Menten. Es va observar una millora estadísticament significativa a l'introduir la variabilitat interindividual a l'aclariment, l'aclariment de distribució i la biodisponibilitat del *trans*-resveratrol, així com en el volum de distribució perifèric del glucurònid. La dosi es va incloure com a covariable a la biodisponibilitat del *trans*-resveratrol disminuint la seva variabilitat interindividual i aportant una millora al model. Les gràfiques de bondat de l'ajust indiquen que el model és capaç de descriure correctament les concentracions plasmàtiques del *trans*-resveratrol i els seus conjugats. La pcVPC demostra que el model desenvolupat és apropiat per descriure el perfil de concentracions plasmàtiques en rates ja que és capaç de captar la tendència mitjana i la dispersió de les dades. El model final mostra una capacitat predictiva satisfactòria ja que les simulacions realitzades pel model d'una dosi de 15 mg/kg de *trans*-resveratrol administrada per via intravenosa estan en concordança amb les dades observades.

Conclusió: El model farmacocinètic poblacional desenvolupat descriu adequadament les concentracions plasmàtiques de *trans*-resveratrol així com les dels seus metabòlits més coneguts, com són el glucurònid i el sulfat.

Pharm Res (2011) 28:1606–1621
DOI 10.1007/s11095-011-0395-8

RESEARCH PAPER

Population Pharmacokinetic Modeling of *trans*-Resveratrol and Its Glucuronide and Sulfate Conjugates After Oral and Intravenous Administration in Rats

Helena Colom • Irene Alfaras • Mònica Maijó • M. Emília Juan • Joana M. Planas

Received: 27 July 2010 / Accepted: 8 February 2011 / Published online: 23 March 2011

ABSTRACT

Purpose To develop a population pharmacokinetic (PK) model which allowed the simultaneous modeling of *trans*-resveratrol and its glucuronide and sulfate conjugates.

Methods Male Sprague–Dawley rats were administered i.v. and p.o. with 2, 10 and 20 $mg \cdot kg^{-1}$ of *trans*-resveratrol. Blood was collected at different times during 24 h. An integrated PK model was developed using a sequential analysis, with non-linear mixed effect modeling (NONMEM). A prediction-corrected visual predictive check (pcVPC) was used to assess model performance. The model predictive capability was also evaluated with simulations after the i.v. administration of 15 $mg \cdot kg^{-1}$ that were compared with an external data set.

Results Disposition PK of *trans*-resveratrol and its metabolites was best described by a three-linked two-compartment model. Clearance of *trans*-resveratrol by conversion to its conjugates occurred by a first-order process, whereas both metabolites were eliminated by parallel first-order and Michaelis-Menten kinetics. The pcVPC confirmed the model stability and precision. The final model was successfully applied to the external data set showing its robustness.

Conclusions A robust population PK model has been built for *trans*-resveratrol and its glucuronide and sulfate conjugates that adequately predict plasmatic concentrations.

H. Colom (✉)
Departament de Farmàcia i Tecnologia Farmacèutica
Facultat de Farmàcia, Universitat de Barcelona
Av. Joan XXIII s/n
08028 Barcelona, Spain
e-mail: helena.colom@ub.edu

I. Alfaras • M. Maijó • M. E. Juan • J. M. Planas
Departament de Fisiologia, Facultat de Farmàcia
Institut de Recerca en Nutrició i Seguretat Alimentària (INSA-UB)
Universitat de Barcelona
Barcelona, Spain

KEY WORDS glucuronide and sulfate conjugates · NONMEM · polyphenols · population pharmacokinetics · *trans*-resveratrol

ABBREVIATIONS

ABC	ATP-binding cassette
AIC	Akaike information criterion
AUC	area under the curve
BCRP	breast cancer resistance protein
DV	observed concentrations
IAV	inter-animal variability
IPRED	individual model predicted concentrations
MRP	multidrug resistance protein
OFV	objective function value
pcVPC	prediction corrected visual predictive check
PD	pharmacodynamic
PK	pharmacokinetic
PRED	population model predicted concentrations
RSE	relative standard error
UGT	UDP-glucuronosyltransferase

INTRODUCTION

trans-Resveratrol (*trans*-3,4′,5-trihydroxystilbene) is found in more than 70 plant species, including grapes, berries and peanuts, where it is biosynthesized in response to different kinds of environmental stress and fungal attack, thus being considered a phytoalexin (1). Furthermore, this polyphenol has been reported to exhibit several beneficial effects on human health, including anti-inflammatory, free-radical scavenging, cardioprotection, immune regulation and anti-tumor activity (1,2). *trans*-Resveratrol also appears to be protective against Alzheimer's and Parkinson's diseases, the

most common neurodegenerative ailments associated with aging (2). In addition, this polyphenol is well tolerated, and no harmful effects have been reported (3,4).

The pharmacokinetic (PK) information existing for *trans*-resveratrol to date is limited despite that different studies have assessed its oral bioavailability both in animals and humans (4). Previous PK studies included either only one dose (5–7), or the parameters were obtained through non-compartmental analyses (8–10). Moreover, none of them provided an adequate description of the intricate processes that determine the bioavailability of *trans*-resveratrol. After p.o. administration, this compound rapidly enters the intestinal epithelium (11). Once in the enterocyte, it is highly metabolized to glucuro and sulfo-conjugates that are excreted back, in part, to the intestinal lumen through specific proteins from the ATP-binding cassette (ABC) family (11). Therefore, the small intestine comes out as the first bottleneck to the entry of *trans*-resveratrol to the organism. In addition, the metabolism in the liver cannot be underestimated (12,13) before the distribution to tissues where ABC proteins are also present. All these processes influence the distribution and subsequent elimination from the organism (14). As a result of this complex interplay between enzyme activities and efflux transporters, the concentrations of *trans*-resveratrol in plasma have been reported to be low (4).

Consequently, owing to the lack of description of the pharmacokinetics of *trans*-resveratrol and its metabolites, we aim to develop a PK model that can simultaneously describe the pharmacokinetics of both the parent compound and its conjugated metabolites and investigate the linearity of the kinetics after i.v. and p.o. administration of three doses of *trans*-resveratrol in Sprague–Dawley rats. Analyses of the plasmatic data through the population PK approach provides important advantages such as overcoming the limitations of blood sampling in studies using experimental animals and at the same time preserving animal individuality.

MATERIALS AND METHODS

Materials

trans-Resveratrol was purchased from Second Pharma CO., LTD (Shangyu, P.R. China). Dose preparation, rat administration and sample treatments were performed in dim light to avoid photochemical isomerization of *trans*-resveratrol to the *cis* form. Acetonitrile and methanol were purchased from J.T. Baker (Deventer, Netherlands) and acetic acid from Scharlau Chemie S.A. (Barcelona, Spain). All these solvents were HPLC grade. All other reagents were analytical grade and purchased from Sigma-Aldrich (St. Louis, MO, USA). Water used in all experiments was passed through a Milli-Q water purification system (18 mΩ) (Millipore, Milan, Italy).

Animals

The protocol of the present study was reviewed and approved by the Ethic Committee of Animal Experimentation of the University of Barcelona (ref. DMAH-4695). All animal handling followed the European Community guidelines for the care and management of laboratory animals. Male Sprague–Dawley rats (218–432 g) were housed in cages ($n=3$/cage) under controlled conditions of a 12 h light:dark cycle, with a temperature of 22 ± 3°C and a relative humidity of 40–70%. Water and a standard diet (2014 Teklad Global 14%, Harlan, Spain) were consumed *ad libitum*. No traces of *trans*-resveratrol were detected in the commercial diet as revealed by the analyses performed according to the method described previously (15). All rat manipulations were carried out in the morning to minimize the effects of circadian rhythm.

trans-Resveratrol Administration and Blood Sampling

Overnight fasted rats received a single p.o. or i.v. administration of *trans*-resveratrol at three different doses of 2 $mg\cdot kg^{-1}$ (8.8 $\mu mol\cdot kg^{-1}$), 10 $mg\cdot kg^{-1}$ (43.8 $\mu mol\cdot kg^{-1}$) or 20 $mg\cdot kg^{-1}$ (87.6 $\mu mol\cdot kg^{-1}$). All doses were adjusted according to the rat weight and were freshly prepared immediately before each administration. Given that *trans*-resveratrol is insoluble in water, this compound was solubilized using hydroxypropyl-β-cyclodextrin, a parentally safe excipient. The i.v. administration was performed in a physiological saline solution (0.9% NaCl) of hydroxypropyl-β-cyclodextrin at 1 $mL\cdot kg^{-1}$ via the tail vein. The p.o. administration was performed in an aqueous solution of hydroxypropyl-β-cyclodextrin (20%, w/v) by gavage at 10 $mL\cdot kg^{-1}$. Blood was collected from the saphenous vein (16) and placed in tubes containing EDTA-K_2 as anticoagulant (Microvette CB300, Sarstedt, Granollers, Spain). Plasma was immediately obtained by centrifugation at 1500 × *g* (Centrifuge MEGAFUGE 1.0R, Heraeus, Boadilla, Spain) for 15 min at 4°C and was kept at 4°C until analysis, which was performed straight away. Sampling times were 0, 0.016, 0.05, 0.083, 0.16, 0.25, 0.5, 0.75, 1, 1.5, 2, 2.5, 3, 4, 6, 8, 10, 12 and 24 h after administration. A sparse sampling design including 20 rats per dose and route, with 3 to 5 samples per animal, and 5 to 6 values per experimental time were used.

trans-Resveratrol and Its Conjugates Plasmatic Concentrations

Plasma samples were subjected to solid-phase extraction through a reversed-phase C_{18} Sep-Pak Cartridge (WAT051910, Waters, Mildford, USA), and *trans*-resveratrol and its

glucuronide and sulfate conjugates were analyzed by HPLC as described elsewhere (15). The method was previously validated observing a mean recovery in plasma of 97.4% and linearity ($R^2>0.99$) within the range of 0.01–5 $\mu mol \cdot L^{-1}$. The intra-day and inter-day precisions were lower than 10%, and the limits of detection and quantification were 1.73 and 5.77 $nmol \cdot L^{-1}$, respectively (15).

PK Modeling

Software

A non-compartmental analysis of the plasmatic concentrations of *trans*-resveratrol and its conjugates after i.v. and p.o. administration was carried out with WinNonlin version 3.3 (WinNonlin™ Copyright ©1998–2001, Pharsight Corporation). PK modeling was performed using nonlinear mixed-effects approach implemented in the software NONMEM, version 6.2 (Icon Development Solutions, MD, USA) (17) using the subroutine ADVAN6 (user-defined non-linear model). The first-order conditional estimation method (FOCE) with interaction was used for estimating the model parameters. The Xpose program version 4.2.1 (http://xpose.sourceforge.net) implemented into R version 2.11.1 (http://www.r-project.com) was used to guide the model-building process (18). Additional graphical and other statistical analysis including evaluation of NONMEN outputs were performed using S-Plus 6.2 for Windows (Insightful, Seattle, WA, USA). The visual predictive check was performed with the Perl speaks-NONMEM (PsN) 3.2.4. Tool-kit (http://psn.sourceforge.net) (19).

PK Data Analysis

The areas under the concentrations *vs* time profiles (AUC) from zero to infinity were estimated by non-compartmental analysis using the trapezoidal rule. Then, the individual plasmatic concentrations of *trans*-resveratrol and its glucuronide and sulfate conjugates were analyzed together to allow integrated modeling of parent drug and metabolites using the population modeling approach. Models were fitted to log-transformed concentrations ($\mu mol \cdot L^{-1}$). Plasmatic concentrations below the limit of quantification were excluded from the analysis. Inter-animal variability (IAV) was modeled exponentially, assuming a log-normal distribution for the PK parameters. Additive and combined error models on log-transformed data were tested for residual variability modeling of plasmatic concentrations of *trans*-resveratrol and its conjugates. Inclusion of IAV on residual error was also tested in all the cases.

Model selection was based on i) the decrease in the objective function value (OFV; -2xlog likelihood); ii) parameter precision expressed as relative standard error (RSE%) and calculated as the estimate of standard error, obtained as part of the standard NONMEM output, divided by the parameter value; iii) visual inspection of goodness-of-fit plots with Xpose 4.2.1. To statistically distinguish between nested models, the difference in the OFV was used because this difference is approximately χ^2 distributed. A significance level of $p<0.005$ that corresponded to a difference in OFV of 7.879 for 1 degree of freedom was considered. For non-hierarchical models, the most parsimonious model with the lowest objective function according to the Akaike information criterion (AIC) was chosen (20).

Base Population PK Model

A sequential pharmacokinetic analysis was performed. First, the intravenous concentrations *vs* time data of the parent compound and its conjugates were modeled. Once the best intravenous model was found, the disposition parameters were fixed, and the oral data of the three compounds were added to estimate the absorption parameters (absorption rate constants and bioavailability).

Intravenous Data Modeling. One-, two- and three-compartment linear models were evaluated to characterize the time course of the intravenous plasmatic concentrations of *trans*-resveratrol and its glucuronide and sulfate conjugates. Linear, non-linear or combined (linear and non-linear) elimination kinetics were tested to describe the elimination either of *trans*-resveratrol or of its conjugates. The models were parameterized in terms of distribution clearances (CL_D), apparent volumes of distribution (V), and elimination clearances (CL) for linear elimination processes or maximal elimination rate (V_m) and concentration of the drug at which the elimination is half maximal (K_m), according to the Michaelis-Menten equation.

Oral Data Modeling. According to previous knowledge existing about the kinetics of *trans*-resveratrol and its conjugates (11), pre-systemic metabolism of the parent compound at the enterocyte was tested by simulating simultaneous oral *trans*-resveratrol and equimolar conjugates dosing. A linear process was considered for *trans*-resveratrol absorption; meanwhile, linear, non-linear and combined (linear and non-linear) absorption/conversion processes were tested for the conjugates. Moreover, as it is known that a portion of glucuronide or of sulfate can be effluxed back from the enterocyte to the intestinal lumen (11), it was also tested in the model by allowing for a portion of the parent compound never to be absorbed into the circulation.

Covariate Analysis and Final Model

When the best base intravenous model was found, the covariate body weight was investigated to explain part of the variability between animals. The body weight was evaluated in order to see if part of the IAV observed in the PK parameters (specifically, CL_{Dr}, CL and V_{pg}) could be explained. Once the best base oral model was found, the actual dose was tested in bioavailability to study if linear or non-linear pharmacokinetic behavior took place. In this case, the inclusion of body weight in bioavailability was not considered biologically plausible. Of note, that dose was tested both as a categorical and continuous covariate in the model. Covariates were incorporated in the model when a drop of OFV of more than 7.879, corresponding to a significance level of $p<0.005$, was observed. The NONMEM code for the final model is included in the Appendix.

Model Validation

A prediction-corrected visual predictive check (pcVPC) was performed to determine whether the final model provides an adequate description of the data (21,22). By using pcVPC, both the observations and model predictions were normalized for the typical model predictions. pcVPCs were constructed with the median, 2.5th and 97.5th percentiles for the observed data, stratifying by compound/administration route. Then, 1000 data sets were simulated from the final model parameter estimates, and the non-parametric 95% confidence intervals for the median, 2.5th and 97.5th percentiles based on the 1000 simulated datasets were calculated and represented together for visual inspection. The extent of the Bayesian shrinkage was also evaluated for each parameter in the final population PK model (23). Large values of shrinkage would be associated with generally poor individual estimates of that parameter.

Model Simulation

Once the final model was proved to be stable through internal validation procedures, its predictive capacity was evaluated by simulating 1000 data sets after the i.v. dose of 15 $mg \cdot kg^{-1}$ of the parent compound. The external validation data were obtained using the same experimental conditions (15). The 2.5th, 50th and 97.5th percentiles of the simulated concentrations of *trans*-resveratrol and its conjugates were calculated for each sampling time and plotted together with external observations corresponding to the i.v. dose of 15 $mg \cdot kg^{-1}$ for visual inspection.

RESULTS

trans-Resveratrol and Its Conjugates Plasmatic Concentrations

The individual plasma concentrations of *trans*-resveratrol and its conjugates following i.v. and p.o. doses of 2, 10 and 20 $mg \cdot kg^{-1}$ are displayed in Figs. 1 and 2. A total of 1039 plasmatic concentrations were obtained for *trans*-resveratrol ($n=449$) and the two conjugates (glucuronide, $n=421$; sulfate, $n=169$) from 120 Sprague–Dawley rats and were used in the final data set. The sampling points adequately defined the overall PK profiles. Plasmatic concentrations were quantified up to 12–24 h post-administration of *trans*-resveratrol with the exception of sulfate conjugate. In this case, plasmatic concentrations were measurable up to around 2 h post-administration after the p.o. doses of 10 and 20 $mg \cdot kg^{-1}$ and were not detected after the lowest dose of 2 $mg \cdot kg^{-1}$. The total percentages of concentration values below the limit of detection or below the limit of quantification were 2.8%, 4.2% and 27.9% for resveratrol, glucuronide and sulfate, respectively.

PK Modeling

Non-compartmental Analysis

Mean values of AUC estimated from the experimental observations for *trans*-resveratrol and its conjugates after each dose/administration route are indicated in Table I. After i.v. and p.o. administration of 2, 10 and 20 $mg \cdot kg^{-1}$, the AUC for *trans*-resveratrol and its conjugates increased with the dose. When AUC was dose normalized (AUC/D), a linear PK behavior was observed for glucuronide and sulfate of *trans*-resveratrol. However, the AUC/D of the parent compound decreased approximately 70% after i.v. administration, while the decrease was 90% in the p.o. administration.

Population PK Model

A schematic of the full model obtained after a sequential population PK analysis is represented in Fig. 3.

Intravenous Data Model. Three-linked two-compartment models were assumed to provide the best intravenous model for both *trans*-resveratrol and its conjugates (glucuronide and sulfate). According to this model, *trans*-resveratrol was administered directly into the central compartment of *trans*-resveratrol (V_{cr}). Once there, all *trans*-resveratrol was assumed to be converted to its glucuronide and sulfate according to first-order elimination

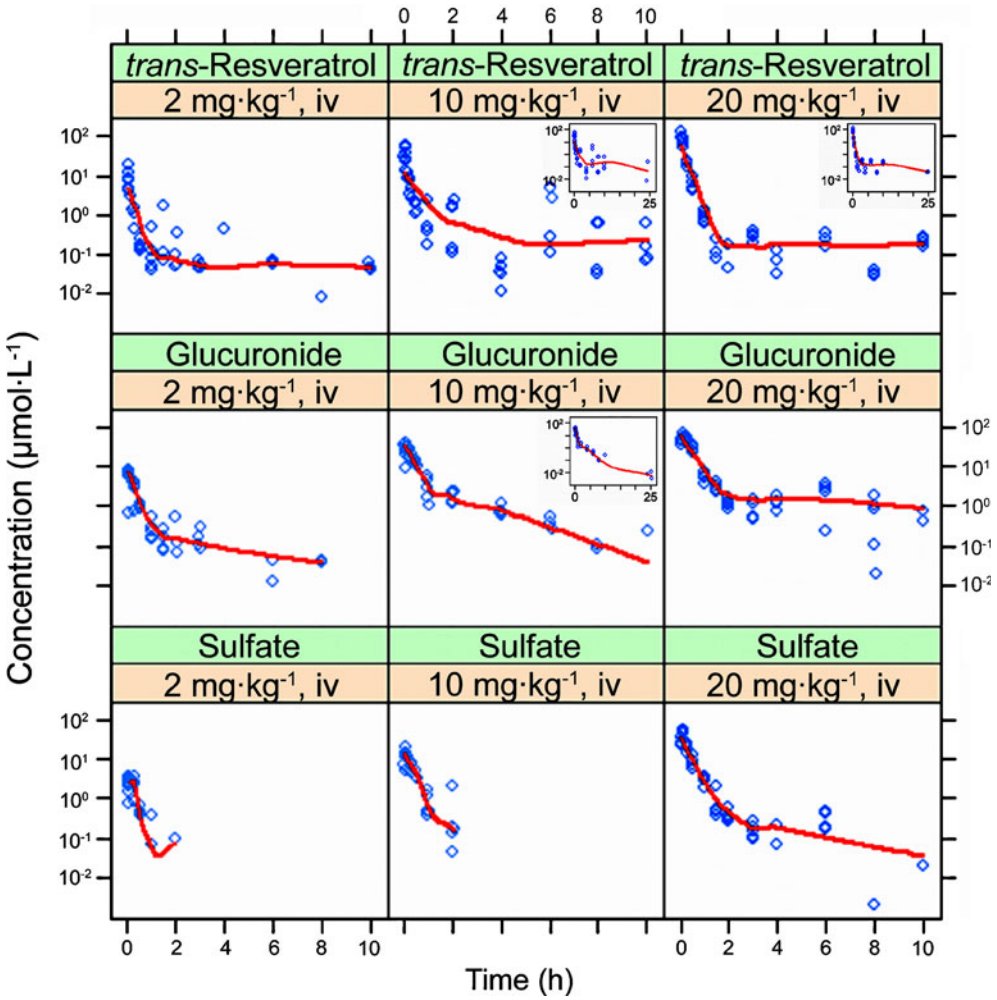

Fig. 1 Plasmatic concentrations *vs* time profile of *trans*-resveratrol and its glucuronide and sulfate conjugates (circles) after i.v. administration of *trans*-resveratrol at the doses of 2 $mg \cdot kg^{-1}$, 10 $mg \cdot kg^{-1}$ and 20 $mg \cdot kg^{-1}$ in rats. *Solid lines* represent the trend line of the observed data. The inserts depict the plasmatic concentrations *vs* time profile from 0 to 25 h.

processes, so two parallel elimination routes were considered. On the other hand, elimination of both metabolites was best described by combined first-order (CL_g and CL_s: clearances associated to the first-order elimination of the glucuronide and sulfate, respectively) and Michaelis-Menten processes (V_{mg}, K_{mg} and V_{ms}, K_{ms}: maximal elimination rates and concentrations of the drug at which the elimination is half maximal for the glucuronide and sulfate, respectively). The inclusion of a parallel Michaelis-Menten elimination process to the linear one, for the glucuronide and sulfate, reduced the AIC values in 17.54 and 3.01 points, respectively. IAV could be included in distributional (CL_{Dr}) and total elimination clearance (CL) of *trans*-resveratrol and peripheral distribution volume of the glucuronide conjugate (V_{pg}). For the other parameters, inclusion of IAV did not improve the fit. Residual error of the three compounds was best described by an additive model on log-transformed data. The clearances associated to the conversion of *trans*-resveratrol to its glucuronide (CL_{fg}) and sulfate (CL_{fs}) were calculated as $CL_{fg} = CL \cdot f_m$, and $CL_{fs} = CL \cdot (1\text{-}f_m)$, where f_m and $1\text{-}f_m$ were the fractions of the parent compound metabolized to the glucuronide and sulfate conjugates, respectively. Since only the parent compound was administered, this model was *a priori* unidentifiable, and f_m, the distribution volumes and the clearances of formation of both metabolites could not be estimated independently. A simultaneous modeling of *trans*-resveratrol and glucuronide intravenous data, performed in a previous step, provided a V_{cg}/f_m value of 0.0970, under the assumption of $f_m = 1$, i.e. total conversion of the parent compound to the metabolite. Consequently, when the plasmatic sulfate data were incorporated into the modeling process, the V_{cg} value was assumed to be 0.05 for the remaining parameter estimation in order to avoid f_m values >1. Then, it was possible to identify f_m, and once f_m was known, $1\text{-}f_m$ could be estimated too, under the assumption that there was no other elimination of *trans*-resveratrol except by formation of glucuronide or sulfate. Therefore, the amount of formed sulfate was known, and the central compartment volume of this metabolite could be identified. By assuming a value for V_{cg}, the clearance values associated to the formation of the metabolites were also identifiable. Of note, the V_{cs} is not necessarily equal to the V_{cg}, but its numerical value is depending on the last. The intravenous

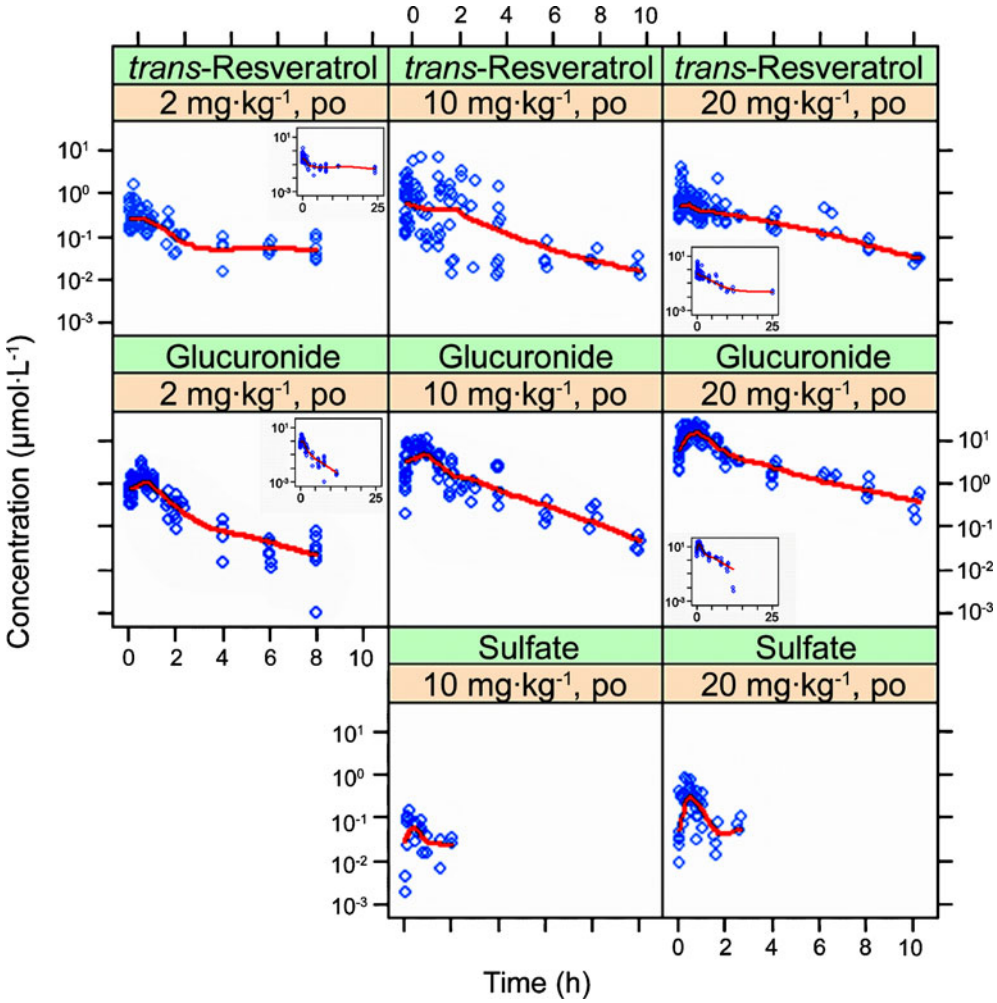

Fig. 2 Plasmatic concentrations *vs* time profile of *trans*-resveratrol and its glucuronide and sulfate conjugates (circles) after p.o. administration of *trans*-resveratrol at the doses of 2 mg·kg^{-1}, 10 mg·kg^{-1} and 20 mg·kg^{-1} in rats. *Solid lines* represent the trend line of the observed data. The inserts depict the plasmatic concentrations *vs* time profile from 0 to 25 h.

PK base model was assessed both with a full variance-covariance matrix and a diagonal variance-covariance matrix for random-effects. The full matrix did not reduce the OFV, and therefore was not considered further.

Covariate Analysis and Final Intravenous Model. The body weight did not show any significant effect when entered in the intravenous model. The parameter estimates for the final PK intravenous model are given in Table II. The

Table I Mean AUC and AUC Normalized by Actual Doses (AUC/D) Values for *trans*-Resveratrol and Its Conjugates Glucuronide and Sulfate after i.v. and p.o. Doses of 2, 10 and 20 mg·kg^{-1}

Dose	Intravenous administration		Oral administration	
	AUC (μmol·L^{-1})·h	AUC/D	AUC (μmol·L^{-1})·h	AUC/D
trans-Resveratrol				
2 mg·kg^{-1}	6.87	2.85	4.04	1.50
10 mg·kg^{-1}	19.8	1.53	4.09	0.3
20 mg·kg^{-1}	25.8	0.95	3.34	0.12
trans-Resveratrol glucuronide				
2 mg·kg^{-1}	5.47	2.27	2.37	0.88
10 mg·kg^{-1}	23.2	1.79	14.7	1.09
20 mg·kg^{-1}	49.5	1.82	36.3	1.24
trans-Resveratrol sulfate				
2 mg·kg^{-1}	1.32	0.55	–	–
10 mg·kg^{-1}	6.16	0.48	0.13	0.01
20 mg·kg^{-1}	16.48	0.61	0.46	0.02

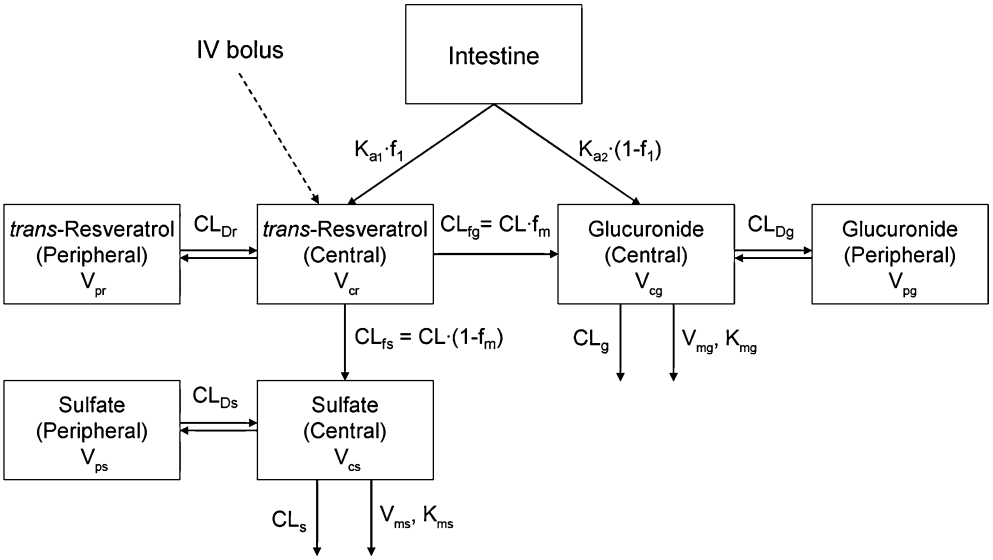

Fig. 3 Schematic representation of the pharmacokinetic model to simultaneously describe the data of *trans*-resveratrol and its glucuronide and sulfate conjugates after i.v. and p.o. administration. The model consists of three-linked two compartments with first-order absorption process and first-order elimination from the central compartment through the metabolites glucuronide and sulfate. The model also allows the inclusion of the pre-systemic metabolism of *trans*-resveratrol to glucuronide in the intestine.

standard errors of the estimated parameters could not be obtained due to matrix algorithmically singular and algorithmically non-positive semidefinite and covariance step aborted. IAV included in CL, CL_{Dr} and V_{pg} were 19.34%, 90.00% and 61.24%, respectively. Large values of residual variabilities (*trans*-resveratrol: 75.96%; glucuronide: 52.73%; sulfate: 41.35%) were found probably due to analytical contributions and model misspecifications. The mean half-life ($t_{1/2\beta}$) value of *trans*-resveratrol after i.v. administration calculated from the Bayesian estimations was 0.55 h.

Oral Data Model. Once the disposition parameters were obtained, they were fixed in order to estimate the absorption parameters (absorption rate constants and bioavailability). Therefore, a depot compartment (intestinal compartment) was added to the intravenous model where *trans*-resveratrol was administered. When going into the gastrointestinal tract, *trans*-resveratrol was supposed to be subject to first-pass metabolism and to reach the systemic circulation intact or as its glucuronide. The data did not support the inclusion of first-pass metabolism of *trans*-resveratrol to sulfate, so the model was simplified to absorption/presystemic metabolism of *trans*-resveratrol to its glucuronide and absorption of the formed glucuronide. The inclusion of a fraction of the parent compound never absorbed, and due to metabolism to the conjugates and efflux of them back into intestine, did not improve the fit. The proportions of absorbed intact *trans*-resveratrol and its glucuronide were estimated as f_1 and ($1\text{-}f_1$), respectively. It was assumed that the total absorption of *trans*-resveratrol and its glucuronide was 100%, and the absorption rate for *trans*-resveratrol was rate limiting; hence, the rate of appearance of glucuronide was set to the absorption rate constant. First-order kinetic processes described the presentation of both *trans*-resveratrol and its glucuronide into the systemic circulation with lower AIC values than Michaelis-Menten kinetics. Different rate constant values for both compounds (*trans*-resveratrol *vs* glucuronide) provided a statistically significant reduction of the OFV in 315.98 points ($p<0.001$). IAV could only be included in f_1. Residual error of the three compounds was best described by an additive model on log-transformed data.

Covariate Analysis and Final Oral Model. The covariate analysis showed a dose-dependency behavior in f_1. The inclusion of dose as a continuous covariate resulted in a higher drop of the OFV than when it was entered as a categorical variable. The inclusion of dose on f_1 reduced the OFV in 81.41 points. The IAV in f_1 was reduced from 96.18% (base model) to 64.80% (final model). According to the final oral model, f_1 decreased significantly with increasing doses from 2 to 20 $mg\cdot kg^{-1}$ ($p<0.001$). Specifically a decrease in f_1 values of 20.62% (from 2 to 10 mg/kg) and 32.12% (from 10 to 20 mg/kg) occurred. The parameter estimates for the oral data model are given in Table II. The RSE of both fixed and random parameters were from 2.70% to 29.29%, which suggests that these parameters were estimated with good precision. As in the intravenous data model, large values of residual variabilities (*trans*-resveratrol: 88.03%; glucuronide: 61.16%; sulfate: 71.62%) were found, probably due to analytical contributions and model misspecifications. Of note, although in the final step of the model development a simultaneous intravenous and oral data modeling was evaluated, the minimization was terminated due to an excess of maximum number of function evaluations and an unreportable number of significant digits.

Table II Population Pharmacokinetic Parameters, Inter-animal and Residual Variability of *trans*-Resveratrol and Its Glucuronide and Sulfate Conjugates after I.V. and P.O. Administration

Parameters	Final model	
Disposition parameters		
trans-Resveratrol	Estimate	RSE (%)
CL ($L \cdot h^{-1}$)	1.24	–[a]
V_{cr} (L)	0.249	–
CL_{Dr} ($L \cdot h^{-1}$)	0.436	–
V_{pr} (L)	2.80	–
f_m	0.540	–
Glucuronide		
CL_g ($L \cdot h^{-1}$)	0.297	–
V_{cg} (L)	0.05	fixed
CL_{Dg} ($L \cdot h^{-1}$)	0.127	–
V_{pg} (L)	0.327	–
V_{mg} ($\mu mol \cdot h^{-1}$)	0.0961	–
K_{mg} ($\mu mol \cdot L^{-1}$)	0.00518	–
Sulfate		
CL_s ($L \cdot h^{-1}$)	0.737	–
V_{cs} (L)	0.0613	–
CL_{Ds} ($L \cdot h^{-1}$)	0.273	–
V_{ps} (L)	0.0770	–
V_{ms} ($\mu mol \cdot h^{-1}$)	0.139	–
K_{ms} ($\mu mol \cdot L^{-1}$)	0.0229	–
Absorption parameters		
K_{a1} (h^{-1})	0.442	23.52
f_1	$\theta_1 \cdot (1-\theta_2 \cdot Dose)$[b]	
	$\theta_1 = 0.474$	12.05
	$\theta_2 = 0.0244$	2.70
K_{a2} (h^{-1})	0.256	7.50
Inter-animal variability[c]		
CL	19.34	–
CL_{Dr}	90.00	–
V_{pg}	61.24	–
f_1	64.80	29.29
Residual variability[c]		
Intravenous data		
trans-Resveratrol	75.96	–
Glucuronide	52.73	–
Sulfate	41.35	–
Oral data		
trans-Resveratrol	88.03	13.16
Glucuronide	61.16	21.95
Sulfate	71.62	25.34

[a] The standard errors of the disposition estimated parameters could not be obtained due to covariance step aborted of the final intravenous data run.

[b] Dose values are expressed in μmol.

[c] Inter-animal and residual variabilities are expressed as coefficient of variation (CV%).

Intravenous and Oral Data Model Evaluations

Figure 4 illustrates the correlation between observed (DV) and population model-predicted (PRED) and between DV and individual model-predicted (IPRED) concentrations for both intravenous and oral data models. These plots indicated that the models adequately described the concentrations of *trans*-resveratrol and its conjugates. Estimates of η-shrinkage for CL, CL_{Dr}, V_{pg} and f_1 were −2.36, −0.035, 0.15 and −0.28, respectively, while those of ε-shrinkage were 0.37 and 0.20 for intravenous and oral data, respectively. According to these values, shrinkage was present, but it did not affect the correct model selection because it was based on standard model building using the objective function values (23), rather than on empirical bayes estimates (EBE's), IPRED and individual weighted residuals (IWRES). Moreover, the condition number for the oral data model was 8.115, which indicates that the parameter estimates were not severely influenced by ill-conditioning.

Model Validation

The results of the pcVPC stratified by compound (*trans*-resveratrol and its metabolites)/administration route are depicted in Fig. 5. These plots indicated that the model predicts the data adequately in such a way that the 2.5%, 50% and 97.5% percentiles of the observed data overlap the corresponding percentiles of the simulated data.

Model Simulations

According to the results of Fig. 6 the final model showed a satisfactory predictive performance for which there was a close agreement between the observed data found after an i.v. administration of 15 $mg \cdot kg^{-1}$ of *trans*-resveratrol and model-predicted concentration data for this dose and administration route.

DISCUSSION

The present study performs an integrated PK analysis of *trans*-resveratrol and its glucuronide and sulfate conjugates using a population approach with the non-linear mixed effects modeling. This approach preserves the individuality of plasma concentration profiles and allows the estimation of the typical PK parameters, the corresponding IAV as well as the residual variability. To this end, all the data (from parent compound and conjugates) obtained after the i.v. and p.o. administrations of three doses of *trans*-resveratrol were modeled using a sequential analysis. First, the intravenous data were modeled, and once the disposi-

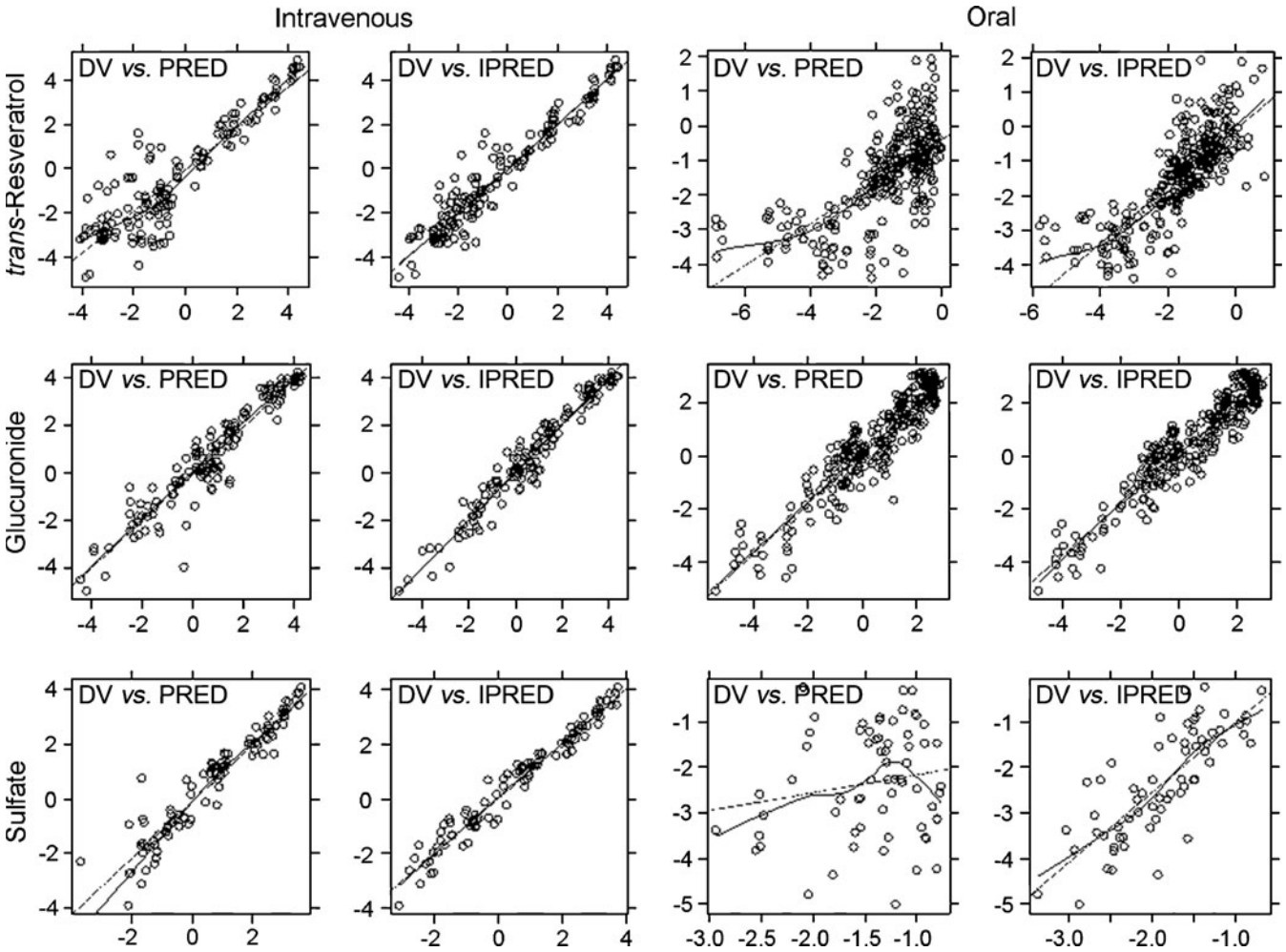

Fig. 4 Goodness-of-fit plots for the final population pharmacokinetic model. The scatter plots show the observed concentrations (DV) *vs* population model predictions (PRED) and observed concentrations (DV) *vs* individual model predictions (IPRED). The *dashed lines* represent the identity line; the *solid lines* display the smooth line indicating the general data trend. Concentrations are given in $\mu mol \cdot L^{-1}$.

tion parameters were obtained, they were fixed, and the oral data were added in order to estimate the absorption parameters. One-, two- and three-compartment linear models were evaluated to characterize the disposition of *trans*-resveratrol and its conjugates. The best full PK intravenous model was achieved by three-linked two compartments.

Elimination of *trans*-resveratrol by conversion to its glucuronide and sulfate took place by a first-order kinetic process. It is noteworthy that the transformation of the parent compound to its conjugates was not saturable even at the plasmatic concentrations achieved after the highest dose assayed (20 $mg \cdot kg^{-1}$). Meanwhile, clearance of *trans*-resveratrol glucuronide and sulfate was best described by parallel first-order and Michaelis-Menten kinetics. These results are in agreement with existing knowledge about elimination mechanisms of both conjugates (14,24). In effect, glucuronide and sulfate can suffer either renal or biliar excretion, and in tubular cells and hepatocytes both first-order and Michaelis-Menten kinetics are implicated. The total clearance value of *trans*-resveratrol was slightly higher than ¾ times the hepatic blood flow in the rat (0.90 L/h for a body weight of 0.25 kg). According to the f_m value obtained (0.540), approximately the same percentage of both metabolites was formed. Clearances of formation of the glucuronide and sulfate were 0.67 and 0.57 $L \cdot h^{-1}$, respectively. Distribution volume of *trans*-resveratrol (total distribution volume = 3.05 L) exceeded the total body water in the rat (0.15 $L \cdot kg^{-1}$ for a body weight of 0.25 kg), suggesting extensive distribution into tissues. A short half-life value was estimated for *trans*-resveratrol (0.55 h) that was in agreement with its clearance and distribution volumes values. By contrast, smaller distribution volumes were found for the metabolites (total distribution

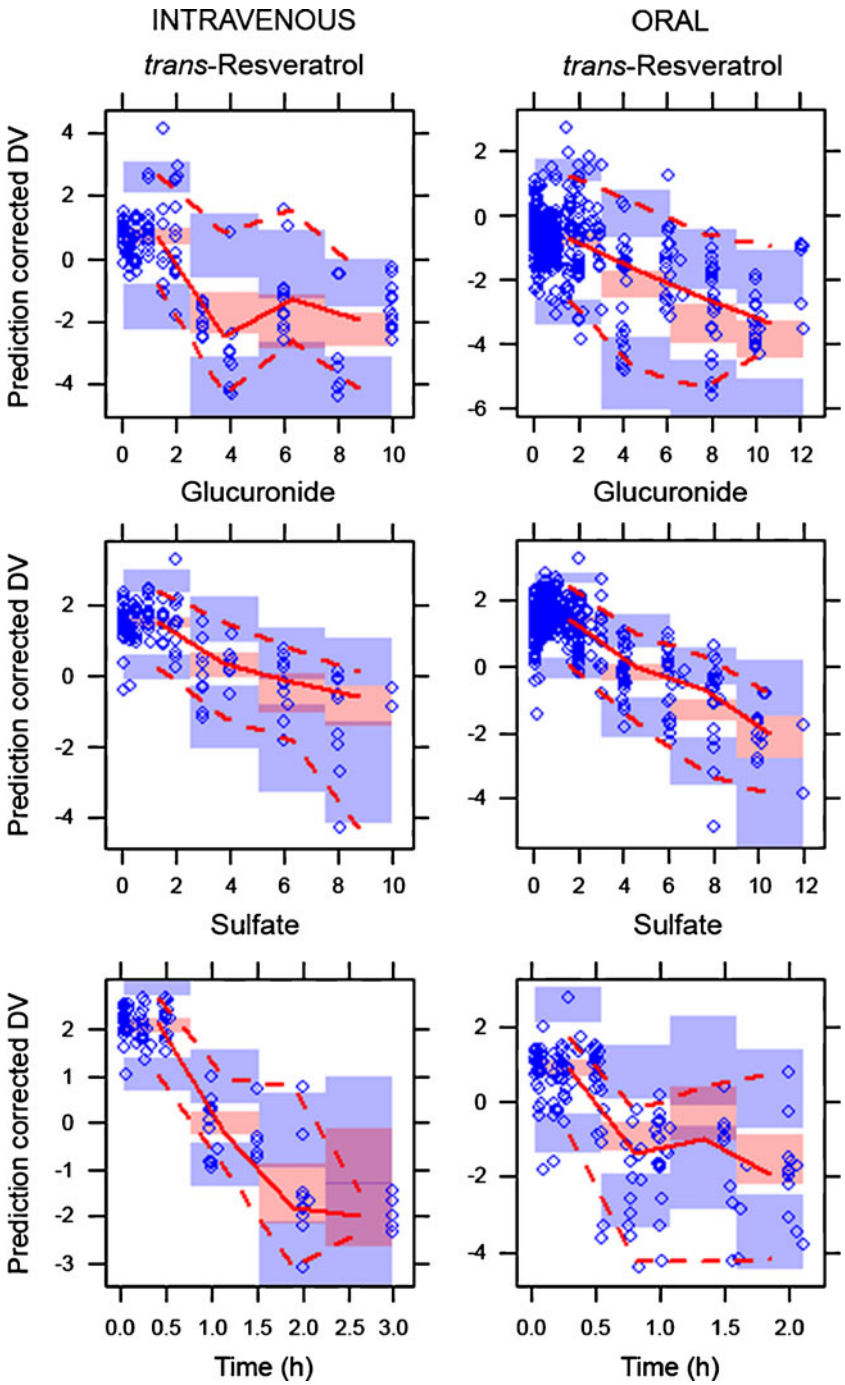

Fig. 5 Prediction-corrected visual predictive check of the pharmacokinetic model for *trans*-resveratrol and its glucuronide and sulfate conjugates after the i.v. and p.o. administrations of 2, 10 and 20 $mg \cdot kg^{-1}$ of *trans*-resveratrol to rats. The *circles* represent the observed data. *Dashed red lines* depict the 2.5th and 97.5th percentiles of the observed concentrations. *Solid red lines* correspond to the 50th percentiles of the observed concentrations. *Shaded blue* areas correspond to the 2.5th and 97.5th percentiles and *shaded red* area to the median calculated from 1000 simulated data sets.

volumes = 0.38 and 0.14 L for the glucuronide and sulfate, respectively).

In the present study, the plasmatic concentrations of *trans*-resveratrol obtained after i.v. and p.o. administration are low and in accordance with previous results obtained by different authors (4–8). The low bioavailability might be explained, at least in part, by the first-pass effect not only in the liver (25–27) but also in the intestine (11,24,28,29). After p.o. administration, *trans*-resveratrol enters to the enterocyte by simple diffusion (11). Then, this compound undergoes extensive metabolism to its glucuronide and sulfate conjugates (25,26) that are excreted back, in part, to the intestinal lumen through the specific proteins multidrug resistance protein 2 (MRP2) and breast cancer resistance protein (BCRP) (11). The metabolism in the liver accounted for an extensive glucuronidation and sulfatation through UDP-glucuronosyltransferase (UGT) and sulfotransferase, respectively (4,27). *trans*-Resveratrol and its

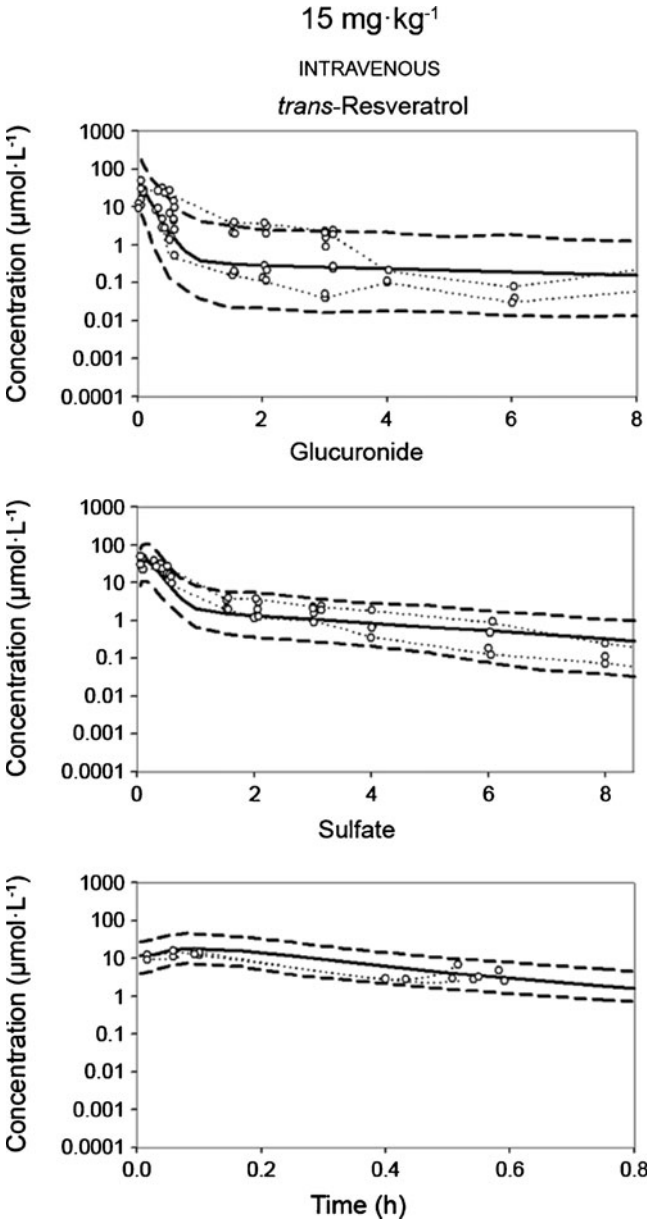

Fig. 6 Model predictive performance of external data. Observed concentrations (*circles*) of an external data set after an i.v. administration of 15 mg·kg^{-1} of *trans*-resveratrol are represented with simulated 50th percentile (*solid line*) and 2.5th and 97.5th percentiles (*dashed lines*) and the actual 2.5th and 97.5th percentiles (*dotted lines*). Simulations (n = 1000) are based on the final model for an i.v. dose of 15 mg·kg^{-1}.

conjugates accumulate significantly in this organ (14,15) and are further excreted into the bile, leading to enterohepatic recirculation (6,27). The contribution of the biliar pathways to the elimination of the conjugated metabolites could not be captured by the present model, although a light rebound was observed after 6 h of the i.v. administration, supporting the occurrence of the enterohepatic cycle. Previously, Marier *et al.* (6) have reported that the enterohepatic recirculation using a linked rat model induced significant increase of plasma concentrations of resveratrol and its glucuronide in bile-recipient rats at 4 to 8 h.

The linearity of the PK after i.v. and p.o. administration of three doses of *trans*-resveratrol was also assessed. The AUC estimated for the parent compound and its conjugated metabolites, by non-compartmental procedures, indicated non-linear PK behavior for *trans*-resveratrol, especially evident after p.o. administration. The linearity of the PK of this polyphenol has scarcely been evaluated previously. Boocock *et al.* (8) performed a pharmacokinetic study after the p.o. administration of 7, 14, 36 and 72 mg·kg^{-1} of *trans*-resveratrol in humans. When plotted *vs* dose, the mean AUC and C_{max} values for *trans*-resveratrol increased with dose but in a slightly less than dose-proportional manner, in accordance with our results. The PK behaviors of *trans*-resveratrol and its metabolites in a living animal are somewhat complex. The important role that the intestine plays not only in the absorption process but also in the metabolism of these compounds might explain, at least in part, the differences observed between the oral and intravenous routes (5,14). The lower exposure (AUC) values found after the oral route compared to the intravenous at the three assayed doses could be attributed to the metabolism occurring at the enterocyte as well as the efflux processes from the enterocyte by transporters such as MRP2 or BCRP (11,14).

The uptake of *trans*-resveratrol through the intestine is best fitted with a first-order kinetic. Our plasmatic data of this compound and its glucuronide and sulfate metabolites only allowed the inclusion of the first-pass metabolism in the intestine of *trans*-resveratrol to its glucuronide, but could not take in the conjugation to *trans*-resveratrol sulfate. One of the reasons why *trans*-resveratrol sulfate could not be included in the presystemic metabolism of *trans*-resveratrol might be the low concentrations of this metabolite that reached the bloodstream. These low concentrations could be attributed to a lower sulfation compared to the glucuronidation of *trans*-resveratrol in the rat intestine (28,29). Moreover, the higher affinity and capacity of BCRP for *trans*-resveratrol sulfate compared to the one observed for the glucuronide could account for a higher efficiency in the secretion of the sulfate (24). Andlauer *et al.* (28) appointed that only 0.3% of the absorbed resveratrol reaches the blood as sulfate. Altogether, these processes could explain why the model did not support the inclusion of presystemic metabolism of *trans*-resveratrol to its sulfate conjugate.

In the final model developed, the rate-limiting step is most likely the absorption process of *trans*-resveratrol and its glucuronide rather than the metabolism. The first-order absorption rate constants (K_{a1}=0.442 h^{-1}, absorption half life = 1.57 h, K_{a2}=0.256 h^{-1}, absorption/metabolism half life = 2.71 h) confirmed rapid absorption/metabolism kinetics for both compounds. Our results show that when the dose administered increased, a lower fraction of *trans*-resveratrol

remained unchanged (f_1 = 0.420, 0.207 and 0.060 for the doses of 2, 10 and 20 mg·kg^{-1}, respectively, and a body weight of 0.25 kg). By contrast, the relative fraction of glucuronide formed/absorbed from the intestine increased with the dose with values of 0.580, 0.793 and 0.94 for the doses of 2, 10 and 20 mg·kg^{-1} and a body weight of 0.25 kg, respectively.

Our work also aimed to develop a PK model for estimation of the time course of *trans*-resveratrol in plasma to be used in future PK-pharmacodynamic (PD) investigation. For this reason, once the model was established and proved to be stable through the internal validation procedures, its predictive capacity was evaluated using an external data set obtained after the i.v. administration of 15 mg·kg^{-1}. The results showed a close agreement between the observed data and the predicted concentrations for the dose and administration route assayed, supporting the hypothesis of the robustness of the model.

In summary, we built a population PK model to adequately describe plasma data of *trans*-resveratrol and its currently known major metabolites in the rat, including the glucuronide and the sulfate. These data not only increase our knowledge to better understand the PK of this polyphenol but also may be applicable to many other polyphenols which have similar PK properties. In addition the model may also be useful for planning future PK–PD studies to establish the relative contribution of the conjugates to the overall efficacy.

ACKNOWLEDGMENTS

This study was supported by the Ministerio de Ciencia y Tecnología grants AGL2005-05728 and AGL2009-12866 and the Generalitat de Catalunya grants 2005-SGR-00632 and 2009-SGR-00471.

APPENDIX

The NONMEM code used in the final model

Modeling of Intravenous Data

```
$PROBLEM trans-resveratrol and its conjugates plasmatic concentrations
$INPUT ID TIME AMT DV MDV EVID CMT WGT ROUT DOSA;DOSA=ACTUAL DOSE
$DATA data.csv IGNORE=#
IGNORE (ROUT.EQ.2)
$SUBROUTINES ADVAN6 TOL=3
$MODEL

  COMP = (CENTRALRESV,DEFOBS)
  COMP = (PERIPHRESV)
  COMP = (CENTRALGLUC)
  COMP = (PERIPHGLUC)
  COMP = (CENTRALSULF)
  COMP = (PERIPHSULF)


$PK
  ;DISPOSITION PARAMETERS

  ;trans-Resveratrol
   TVCL1              = THETA(1)
   CL1                = TVCL1*EXP(ETA(1))     ;Plasmatic CL of resveratrol
   V1                 = THETA(2)              ;Central compartment V of resveratrol
   Q                  = THETA(3)*EXP(ETA(2))  ;Distributional CL of resveratrol
   V2                 = THETA(4)              ;Peripheral compartment V of resveratrol
  ;Glucuronide
   V3                 = 0.05                  ;Central compartment V of the glucuronide
```

```
 QM1                    = THETA(5)              ;Distributional CL of the glucuronide
 V4                     = THETA(6) *EXP(ETA(3)) ;Peripheral compartment V of the glucuronide
 ;Linear elimination process
 CL2                    = THETA(7)              ;Plasmatic CL of the glucuronide
 ;Non-linear elimination
   process
 VMG                    = THETA(8)              ;Maximal elimination rate of the glucuronide
 KMG                    = THETA(9)              ;Concentration of the glucuronide at which the elimination is half maximal
 FM                     = THETA(10)             ;Fraction of resveratrol converted to its glucuronide
;Sulfate
 V5                     = THETA(11)             ;Central compartment V of the sulfate
 V6                     = THETA(12)             ;Peripheral compartment V of the sulfate
 QM2                    = THETA(13)             ;Distributional CL of the sulfate
 ;Linear elimination process
 CL3                    = THETA(14)             ;Plasmatic CL of the sulfate
 ;Non-linear elimination
   process
 VMS                    = THETA(15)             ;Maximal elimination rate of the sulfate
 KMS                    = THETA(16)             ;Concentration of the sulfate at which the elimination is half maximal

;SCALE FACTORS

 S1 = V1
 S3 = V3
 S5 = V5

;RATE CONSTANTS

 K12 = Q/V1
 K21 = Q/V2
 K30 = CL2/V3
 K34 = QM1/V3
 K43 = QM1/V4
 K56 = QM2/V5
 K65 = QM2/V6
 K50 = CL3/V5

;DIFFERENTIAL EQUATIONS
$DES

 DADT(1)                = -K12*A(1)+K21*A(2)-(CL1/V1)*FM*A(1)-(CL1/V1)*(1-FM)*A(1)
 DADT(2)                = K12*A(1)-K21*A(2)
 DADT(3)                = (CL1/V1)*FM*A(1)-K30*A(3)+K43*A(4)-K34*A(3)-(VMG*A(3))/(KMG+A(3))
 DADT(4)                = K34*A(3)-K43*A(4)
 DADT(5)                = (CL1/V1)*(1-FM)*A(1)-K56*A(5)+K65*A(6)-K50*A(5))-(VMS*A(5))/(KMS+A(5))
 DADT(6)                = K56*A(5)-K65*A(6)

;RESIDUAL ERROR FOR LOG-TRANSFORMED DATA
$ERROR

 IPRED                  = -5
 IF(F.GT.0)             IPRED= LOG(F)
 IF(CMT.EQ.1)           Y= IPRED+EPS(1)
 IF(CMT.EQ.3)           Y= IPRED+EPS(2)
```

```
   IF(CMT.EQ.5)              Y= IPRED + EPS(3)
   IWRES                     = (DV-IPRED)

;INITIAL ESTIMATES
$THETA
$OMEGA
$SIGMA
$ESTIMATION
$COVARIANCE
```

Modeling of Oral Data

```
$PROBLEM trans-resveratrol and its conjugates plasmatic concentrations
$INPUT ID TIME AMT DV MDV EVID CMT WGT ROUT DOSA;DOSA=ACTUAL DOSE
$DATA data.csv IGNORE=#
IGNORE (ROUT.EQ.1)
$SUBROUTINES ADVAN6 TOL=3
$MODEL

   COMP = (DEPOT)
   COMP = (CENTRALRESV,DEFOBS)
   COMP = (PERIPHRESV)
   COMP = (CENTRALGLUC)
   COMP = (PERIPHGLUC)
   COMP = (CENTRALSULF)
   COMP = (PERIPHSULF)

$PK
   "FIRST
   " COMMON/PRCOMG/IDUM1,IDUM2,IMAX,IDUM4,IDUM5
   " INTEGER IDUM1,IDUM2,IMAX,IDUM4,IDUM5
   " IMAX=70000000
  ;DISPOSITION PARAMETERS

  ;trans-Resveratrol
   TVCL1                     = THETA(1)
   CL1                       = TVCL1*EXP(ETA(1))     ;Plasmatic CL of resveratrol
   V2                        = THETA(2)              ;Central compartment V of resveratrol
   Q                         = THETA(3)*EXP(ETA(2))  ;Distributional CL of resveratrol
   V3                        = THETA(4)              ;Peripheral compartment V of resveratrol
  ;Glucuronide
   V4                        = 0.05                  ;Central compartment V of the glucuronide
   QM1                       = THETA(5)              ;Distributional CL of the glucuronide
   V5                        = THETA(6) *EXP(ETA(3)) ;Peripheral compartment V of the glucuronide
   FM                        = THETA(7)              ;Fraction of resveratrol converted to its glucuronide
   ;Linear elimination process
   CL2                       = THETA(8)              ;Plasmatic CL of the glucuronide
   ;Non-linear elimination process
   VMG                       = THETA(9)              ;Maximal elimination rate of the glucuronide
   KMG                       = THETA(10)             ;Concentration of the glucuronide at which the elimination is half maximal
  ;Sulfate
   V6                        = THETA(11)             ;Central compartment V of the sulfate
   V7                        = THETA(12)             ;Peripheral compartment V of the sulfate
   QM2                       = THETA(13)             ;Distributional CL of the sulfate
   ;Linear elimination process
```

```
CL3                          = THETA(14)          ;Plasmatic CL of the sulfate
;Non-linear elimination process
VMS                          = THETA(15)          ;Maximal elimination rate of the sulfate
KMS                          = THETA(16)          ;Concentration of the sulfate at which the elimination is half maximal
```

;ABSORPTION PARAMETERS

```
KA1          = THETA(17)                          ;Absorption rate constant
KA2          = THETA(18)                          ;Transformation (from the parent compound to the glucuronide)/Absorption rate constant
TVF1         = THETA(19)*(1-THETA(20)*DOSA)
F1           = TVF1*EXP(ETA(4))                   ;Bioavailability
```

;SCALE FACTORS

```
S2 = V2
S4 = V4
S6 = V6
```

;RATE CONSTANTS

```
K23 = Q/V2
K32 = Q/V3
K40 = CL2/V4
K45 = QM1/V4
K54 = QM1/V5
K67 = QM2/V6
K76 = QM2/V7
K60 = CL3/V6
```

;DIFFERENTIAL EQUATIONS
$DES

```
DADT(1)                      = -KA1*F1*A(1)-KA2*(1-F1)*A(1)
DADT(2)                      = KA1*F1*A(1)-K23*A(2)+K32*A(3)-(CL1/V2)*FM*A(2)-(CL1/V2)*(1-FM)*A(2)
DADT(3)                      = K23*A(2)-K32*A(3)
DADT(4)                      = KA2*(1-F1)*A(1)+(CL1/V2)*FM*A(2)-K40*A(4)+K54*A(5)-K45*A(4)-(VMG*A(4))/(KMG+A(4))
DADT(5)                      = K45*A(4)-K54*A(5)
DADT(6)                      = (CL1/V2)*(1-FM)*A(2)-K67*A(6)+K76*A(7)-K60*A(6))-(VMS*A(6))/(KMS+A(6))
DADT(7)                      = K67*A(6)-K76*A(7)
```

;RESIDUAL ERROR FOR LOG-TRANSFORMED DATA
$ERROR

```
IPRED        = -5
IF(F.GT.0)   IPRED        = LOG(F)
IF(CMT.EQ.2) Y            = IPRED+EPS(1)
IF(CMT.EQ.4) Y            = IPRED+EPS(2)
IF(CMT.EQ.6) Y            = IPRED+EPS(3)
IWRES        = (DV-IPRED)
```

;INITIAL ESTIMATES
$THETA
$OMEGA
$SIGMA
$ESTIMATION
$COVARIANCE

REFERENCES

1. Pervaiz S, Holme AL. Resveratrol: its biologic targets and functional activity. Antioxid Redox Signal. 2009;11(11):2851–97.
2. Brisdelli F, D'Andrea G, Bozzi A. Resveratrol: a natural polyphenol with multiple chemopreventive properties. Curr Drug Metab. 2009;10(6):530–46.
3. Juan ME, Vinardell MP, Planas JM. The daily oral administration of high doses of *trans*-resveratrol to rats for 28 days is not harmful. J Nutr. 2002;132(2):257–60.
4. Cottart CH, Nivet-Antoine V, Laguillier-Morizot C, Beaudeux JL. Resveratrol bioavailability and toxicity in humans. Mol Nutr Food Res. 2010;54(1):7–16.
5. Juan ME, Buenafuente J, Casals I, Planas JM. Plasmatic levels of *trans*-resveratrol in rats. Food Res Int. 2002;35(2–3):195–9.
6. Marier JF, Vachon P, Gritsas A, Zhang J, Moreau JP, Ducharme MP. Metabolism and disposition of resveratrol in rats: extent of absorption, glucuronidation, and enterohepatic recirculation evidenced by a linked-rat model. J Pharmacol Exp Ther. 2002;302(1):369–73.
7. Sale S, Verschoyle RD, Boocock D, Jones DJ, Wilsher N, Ruparelia KC, *et al.* Pharmacokinetics in mice and growth-inhibitory properties of the putative cancer chemopreventive agent resveratrol and the synthetic analogue trans 3, 4, 5, 4′-tetramethoxystilbene. Br J Cancer. 2004;90(3):736–44.
8. Boocock DJ, Faust GE, Patel KR, Schinas AM, Brown VA, Ducharme MP, *et al.* Phase I dose escalation PK study in healthy volunteers of resveratrol, a potential cancer chemopreventive agent. Cancer Epidemiol Biomark Prev. 2007;16(6):1246–52.
9. Almeida L, Vaz-da-Silva M, Falcão A, Soares E, Costa R, Loureiro AI, *et al.* PK and safety profile of *trans*-resveratrol in a rising multiple-dose study in healthy volunteers. Mol Nutr Food Res. 2009;53 Suppl 1:S7–15.
10. Nunes T, Almeida L, Rocha JF, Falcão A, Fernandes-Lopes C, Loureiro AI, *et al.* Pharmacokinetics of *trans*-resveratrol following repeated administration in healthy elderly and young subjects. J Clin Pharmacol. 2009;49(12):1477–82.
11. Juan ME, González-Pons E, Planas JM. Multidrug resistance proteins restrain the intestinal absorption of *trans*-resveratrol in rats. J Nutr. 2010;140(3):489–95.
12. Hebbar V, Shen G, Hu R, Kim BR, Chen C, Korytko PJ, *et al.* Toxicogenomics of resveratrol in rat liver. Life Sci. 2005;76 (20):2299–314.
13. Lançon A, Hanet N, Jannin B, Delmas D, Heydel JM, Lizard G, *et al.* Resveratrol in human hepatoma HepG2 cells: metabolism and inducibility of detoxifying enzymes. Drug Metab Dispos. 2007;35(5):699–703.
14. Alfaras I, Pérez M, Juan ME, Merino G, Prieto JG, Planas JM, *et al.* Involvement of breast cancer resistance protein (BCRP1/ABCG2) in the bioavailability and tissue distribution of *trans*-resveratrol in knockout mice. J Agric Food Chem. 2010;58 (7):4523–8.
15. Juan ME, Maijó M, Planas JM. Quantification of *trans*-resveratrol and its metabolites in rat plasma and tissues by HPLC. J Pharm Biomed Anal. 2010;51(2):391–8.
16. Hem A, Smith AJ, Solberg P. Saphenous vein puncture for blood sampling of the mouse, rat, hamster, gerbil, guinea pig, ferret and mink. Lab Anim. 1998;32(4):364–8.
17. Beal SL, Sheiner LB. NONMEM User's guide. Icon Development Solutions: Ellicot City, MD 1989–2006.
18. Jonsson EN, Karlsson MO. Xpose: an S-PLUS based population pharmacokinetic/pharmacodynamic model building aid for NONMEM. Comput Meth Programs Biomed. 1999;58(1):51–64.
19. Lindbom L, Pihlgren P, Jonsson N. PsN-Toolkit: a collection of computer intensive statistical methods for non-linear mixed effect modeling using NONMEM. Comput Meth Programs Biomed. 2005;79(3):241–57.
20. Yamaoka T, Nakagawa T. Uno, Application of Akaike's Information Criterion (AIC) in the evaluation of linear pharmacokinetics equations. J Pharmacokinet Biopharm. 1978;6(2):165–75.
21. Karlsson MO, Holford NH. A Tutorial on Visual Predictive Checks. 2008, pp 17 (Abstract 1434). Available at: http://www.page-meeting.org/?abstract=1434.
22. Bergstrand M, Hooker AC, Wallin JE, Karlsson MO. Prediction-Corrected Visual Predictive Checks for Diagnosing Nonlinear Mixed-Effects Models. AAPS J. 2011. doi:10.1208/s12248-011-9255-z.
23. Savic RM, Karlsson MO. Importance of shrinkage in empirical bayes estimates for diagnostics: problems and solutions. AAPS J. 2009;11(3):558–69.
24. van de Wetering K, Burkon A, Feddema W, Bot A, de Jonge H, Somoza V, *et al.* Intestinal breast cancer resistance protein (BCRP)/Bcrp1 and multidrug resistance protein 3 (MRP3)/Mrp3 are involved in the pharmacokinetics of resveratrol. Mol Pharmacol. 2009;75(4):876–85.
25. de Santi C, Pietrabissa A, Mosca F, Pacifici GM. Glucuronidation of resveratrol, a natural product present in grape and wine, in the human liver. Xenobiotica. 2000;30(11):1047–54.
26. Sabolovic N, Humbert AC, Radominska-Pandya A, Magdalou J. Resveratrol is efficiently glucuronidated by UDP-glucuronosyltransferases in the human gastrointestinal tract and in Caco-2 cells. Biopharm Drug Dispos. 2006;27(4):181–9.
27. Maier-Salamon A, Hagenauer B, Reznicek G, Szekeres T, Thalhammer T, Jäger W. Metabolism and disposition of resveratrol in the isolated perfused rat liver: role of Mrp2 in the biliary excretion of glucuronides. J Pharm Sci. 2008;97(4):1615–28.
28. Andlauer W, Kolb J, Siebert K, Fürst P. Assessment of resveratrol bioavailability in the perfused small intestine of the rat. Drugs Exp Clin Res. 2000;26(2):47–55.
29. Kuhnle G, Spencer JP, Chowrimootoo G, Schroeter H, Debnam ES, Srai SK, *et al.* Resveratrol is absorbed in the small intestine as resveratrol glucuronide. Biochem Biophys Res Commun. 2000;272(1):212–7.